AAMRL-SR-90-510

AD-A232 814

QUANTIFYING PERFORMANCE DEGRADATION DUE TO THE HUMAN-MACHINE INTERFACE OF TELEMANIPULATORS

Steven J. Remis
Daniel W. Repperger

Biodynamics and Bioengineering Division
Harry G. Armstrong Aerospace Medical Research Laboratory
Wright-Patterson Air Force Base, OH 45433-6573

December 1990

Interim Report for the Period January 1990 through December 1990

HARRY G. ARMSTRONG AEROSPACE MEDICAL RESEARCH LABORATORY
HUMAN SYSTEMS DIVISION
AIR FORCE SYSTEMS COMMAND
WRIGHT-PATTERSON AIR FORCE BASE, OHIO 45433-6573

REPORT DOCUMENTATION PAGE

Form Approved
OMB No. 0704-0188

1. AGENCY USE ONLY (Leave blank)	2. REPORT DATE	3. REPORT TYPE AND DATES COVERED
	December 1990	Interim - Jan 90 - Dec 90

4. TITLE AND SUBTITLE

Quantifying Performance Degradation Due to the Human-Machine Interface of Telemanipulators

5. FUNDING NUMBERS

PE - 62202F
PR - 7231
TA - 38
WU - 08

6. AUTHOR(S)

Steven J. Remis; Daniel W. Repperger

7. PERFORMING ORGANIZATION NAME(S) AND ADDRESS(ES)

Biodynamics and Bioengineering Division
Harry G. Armstrong Aerospace Medical Research Laboratory
Wright-Patterson AFB, OH 45433-6573

8. PERFORMING ORGANIZATION REPORT NUMBER

9. SPONSORING/MONITORING AGENCY NAME(S) AND ADDRESS(ES)

Harry G. Armstrong Aerospace Medical Research Laboratory
Human Systems Division
Air Force Systems Command
Wright-Patterson AFB, OH 45433-6573

10. SPONSORING/MONITORING AGENCY REPORT NUMBER

AAMRL-SR-90-510

11. SUPPLEMENTARY NOTES

12a. DISTRIBUTION/AVAILABILITY STATEMENT

Approved for public release; distribution is unlimited

12b. DISTRIBUTION CODE

13. ABSTRACT *(Maximum 200 words)*

As a first step in evaluating operator interfaces to telerobots, task performance data were collected from humans hands-on, with and without the subjects wearing a unilateral exoskeletal device. These baseline studies show the degradation in task performance caused solely by the exoskeleton, exclusive of any slave robotic system. This subsystems-level approach to performance measurement is motivated by the increasing modularity among robotic designs, and the need to quantify the performance degradation caused by each subsystem. The experiments described in this paper show that the unilateral exoskeleton decreases the human's available information capacity by approximately 36 percent, depending on the subject and the difficulty of the task. This decrease in available information capacity is similar when viewing the peg-into-hole task using the one dimension of Fitts' Law or when breaking this task into the two tasks of ballistic motion and accurate positioning. Future work involves evaluating the teleoperated performance of these tasks, plus similar hands-on and teleoperated experiments with the operator wearing a bilateral exoskeleton. This matrix of experiments can be repeated for other telerobotic interfaces to understand the benefits and limitations of the variety of available human-machine interfaces.

14. SUBJECT TERMS			15. NUMBER OF PAGES
Teleoperation	Human-machine interface	Telerobotics	99
Force reflection	Robotic telepresence	Exoskeleton	16. PRICE CODE

17. SECURITY CLASSIFICATION OF REPORT	18. SECURITY CLASSIFICATION OF THIS PAGE	19. SECURITY CLASSIFICATION OF ABSTRACT	20. LIMITATION OF ABSTRACT
UNCLASSIFIED	UNCLASSIFIED	UNCLASSIFIED	UL

GENERAL INSTRUCTIONS FOR COMPLETING SF 298

The Report Documentation Page (RDP) is used in announcing and cataloging reports. It is important that this information be consistent with the rest of the report, particularly the cover and title page. Instructions for filling in each block of the form follow. It is important to ***stay within the lines*** to meet ***optical scanning requirements***.

Block 1. Agency Use Only *(Leave blank)*.

Block 2. Report Date. Full publication date including day, month, and year, if available (e.g. 1 Jan 88). Must cite at least the year.

Block 3. Type of Report and Dates Covered. State whether report is interim, final, etc. If applicable, enter inclusive report dates (e.g. 10 Jun 87 - 30 Jun 88).

Block 4. Title and Subtitle. A title is taken from the part of the report that provides the most meaningful and complete information. When a report is prepared in more than one volume, repeat the primary title, add volume number, and include subtitle for the specific volume. On classified documents enter the title classification in parentheses.

Block 5. Funding Numbers. To include contract and grant numbers; may include program element number(s), project number(s), task number(s), and work unit number(s). Use the following labels:

C	- Contract	**PR**	- Project
G	- Grant	**TA**	- Task
PE	- Program Element	**WU**	- Work Unit Accession No.

Block 6. Author(s). Name(s) of person(s) responsible for writing the report, performing the research, or credited with the content of the report. If editor or compiler, this should follow the name(s).

Block 7. Performing Organization Name(s) and Address(es). Self-explanatory.

Block 8. Performing Organization Report Number. Enter the unique alphanumeric report number(s) assigned by the organization performing the report.

Block 9. Sponsoring/Monitoring Agency Name(s) and Address(es). Self-explanatory.

Block 10. Sponsoring/Monitoring Agency Report Number. *(If known)*

Block 11. Supplementary Notes. Enter information not included elsewhere such as: Prepared in cooperation with...; Trans. of...; To be published in.... When a report is revised, include a statement whether the new report supersedes or supplements the older report.

Block 12a. Distribution/Availability Statement. Denotes public availability or limitations. Cite any availability to the public. Enter additional limitations or special markings in all capitals (e.g. NOFORN, REL, ITAR).

- **DOD** - See DoDD 5230.24, "Distribution Statements on Technical Documents."
- **DOE** - See authorities.
- **NASA** - See Handbook NHB 2200.2.
- **NTIS** - Leave blank.

Block 12b. Distribution Code.

- **DOD** - Leave blank.
- **DOE** - Enter DOE distribution categories from the Standard Distribution for Unclassified Scientific and Technical Reports.
- **NASA** - Leave blank.
- **NTIS** - Leave blank.

Block 13. Abstract. Include a brief *(Maximum 200 words)* factual summary of the most significant information contained in the report.

Block 14. Subject Terms. Keywords or phrases identifying major subjects in the report.

Block 15. Number of Pages. Enter the total number of pages.

Block 16. Price Code. Enter appropriate price code *(NTIS only)*.

Blocks 17. - 19. Security Classifications. Self-explanatory. Enter U.S. Security Classification in accordance with U.S. Security Regulations (i.e., UNCLASSIFIED). If form contains classified information, stamp classification on the top and bottom of the page.

Block 20. Limitation of Abstract. This block must be completed to assign a limitation to the abstract. Enter either UL (unlimited) or SAR (same as report). An entry in this block is necessary if the abstract is to be limited. If blank, the abstract is assumed to be unlimited.

Contents

1 Introduction

Since 1986 the Harry G. Armstrong Aerospace Medical Research Laboratory (AAMRL) has been developing technologies for sensory feedback involving remote robotic systems. Of the three active areas of research (coarse positioning, fine manipulation, and tactile stimulation), this paper investigates the control of robotic slaves in the coarse positioning arena. Specifically, the report presents the results of a preliminary research effort to understand the limitations of exoskeletal devices when used as the human arm interfaces to these teleoperated systems.

To quantify the performance degradation caused by these exoskeletal interfaces, first it is necessary to develop baseline data for future comparisons. The baseline studies must quantify the degradation caused by the exoskeleton without adding bias from the particular slave robots used. A testbed, coined the Force-Reflecting Interfaces to Telemanipulators Testing System (FITTS)[8], has been developed at AAMRL to perform these experiments. With the FITTS, the degradations due to various operator interfaces to teleoperated systems may be compared directly. These data may also be compared to the nondegraded data from a human completing the same tasks hands-on.

Before presenting results of the preliminary experiments conducted with the FITTS, a discussion is given about the increasing need for subsystems-level performance measurement of teleoperated systems. The trend towards modular robotic designs is shown to demand this approach. Next a brief description of the FITTS testbed is presented, along with current and future baseline experiments to be conducted at this facility. Fitts' Law, the metric used for performance comparisons, is then analyzed in detail. Next it is shown that these tasks can also be viewed as dual tasks, with the first task being the ballistic motion phase of the peg transfer task, and the second being the accurate positioning task required to insert the peg into the target hole. The protocol for the preliminary experiments is then given, and data from these experiments are subsequently presented. Finally, an analysis of these data is conducted and conclusions are drawn about this approach to teleoperator subsystem evaluations.

2 The Need for Teleoperator Subsystem Testing

The degree of modularity among robotic devices, including autonomous robots, teleoperators, and telepresence systems, is increasing rapidly. This new-found modularity will someday allow users of robotic systems to "pick and choose" the characteristics of the available equipment, both master subsystems and slave subsystems, to best suit the requirements of a particular task. Modularity creates a virtual, if not physical, separation between the master subsystems and those of the slave devices. The control algorithms, mechanical apparatus, sensor suites, and processing architectures all become *black boxes,* with well-defined inputs and outputs; this allows master subsystems and slave subsystems with completely different characteristics to work together.

However, adding modularity to systems does not inherently increase their utility. In fact, the converse might be true if an analysis of the costs *vs.* benefits of the specific subsystems is not conducted. The extensive work on modular robotics occurring in academia [13] and in industry [11] seems to be concentrating more on kinematic and ease-of-implementation issues than on performance evaluations of specific designs and devices. The increased cost and complexity of the added modularity becomes self-defeating unless users are given the conditions for which a specific device is capable, or the system is intelligent enough to make this decision itself.

To measure the performance capabilities of teleoperated systems, most researchers and systems

developers compare teleoperated task performance to the performance of similar tasks by humans hands-on [3] [5]. This systems-level approach is helpful for understanding the degrading effect the teleoperator has on task performance, but it provides no information about the individual parameters of the complete teleoperator system which contribute to the performance degradation. Two factors have historically prevented the telerobotics community from conducting these specialized, subsystems-level analyses. The first factor is the prohibitive cost involved. This cost includes not only the cost of developing a testbed, but also the expense of the teleoperator systems themselves. Hopefully modularity will continue finding its way into new designs, requiring only specific subsystems of the complete system for the performance measurement tests. The second factor preventing subsystems-level testing is the specificity of both the hardware and the software of existing systems. This specificity is gradually decreasing as designers incorporate the newer architectures, languages, and communications protocols specifically designed for modularity [1]. The future designs should allow comparisons among subsystems, similar to today's computer industry (e.g., megaflops for architectures, benchmark programs for software, access times and storage density for media).

The next section describes a first step to generate parameters for comparisons of teleoperator operator interfaces. It is hoped that using the FITTS testbed to conduct independent examinations will enable the objective analysis of the costs *vs.* performance for the variety of available human-machine interface devices. The remainder of the report then focuses on one specific type of interface: the exoskeleton.

3 Exoskeletal Interfaces: Baselines for Comparison

The FITTS testbed has been developed to evaluate human-machine interfaces to teleoperated systems. This testbed includes a left/right pair of 6 DOF slave robots (American Cimflex Merlin 6500 robots), the AF/Navy Teleoperator Performance Evaluation Battery [12], and associated sensors, controllers, and computers [8]. The AF/Navy Teleoperator Performance Evaluation Battery, also known as the taskboard, contains simple, peg-into-hole tasks structured to provide a linear progression of difficulty when viewed using a Fitts' Law paradigm [4]. This paradigm is discussed in Section 4.

To use FITTS for evaluating specific human-machine interfaces, it is first necessary to develop performance baselines for comparison. In the FITTS testbed, several performance baselines are being applied for exoskeletal interfaces (see Table 1). The first baseline is derived by testing humans hands-on, unencumbered by any system component. This baseline is the optimal performance we would expect a true *telepresence* [7] system to achieve, although it is recognized that synergism between the man and the machine could eventually surpass this now-optimal baseline. The second baseline is found by evaluating the operator wearing the unilateral exoskeleton described in reference [10], performing the same tasks (without any slave robotic devices). By wearing the unilateral device, the operator's performance will be degraded by many factors, such as added inertias, friction, and kinematic constraints. This second baseline can be thought of as worst-case for exoskeletons, since bilateral exoskeletons should include compensation for the exoskeleton's dynamics (inertias, friction, gravity, Coriolis and centripetal forces) which the unilateral device cannot provide. The third baseline is derived by measuring the teleoperated performance of the same tasks while the human wears the unilateral exoskeleton. Once again, this baseline is worst-case for performance, since bilateral exoskeletons will include kinesthetic feedback from the slave robot during task performance while compensating for exoskeleton dynamics.

Table 1: Baseline Evaluations for Exoskeletal Interfaces

Baseline	Description
1	Human unencumbered; hands-on
2	Human wearing unilateral exoskeleton; hands-on
3	Human wearing unilateral exoskeleton; teleoperation

Once the three baselines of Table 1 are established, performance evaluations of bilateral exoskeletons can occur, as shown in Table 2. The first complete subsystem evaluation will be to study the performance of a human wearing the bilateral exoskeleton without interfacing to a slave robot, but including gravitational, Coriolis, centripetal, and friction compensation (if these algorithms are normally part of the exoskeleton's control code). This test, which is the Mode 2 condition of Table 2, measures the kinematic and controller constraints of the exoskeleton, and can be compared against the second baseline established above. The data can also be thought of as the expected performance of the teleoperator system assuming perfectly transparent slave robots are used.

Table 2: Experimental Conditions for Evaluating Teleoperator Human-Machine Interfaces. *Modes are numbered to correspond with the experimental conditions for the baseline experiments.*

Mode	Condition
2	Hands-on task performance
3	Teleoperated task performance

Of course, the final complete subsystem test for the exoskeletal interface is to study the task performance of a human wearing the force-reflecting exoskeleton, while controlling the slave robot (bilateral teleoperation; Mode 3). Comparing these data to the third baseline established above will show the benefits of force reflection and dynamics compensation. Comparing the data to the first baseline will determine how much improvement remains before *telepresence* [6] is achieved.

More discriminating experiments are also possible using the above protocols. For example, assuming the teleoperator human interface control code contains compensation terms for gravity, Coriolis, centripetal, and friction dynamics, it is often a trivial exercise to remove one of these terms from the control equations. The relative importance of each term will be shown by removing the compensation for each dynamical effect individually, and then conducting a Mode 2 experiment using the revised control equations. These data will lead to an understanding of a human's ability to compensate for selected dynamics. Similar experiments will lead to an understanding of the subsystem's dependence on control loop rate (controller bandwidth), by incrementally degrading the controller bandwidth and then conducting Mode 2 experiments. These understandings of the control equations and controller bandwidth effects on the human-machine interface will benefit future designs of human interfaces. A similar matrix of experiments is possible using Mode 3 experiments. These experiments should be conducted by not only limiting the teleoperator human

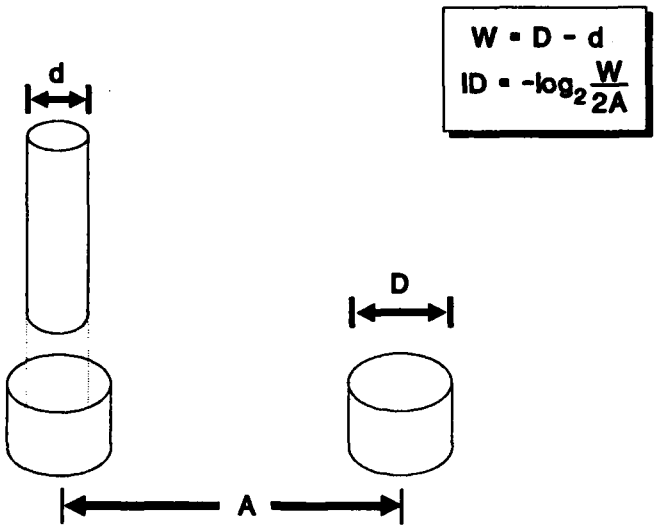

Figure 1: Measurements used to define task difficulty.

interface dynamics compensation terms, but also by selectively degrading other system variables, such as inter-subsystem communication rates, force feedback ratio, and force sensor bandwidth. Once again, these data will permit future teleoperator designers to consider the most important parameters of telemanipulators during the design process.

4 Fitts' Law for Performance Measurement

Fitts [4] defined the Index of Difficulty, ID, for one-dimensional tasks as

$$ID = -log_2 \frac{W}{2A} \qquad (bits/response) \tag{1}$$

where W is the peg tolerance (the difference between the hole diameter and the peg diameter) and A is the amplitude of the movement. The variables are shown in Figure 1.

Fitts' Law [4] relates the time to complete tasks, as a function of task ID, by defining the movement time, mt, as follows:

$$mt = k_1 ID + k_2 \qquad (sec) \tag{2}$$

with k_1 and k_2 varying by individual.

k_1 is simply the slope of the mt *vs.* ID curve. The reciprocal of k_1 has units of $\frac{bits}{sec}$, which is identical to units of capacity for an information channel. Thus $\frac{1}{k_1}$ has been accepted as a measure of human information processing capacity. This has also been related to the bandwidth of human performance when the information processing system is modelled as a low-pass filter [10]. Larger values of k_1 have been shown to be comparable to an information channel with a lower signal-to-noise ratio [2].

The value k_2 is physiologically the reaction time of the human operator. This can be seen by considering a task of $ID = 0$. For this to be true, $\frac{W}{2}$ must equal A. Referring to Figure 2, at the limit, as $\frac{W}{2} \rightarrow A$, the amplitude of motion A may be arbitrary. For this task, were it possible to measure for completion, the subject must process all of the information required to move the peg. Once motion begins, the task is completed, because $A \equiv \frac{W}{2}$, and the peg is already in the target hole. In other words, the peg starts in the same hole it is required to have the run terminated in.

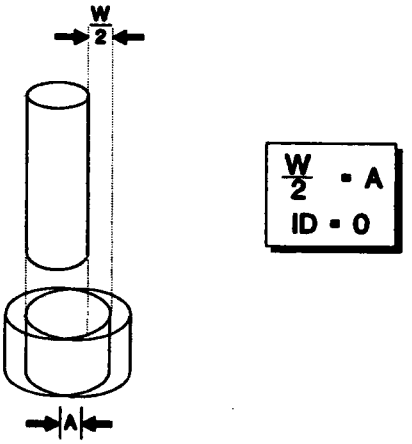

Figure 2: A task with $ID = 0$.

Thus mt is pure reaction time for this task. Although no method exists for measuring these types of tasks, it is possible, with caution, to extrapolate from the measured data to $ID = 0$.

The time required to complete the tasks is expected to increase when the operator wears an exoskeleton. Using the task difficulty, ID, as defined in equation (1), the expected movement time for the subject encumbered by the exoskeleton becomes

$$mt_{enc} = k_1' ID + k_2' \qquad (sec) \tag{3}$$

where k_1' and k_2' are the measured slope and intercept of the Fitts' Law curve for this encumbered condition.

Using k_1 and k_2 from equation (2) (the unencumbered condition), and k_1' and k_2' from equation (3), the following degradation parameters are defined:

$$m_{enc} = \frac{k_1'}{k_1} \tag{4}$$

$$r_{enc} = \frac{k_2'}{k_2} \tag{5}$$

where the m_{enc} ratio represents the change in slope of the Fitts' Law curve, and r_{enc} represents the change in reaction time due to the requirement of wearing the exoskeleton device. The percentage increase in these values, represented by the quantity

$$\frac{k_x' - k_x}{k_x} \tag{6}$$

where x is either one or two, is easily extracted from m_{enc} and r_{enc} by subtracting unity from these ratios.

The slope of the Fitts' Law curve is expected to be greater for the subjects when wearing the exoskeleton than when unencumbered, i.e., $m_{enc} > 1$. This means that some of the human's information channel capacity will be used to overcome the encumbrance of the exoskeleton. It is apparent that the human's requirement to process information when using the exoskeleton, involving such variables as joint frictions, kinematic constraints, added inertias, etc., will reduce the amount of human resources available to process task information.

It is also expected that the physiological reaction time will increase when the subjects wear the encumbering exoskeleton ($r_{enc} > 1$). One would intuitively expect k_2 to increase based on two considerations. First, because the exoskeleton adds substantially more mass to the arm and the upper body, the finite energy available by the human when applied to this new mass results in slower accelerations. If added friction exists in the initial movement, the overall pure reaction time will be subsequently increased. A second reason the encumbrance of the exoskeleton will slow the reaction time is because humans tend to think about and plan their moves before any movement occurs. As a consequence of wearing the exoskeleton, subjects need a longer time to plan their moves before initiating an action.

Note that there is no physical basis for $m_{enc} = r_{enc}$. This is because m_{enc} refers to the change in slope (the reciprocal of capacity) and r_{enc} refers to the change in reaction time. Both of these metrics are the results of different physiological processes within the human; however, as described above, both m_{enc} and r_{enc} should be greater than 1.0.

For certain tasks, Fitts' Law ceases to hold. This occurs when the task essentially becomes two tasks, and the subject must change movement strategies to complete the overall task. For the taskboard, the largest amplitude of motion requires the operator to rotate the torso, lean at the waist, or use finger adjustments of the peg to complete these tasks. k_1 then increases beyond that expected by a simple first-order model of the human's information channel, as shown in Figure 3. To evaluate this data it will be shown in the next section how to break these one-dimensional tasks into dual tasks. However, for the evaluations using only Fitts' one-dimensional paradigm, we will exclude these more complex task situations, with 64 *cm* amplitudes of motion, from the analyses.

5 Extending Fitts' Law to A Dual Task Paradigm

As mentioned above, data from some tasks do not support Fitts' one dimension of task performance. For the experiments reported here, those tasks with amplitude $A = 64$ *cm* do not fit the one-dimensional model, as shown in Figure 3. These tasks require the subjects to either rotate the torso, lean at the waist, or use fine adjustments with the fingers to position the pegs.

The analysis described in reference [14] will be conducted for these more complex tasks. Instead of assuming one linear *mt vs. ID* relationship, the single task is divided into the two tasks of ballistic motion and accurate positioning. The ballistic motion task occurs from the time the subject begins moving the peg until the peg makes first contact with the target hole. If the subject makes a "clean insertion," that is, the peg never contacts the sides of the target hole, then the ballistic phase occurs from the time the subject begins moving the peg until any part of the peg intersects the volume of the target hole. The positioning task occurs from the end of the ballistic task until the peg insertion is completed.

The movement time for the overall peg transfer task, *mt*, is the sum of the movement times for the two tasks:

$$mt = mt_{ballistic} + mt_{positioning} \tag{7}$$

Both movement times on the right side of the above equation are assumed to be linearly dependent on each task's difficulty, similar to equation (2) for the Fitts' Law analysis.

Of particular interest in this study is the capacity for performing tasks of various difficulties, which was shown to be equivalent to the reciprocal of the slope of the *mt vs. ID* line. Using the

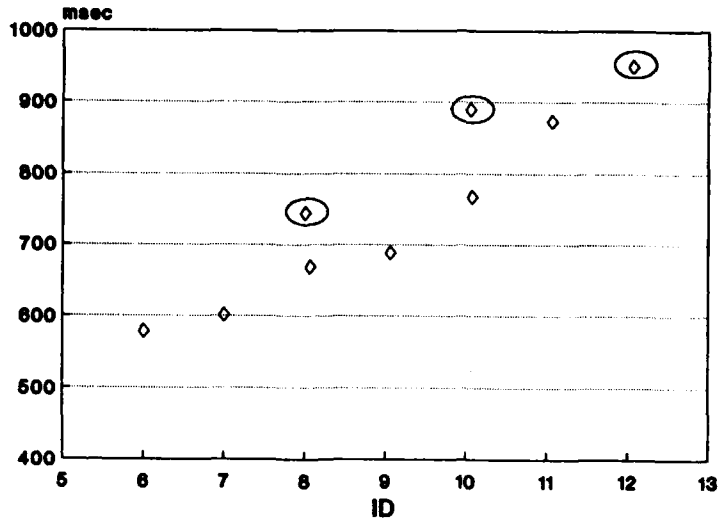

Figure 3: Subject 4's performance times, unencumbered, show that the more difficult tasks of $A = 64$ cm (circled) do not fall in line with the movement times predicted by Fitts' Law.

data collected for the Fitts' Law paradigm, it is possible to extract measures of capacity for ballistic tasks and for positioning tasks, as follows.

Define a to be the slope of the ballistic task. This value can be determined by using data from the tasks which use the smallest peg (and the greatest tolerance $\frac{11'}{2}$), and considering tasks of all amplitudes A for this peg. Because this peg is the easiest to insert into the target holes, the ballistic phase will have the highest possible influence on these data, recognizing that the empirical data consider the overall movement times for both tasks. This analysis assumes that the positioning task is constant for all peg insertions using this particular tolerance, $\frac{11'}{2}$. Although this is an approximation of the task realities, because the difficulty inserting the pegs is also a function of visual acumen and kinematic considerations, in general the assumption is valid. Thus, a is the slope of the performance times versus task difficulty for these ballistic tasks, and $\frac{1}{a}$ is the information channel capacity for performing ballistic tasks.

In a similar way define b to be the slope of the positioning task. This slope is best determined by using data from the tasks which require the shortest amplitude A, but considering all peg diameters for the shortest amplitude. Then, because these tasks require the shortest ballistic motion, the positioning phase will have the highest possible influence on these data. Once again, it is recognized that the empirical data record the sum of the movement times for the ballistic and the positioning tasks, and the slope b is derived with the assumption that the ballistic task is constant for each trial using the shortest amplitude A. Although the difference in mass for each peg may cause the human's ballistic motion to differ slightly, in general the assumption holds. Therefore b is the slope of the positioning task performance times versus task difficulty, and $\frac{1}{b}$ is the subject's capacity for performing positioning tasks.

Comparing the slopes a and b from the unencumbered to the encumbered experimental conditions is similar to the above measures of encumbrance m_{enc} and r_{enc}. If a and b are the ballistic phase and positioning phase slopes when unencumbered, respectively, and a' and b' the same values

Table 3: Taskboard Indices of Difficulty

Peg Diameter (cm)	Hole Diameter (cm)	Amplitude (cm)	ID (bits/response)
1.50	2.00	16	6.000
		32	7.000
		64	8.000
1.88	2.00	16	8.006
		32	9.006
		64	10.006
1.97	2.00	16	10.060
		32	11.060
		64	12.060

when wearing the exoskeleton, define

$$a_{enc} = \frac{a'}{a} \tag{8}$$

$$b_{enc} = \frac{b'}{b} \tag{9}$$

It is expected that overcoming the kinematic and dynamic constraints of the exoskeleton will make it more difficult for the subjects to make ballistic motions ($a_{enc} > 1$). It is also expected to be more difficult to position the pegs into the holes when wearing the exoskeleton ($b_{enc} > 1$). For the MBA exoskeleton, b_{enc} is particularly influenced by a physical obstruction of one's vision of the target hole in some orientations, due to a panel of lights attached next to the handgrip of the exoskeleton. As was done earlier with the values m_{enc} and r_{enc}, subtract unity from the ratios a_{enc} and b_{enc} to determine the percentage increase in slopes.

6 Experimental Protocol

Seven subjects were used for this study. The AF/Navy Teleoperator Performance Evaluation Battery (the taskboard) contained the tasks performed by the subjects. This taskboard consists of sixteen holes of 2.00 *cm* diameter, and 10 *cm* long pegs of 1.50, 1.88, and 1.97 *cm* diameters. Although the taskboard may be fitted with 1 *cm* diameter holes and respective smaller-diameter pegs, these conditions were not evaluated in these experiments. The distance between the start hole and the destination hole was either 16, 32, or 64 *cm* for a particular task. Thus the tasks consisted of the IDs listed in Table 3. Note that the ratio of the amplitudes A forms a geometric series with a ratio $1:2:4$. This is no coincidence: on a log scale it provides a linear dynamic range to collect empirical data.

The goal of these tasks was to transfer the peg from one hole to the next as quickly as possible. Time was recorded from when the subject removed the peg from the start hole (a microswitch opened) until the subject inserted the peg into the destination hole (closing a second microswitch).

Figure 4: A demonstration on how the peg transfer task is performed while unencumbered.

Each subject completed the series of experiments unencumbered, then completed the experiments while wearing the unilateral exoskeleton. Each series of experiments consisted of a practice day (72 practice tasks) followed by three data days (24 practice tasks followed by 72 timed tasks). The order of the peg sizes varied among subjects, although inter-series learning was not a significant concern for these simple tasks. Figure 4 demonstrates how a subject would perform a task from the first series of experiments.

7 Results of Experiments

During the discussion of results, the following graphs, summary charts, and tables are presented in the text:

- Values for k_1, k_2, k_1', k_2', m_{cnc}, and r_{cnc} are given for each subject in Table 4.
- Figure 5 plots all *mt vs.* ID curves for both the unencumbered and encumbered conditions, excluding the nonlinear data points. This graph is the Fitts' Law analysis of these data.
- Coefficients of variation for all task conditions are shown in Figure 6.
- Values for a, b, a', b', a_{enc}, and b_{enc} are given for each subject in Table 5.

These graphs, charts, and tables have been drawn from the complete data set which is given in the appendices. The appendices contain data listed in the following order:

Unencumbered

A Raw data for each subject, grouped by task ID.

B *mt vs.* ID for all tasks.

Table 4: Fitts' Law Data for Both Test Conditions

	Unencumbered		Wearing MBA exoskeleton			
Subject	k_1	k_2	k_1'	k_2'	m_{enc}	r_{enc}
1	61	289	73	322	1.197	1.114
2	67	120	78	147	1.164	1.225
3	61	180	73	190	1.197	1.056
4	56	218	63	364	1.125	1.670
5	61	98	62	204	1.016	2.082
6	46	318	99	152	2.152	0.478
7	38	273	90	-36	2.368	-0.132

C *mt vs.* ID, excluding nonlinear data points.

D *mt vs.* ID extrapolated to $ID = 0$.

Wearing MBA Exoskeleton

E Raw data for each subject, grouped by task ID.

F *mt vs.* ID for all tasks.

G *mt vs.* ID, excluding nonlinear data points.

H *mt vs.* ID extrapolated to $ID = 0$.

Other

I Coefficients of variation for each condition, unencumbered and wearing exoskeleton.

J Two-dimensional (ballistic phase and positioning phase) analysis for each subject, unencumbered and wearing the exoskeleton.

8 Discussion

8.1 Fitts' Law Paradigm

Referring to Table 4, which is repeated for $5 < ID < 13$ in Figure 5, both k_1 and k_2 were expected to increase when the MBA exoskeleton was worn. The data show the average increase in slope k_1, as represented by $\overline{m_{enc}}$ (where the overbar indicates mean value across subjects), is approximately 48 per cent. It is also seen from these data that the increase in reaction time k_2, as represented by $\overline{r_{enc}}$, is approximately 7 per cent. The significance of these results is discussed next.

m_{enc} appears to be a reliable indicator of performance. Recall that m_{enc} refers to the ratio of slopes of the Fitts' Law curves, with a higher value resulting from a larger amount of encumbrance, and a corresponding decrease in usable information channel capacity related by $(\frac{1}{m_{enc}})$. Therefore,

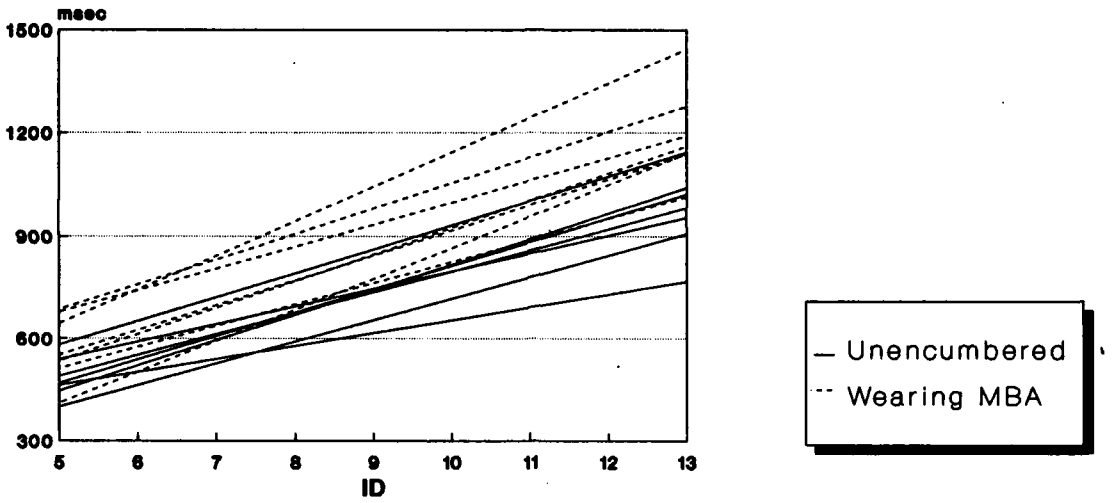

Figure 5: Performance curves for all subjects, both unencumbered and wearing the MBA exoskeleton. Recall that the nonlinear data points are excluded from these analyses (Section 5).

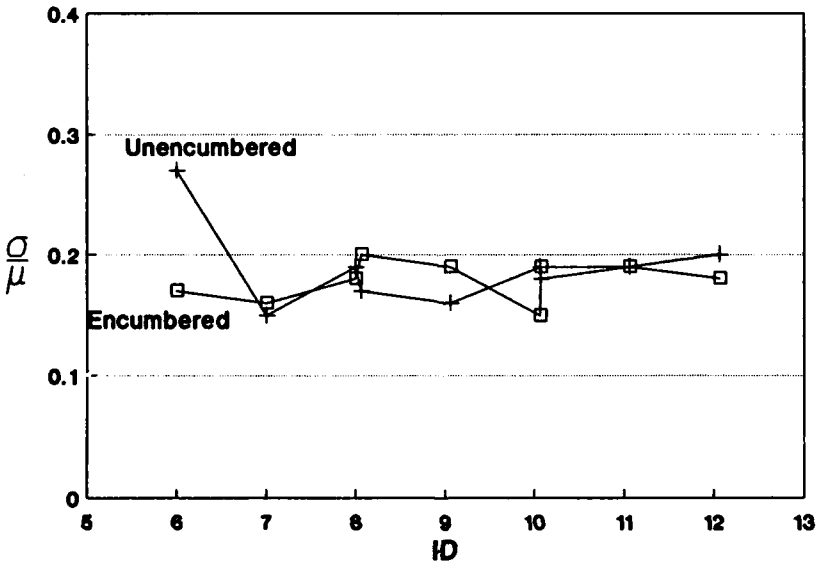

Figure 6: Coefficients of variation for all task conditions, averaged across subjects.

on average, a subject was able to use only 68 per cent ($\frac{1}{1.48}$) of the original information channel capacity to process task data when wearing the MBA exoskeleton. The remaining 32 per cent was used to process kinematic and dynamic information about controlling the MBA exoskeleton. Recall that this analysis excludes those tasks of amplitude $A = 64$ *cm*.

As expected, k_2 also increased when the subjects wore the exoskeleton, with $\overline{r_{enc}} = 1.07$. This equates to an average 7 per cent increase in reaction time resulting from increased initial processing requirements and the need to overcome the exoskeleton's dynamic effects with a finite amount of human input energy available. However, this analysis depends on extrapolating to $ID = 0$, when tasks with $0 \leq ID < 6$ were not measured. Even a minor change in slope k_1 results in significant changes in reaction time k_2 when extrapolating this far. This can be seen by excluding Subject 7's results from the above analysis. In this case $\overline{r_{enc}} = 1.27$, and the average increase in reaction time due to the requirement to wear the exoskeleton more than triples, from 7 per cent to 27 per cent. Obviously a particular subject's data should not have this much influence on the net result. It is apparent that an increased dynamic range of Fitts' Law tasks, including values of $0 < ID < 6$, is required to reduce the sensitivity of this analysis and enable accurate measurement of the degradation of the operator's reaction time response.

8.2 Coefficient of Variation

The coefficient of variation measures the repeatability of a trial by comparing two or more replications of the same experimental condition. This metric is calculated by dividing the standard deviation of a set of trials by the mean value. This ratio is almost always greater than 0.1 and less than 0.4 if an experiment using human subjects was conducted in a manner that is repeatable. The coefficient of variation is a good measure of the reproducibility of the experiment's data if it were to be rerun or if another facility were to replicate the original experiments.

To develop the coefficients of variation for this experiment (individually for each subject), it is necessary, at each $\frac{2A}{W}$ value, to form the ratio of $\frac{\sigma}{\mu}$. σ represents the standard deviation and μ is the mean of these data for each discrete task condition. Statisticians use the coefficient of variation to quickly ascertain the validity of the data within the framework of the overall experiment.

These experiments appear to be quite repeatable, with most of the coefficients of variation falling below 0.2. Figure 6 illustrates the coefficients of variation for these tasks averaged across subjects. No noticeable increase in variability is seen when the subjects wore the exoskeleton versus the unencumbered condition. Two obvious exceptions occurred during these experiments, causing individual coefficients of variation to exceed 0.4. These exceptions are found in Appendix I - one for subject 7 and one for subject 6. Neither of these isolated circumstances can be explained by the experimental protocol.

8.3 Dual Task Paradigm

Table 5 lists the data for the two separate tasks of ballistic motion and accurate positioning, using all the data points. These data show the average degradation in ballistic motion, represented by $\overline{a_{enc}}$, to be 1.69. The average degradation in accurate positioning, represented by $\overline{b_{enc}}$, is 1.52. These values correspond to an average decrease in usable ballistic motion capacity to 59 per cent ($\frac{1}{1.69}$) of the original capacity, and a similar decrease in available accurate positioning capacity to 66 percent ($\frac{1}{1.52}$) of the original quantity.

Table 5: Two-Dimensional Analysis of Data

Subject	Unencumbered		Wearing MBA exoskeleton			
	a	b	a'	b'	a_{enc}	b_{enc}
1	115	44	194	66	1.69	1.50
2	120	65	173	69	1.44	1.06
3	106	51	146	73	1.38	1.43
4	82	46	48	66	0.585	1.43
5	96	64	80	68	0.833	1.06
6	98	51	166	98	1.69	1.92
7	37	35	155	79	4.19	2.26

Two subjects, Subject 4 and Subject 5, show a *decrease* in ballistic phase slope, which corresponds to an increase in ballistic capacity when wearing the exoskeleton. This result, though unexpected, agrees with earlier studies which found that humans sometimes use the dynamics of an interface to dampen human-input noise [9]. Another possible explanation is due to the stimulation which sometimes occurs when humans are subjected to stress, such as when wearing the MBA exoskeleton. When subjected to stress situations, humans sometimes change their perceptions about the goals of the task, or they change their individual expectations. Consequently the humans might "try harder," or appear to be more motivated because of the change in their internal perception of the task at hand. Note, however, that this accommodation does not occur for the positioning phase, nor should it. The kinematic and visual constraints of the MBA exoskeleton prevented all subjects from performing the accurate positioning phase as well when wearing the MBA exoskeleton as compared to the case when the subjects were unencumbered.

Considering only the data for Subject 7, it is noted that a is very nearly equal to b for this subject's unencumbered condition. This indicates that a subject's data is very close to Fitts' one-dimensional model, even including the tasks of 64 *cm* amplitude. Also notice how much the exoskeleton increased this subject's ballistic slope a - over 400 per cent - demonstrating that the exoskeleton had the greatest effect on this subject's ballistic performance. This is confirmed by the Fitts' Law analysis, where $m_{enc} = 2.368$, also the largest.

There are several reasons why this exoskeleton affected Subject 7 the most. Although exact correlation between subjects' characteristics (biophysical data, motivation, and task completion strategies) and amount of performance degradation was not accomplished, it was noted that Subject 7 has the shortest arm lengths of the subject pool - noticeably shorter than the link lengths of the exoskeleton. Therefore the axes of rotation of the exoskeleton do not coincide with the axes of rotation of this subject's arm joints. This kinematic discrepancy will degrade one's ballistic motion by changing arm trajectories to make the Cartesian displacement of each arm link, given by $l_i\ \theta_{(i-1)}$, equate to the displacement of the exoskeleton's link, given by $l'_i\ \theta'_{(i-1)}$. Here the l_i and l'_i terms represent the length of the i^{th} link of the arm and the exoskeleton, respectively, and the $\theta_{(i-1)}$ and $\theta'_{(i-1)}$ terms represent the angular displacement of the joints which rotate these links.

Subject 7 was also extremely motivated for speed of task completion. This motivation led to some very quick peg insertions (typically for short amplitudes of motion), but the subject's attempts

to make very fast insertions also resulted in attempts to complete these tasks using only ballistic motion. It seemed that only when a rapid, ballistic motion was unsuccessful in inserting the peg into the target hole, did the subject complete the peg insertion task with an accurate positioning response. These failed insertion attempts may be categorized as errors, and they occurred for each subject. No attempt was made to correlate numbers of errors with the expected degradation because the subjects were not penalized for making errors, and speed of task completion was the sole motivation used in these experiments. It was apparent, however, that many more insertion errors were made by Subject 7 when wearing the exoskeleton than when unencumbered. Although this may or may not have been true for all subjects, it was only readily apparent for Subject 7.

9 Conclusions

The experiments described in this report have verified a new analytical technique which allows one to derive the degradation in available information channel capacity caused by a requirement to use the interface of a telemanipulation system when performing standard tasks. It has been shown how to extend Fitts' Law to include a measure of the degrading effect of the human interface, as long as the tasks hold to the one-dimensional assumptions inherent in Fitts' Law. A similar, but separate, analytical technique has shown how to derive the degradation to the operator's available capacities for both ballistic motion and accurate positioning tasks. The data from these experiments reveal that the MBA exoskeleton degrades the human's available information channel capacity for ballistic tasks, accurate positioning tasks, and one-dimensional tasks by 41 per cent, 34 per cent, and 32 per cent respectively. The data also show that the requirement to wear this exoskeleton increases the operator's physiological reaction time, although this result is very sensitive to the experimental conditions.

It is not possible with these studies, however, to predict the quantity of information channel capacity degradation expected for a particular telemanipulation operator. The many variables which may cause one subject to be more or less affected by this exoskeleton than another subject were not measured; thus, correlation between independent variables and results was not conducted. Further experiments to correlate subjects' anthropometric data, motivational impetus, and task completion techniques with the degradation in available information channel capacity are required if this analytical technique is to be extended to a predictive quantity. It will also be beneficial if subjects are penalized for making errors, or if an accurate account of insertion errors is maintained during the future experiments. It may be found that a correlation exists between one of the above metrics and the number of errors.

These experiments have enabled the quantification of the performance degradation caused by a unilateral exoskeleton. Additional value from these studies will be derived after the third and final baseline is measured (unilateral teleoperation); from these studies bilateral exoskeletons can then be evaluated as human interfaces to telemanipulation systems. The subsystems-level approach adopted here for teleoperator testing will allow future comparisons of the variety of operator interface devices, in addition to exoskeletons, which are available for teleoperated systems. Because of the increasing modularity among new robotic designs, these comparisons will aid those selecting telemanipulator subsystems for future applications. This is necessary, because the human limitations with or without such devices should drive the design of human interfaces. These limitations should be objectively quantified by metrics that can be easily understood and can be used to compare one experimental condition, using a specific operator interface, versus another condition. The

information capacity metrics presented herein meet these requirements.

References

[1] Albus, J. S., McCain, H. G., and Lumia, R., "NASA/NBS Standard Reference Model Telerobot Control System Architecture (NASREM)," *NBS Technical Note 1235*, 1987.

[2] Chan, R. B. and Childress, D. S., "On a Unifying Noise-Velocity Relationship and Information Transmission in Human-Machine Systems," *IEEE Trans. Syst. Man Cybern.*, vol. 20, no. 6, pp. 1125-1135, Sep/Oct 1990.

[3] Draper, J. V., Moore, W. E., and Herndon, J. N., "Effects of Force Reflection on Servomanipulator Task Performance," *Proc. USDOE/FRG Specialists' Meeting on Remote Systems Technology*, Oak Ridge, TN, 1987.

[4] Fitts, P. M., "The Information Capacity of the Human Motor System in Controlling the Amplitude of a Movement," *J. Exp. Psych.*, vol. 47, pp. 381-391, 1954.

[5] Hannaford, B. and Wood, L., "Performance Evaluation of a 6 Axis High Fidelity Generalized Force Reflecting Teleoperator," *Proc. NASA Conf. on Space Telerobotics*, Pasadena, CA, 1989.

[6] Julian, R. G. and Anderson, T. A., "Robotic telepresence: Applications of human controlled robots in Air Force maintenance," *Aerospace Simulation 1988, Proc. SCS Multiconf. on Aerospace Simulation III*, pp. 59-67, 1988.

[7] Mohr, G. C., "Robotic Telepresence," *Proc. Human Factors Society - 30th Annual Meeting*, Santa Monica, CA, pp. 43-44, 1986.

[8] Remis, S. J. and Nelson, D. K., "Force-Reflecting Interfaces to Telerobotics Testing System (FITTS) Interim User's Guide," *AAMRL Special Report*, Wright-Patterson AFB, OH, Dec 1990.

[9] Repperger, D. W., "Force Reflection Devices in Teleoperation," *IEEE Control Systems Magazine*, Jan 1991.

[10] Repperger, D. W., Remis, S. J., and Merrill, G., "Performance Measures of Teleoperation Using an Exoskeleton Device," *Proc. 1990 IEEE Int. Conf. Robot. Automat.*, vol. 1, pp. 552-557, 1990.

[11] Sciaky, M., "Modular Robots Implementation," *Handbook of Industrial Robotics*, S. Y. Noff, Ed. New York: John Wiley & Sons, Inc., 1985.

[12] Spain, E. H. and Coppock, D. A., "Toward Performance Standards for Remote Manipulation," *Proc. IEEE EMBS 11th Ann. Conf.*, Seattle, WA, Nov 1989.

[13] Tesar, D., "Next Generation of Technology for Robotics," Mechanical Engineering Department, The University of Texas at Austin, Feb 1985.

[14] Wiker, S. F., Langolf, G. D., and Chaffin, D. B., "Arm Posture and Human Movement Capability," *Human Factors*, vol. 31, no. 4, pp. 421-441, 1989.

Appendix A

Unencumbered Raw Data Grouped by Task *ID*

Subject 1 - Unencumbered

Peg diameter (cm)	$\frac{W}{2}$ (cm)	A (cm)	ID $\frac{bits}{response}$	n	$\overline{mt}$ (msec)	σ (msec)
1.50	0.250	16	6.000	24	667.542	131.816
1.88	0.060	32	7.000	24	750.167	91.409
1.97	0.015	64	8.000	24	897.458	172.082
1.50	0.250	16	8.006	24	748.208	92.574
1.88	0.060	32	9.006	24	833.792	146.186
1.97	0.015	64	10.006	24	1046.042	363.014
1.50	0.250	16	10.060	24	846.667	133.294
1.88	0.060	32	11.060	24	1028.583	212.253
1.97	0.015	64	12.060	24	1021.958	155.836

Subject 2 - Unencumbered

Peg diameter (cm)	$\frac{W}{2}$ (cm)	A (cm)	ID $\frac{bits}{response}$	n	$\overline{mt}$ (msec)	σ (msec)
1.50	0.250	16	6.000	24	500.333	96.243
1.88	0.060	32	7.000	24	641.292	98.722
1.97	0.015	64	8.000	24	740.250	81.570
1.50	0.250	16	8.006	24	642.667	121.381
1.88	0.060	32	9.006	24	740.333	99.022
1.97	0.015	64	10.006	24	908.792	152.797
1.50	0.250	16	10.060	24	762.417	126.802
1.88	0.060	32	11.060	24	886.750	193.425
1.97	0.015	64	12.060	24	1080.333	197.644

Subject 3 - Unencumbered

Peg diameter (cm)	$\frac{W}{2}$ (cm)	A (cm)	ID $\frac{bits}{response}$	n	$\overline{mt}$ (msec)	σ (msec)
1.50	0.250	16	6.000	24	528.417	75.541
1.88	0.060	32	7.000	24	616.917	77.614
1.97	0.015	64	8.000	24	739.458	115.679
1.50	0.250	16	8.006	24	664.458	123.431
1.88	0.060	32	9.006	24	775.125	99.014
1.97	0.015	64	10.006	24	909.000	123.561
1.50	0.250	16	10.060	24	734.750	85.207
1.88	0.060	32	11.060	24	867.708	184.425
1.97	0.015	64	12.060	24	968.083	201.722

Subject 4 - Unencumbered

Peg diameter (cm)	$\frac{W}{2}$ (cm)	A (cm)	ID $\frac{bits}{response}$	n	$\overline{mt}$ (msec)	σ (msec)
1.50	0.250	16	6.000	24	579.042	140.099
1.88	0.060	32	7.000	24	601.208	106.348
1.97	0.015	64	8.000	24	743.958	120.894
1.50	0.250	16	8.006	24	668.875	137.326
1.88	0.060	32	9.006	24	688.500	78.070
1.97	0.015	64	10.006	24	889.792	142.285
1.50	0.250	16	10.060	24	767.042	145.351
1.88	0.060	32	11.060	24	873.833	162.670
1.97	0.015	64	12.060	24	950.833	156.811

Subject 5 - Unencumbered

Peg diameter (cm)	$\frac{W}{2}$ (cm)	A (cm)	ID $\frac{bits}{response}$	n	$\overline{mt}$ (msec)	σ (msec)
1.50	0.250	16	6.000	24	463.625	98.970
1.88	0.060	32	7.000	24	521.958	85.744
1.97	0.015	64	8.000	24	656.083	144.441
1.50	0.250	16	8.006	24	619.208	134.272
1.88	0.060	32	9.006	24	612.792	64.414
1.97	0.015	64	10.006	24	760.708	128.700
1.50	0.250	16	10.060	24	722.750	111.463
1.88	0.060	32	11.060	24	778.792	148.622
1.97	0.015	64	12.060	24	962.250	252.253

Subject 6 - Unencumbered

Peg diameter (cm)	$\frac{W}{2}$ (cm)	A (cm)	ID $\frac{bits}{response}$	n	$\overline{mt}$ (msec)	σ (msec)
1.50	0.250	16	6.000	24	560.750	105.581
1.88	0.060	32	7.000	24	678.750	104.435
1.97	0.015	64	8.000	24	756.875	192.863
1.50	0.250	16	8.006	24	681.875	78.964
1.88	0.060	32	9.006	24	760.333	133.119
1.97	0.015	64	10.006	24	895.167	120.506
1.50	0.250	16	10.060	24	766.958	131.590
1.88	0.060	32	11.060	24	820.083	90.741
1.97	0.015	64	12.060	24	1069.208	233.921

Subject 7 - Unencumbered

Peg diameter (cm)	$\frac{W}{2}$ (cm)	A (cm)	ID $\frac{bits}{response}$	n	$\overline{mt}$ (msec)	σ (msec)
1.50	0.250	16	6.000	24	542.000	382.300
1.88	0.060	32	7.000	24	507.750	95.366
1.97	0.015	64	8.000	24	615.792	127.930
1.50	0.250	16	8.006	24	544.583	85.468
1.88	0.060	32	9.006	24	607.250	176.499
1.97	0.015	64	10.006	24	707.792	140.921
1.50	0.250	16	10.060	24	682.667	200.220
1.88	0.060	32	11.060	24	693.333	123.407
1.97	0.015	64	12.060	24	780.875	155.605

Appendix B

Unencumbered *mt vs. ID* for All Tasks

Subject 1 Unencumbered
All Data Points

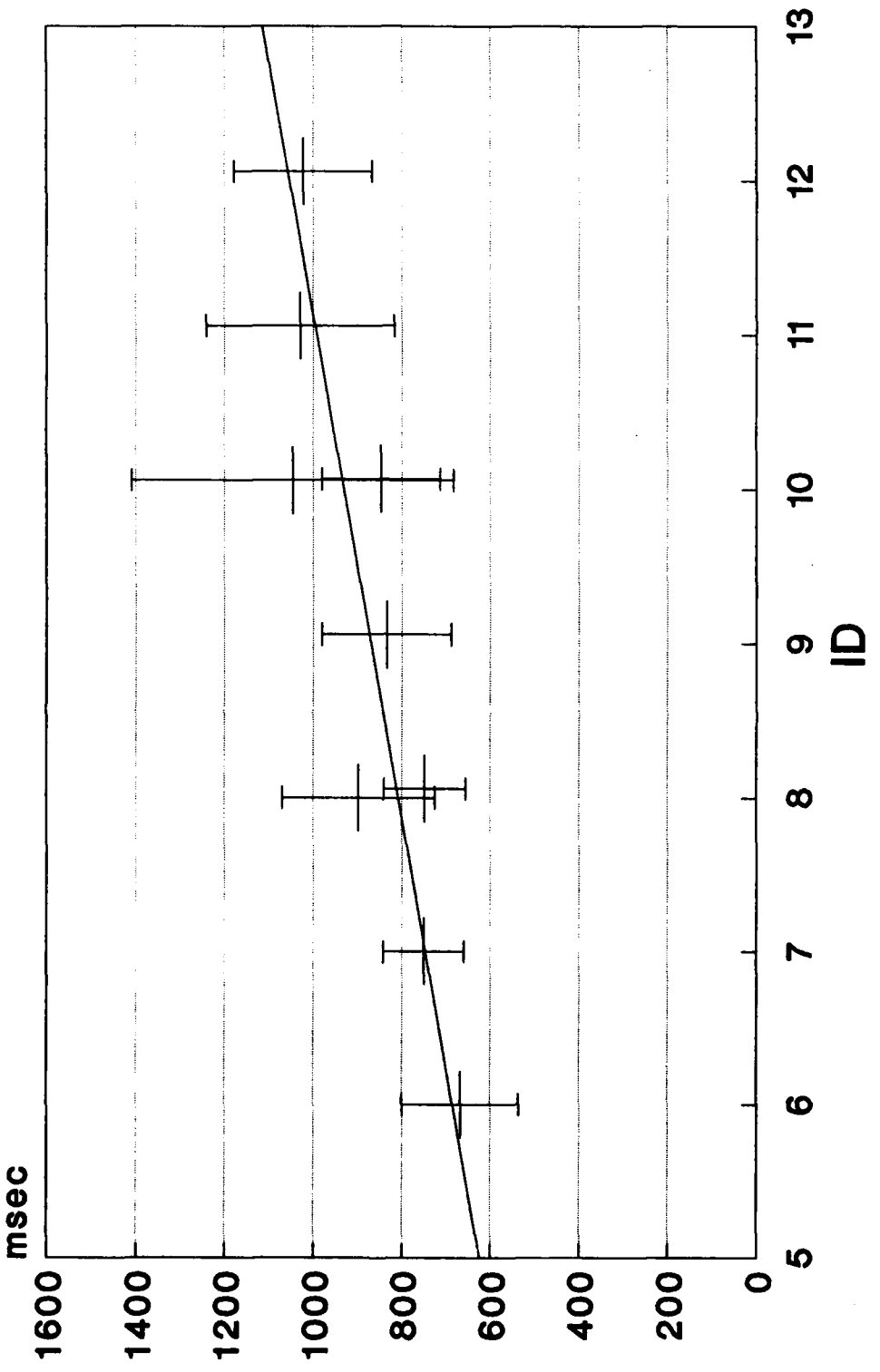

Subject 2 Unencumbered
All Data Points

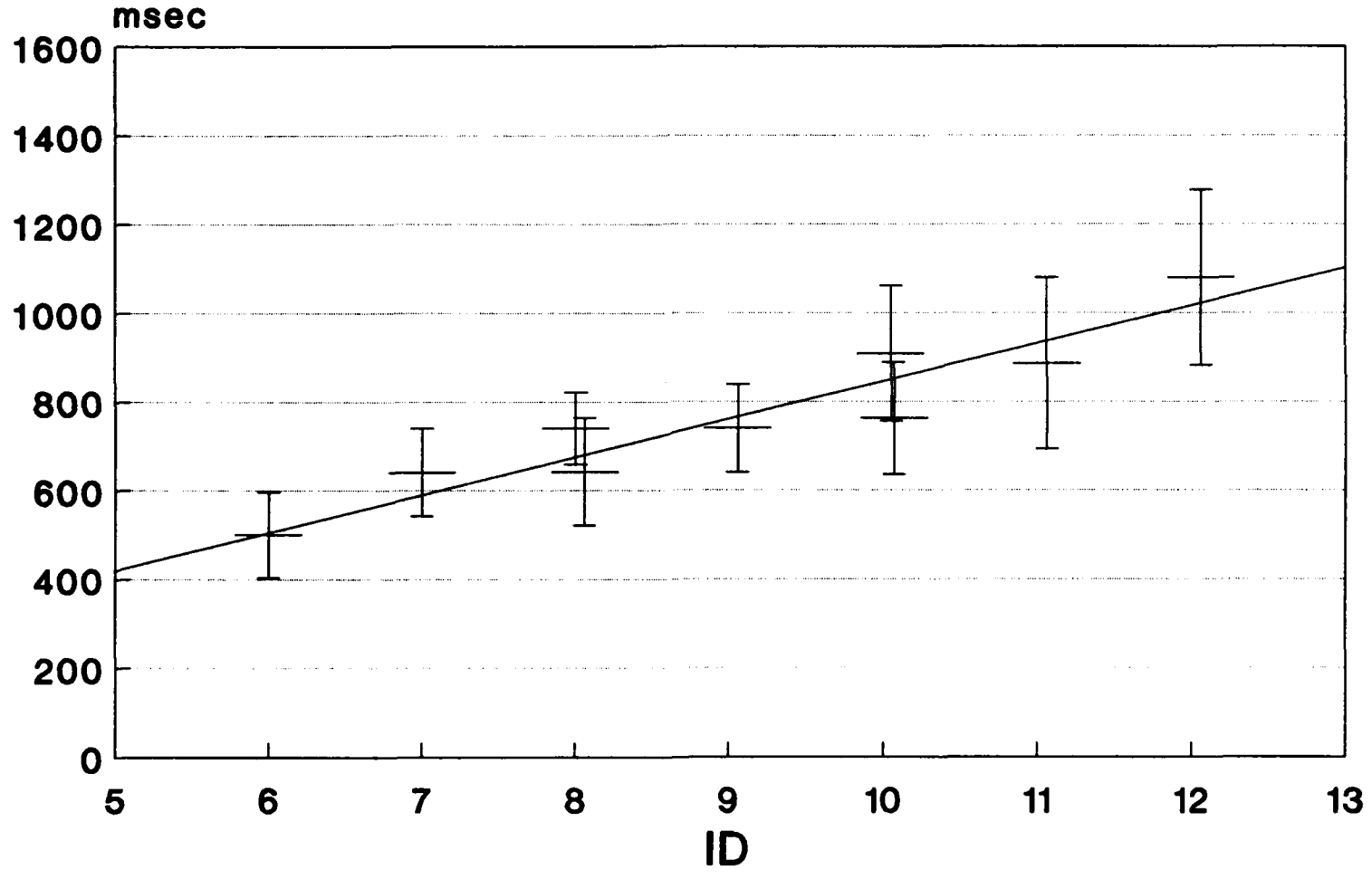

Subject 3 Unencumbered

All Data Points

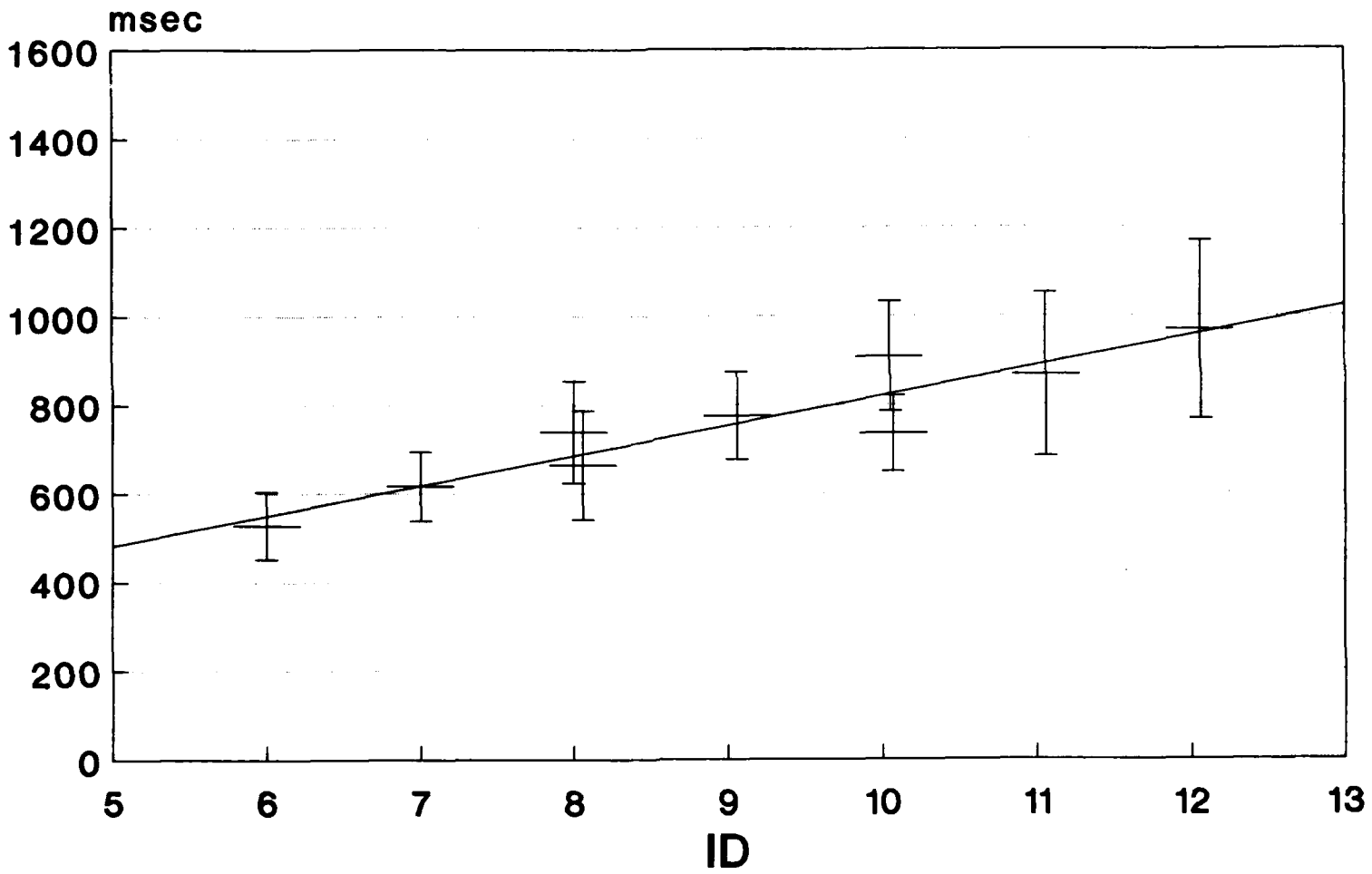

Subject 4 Unencumbered
All Data Points

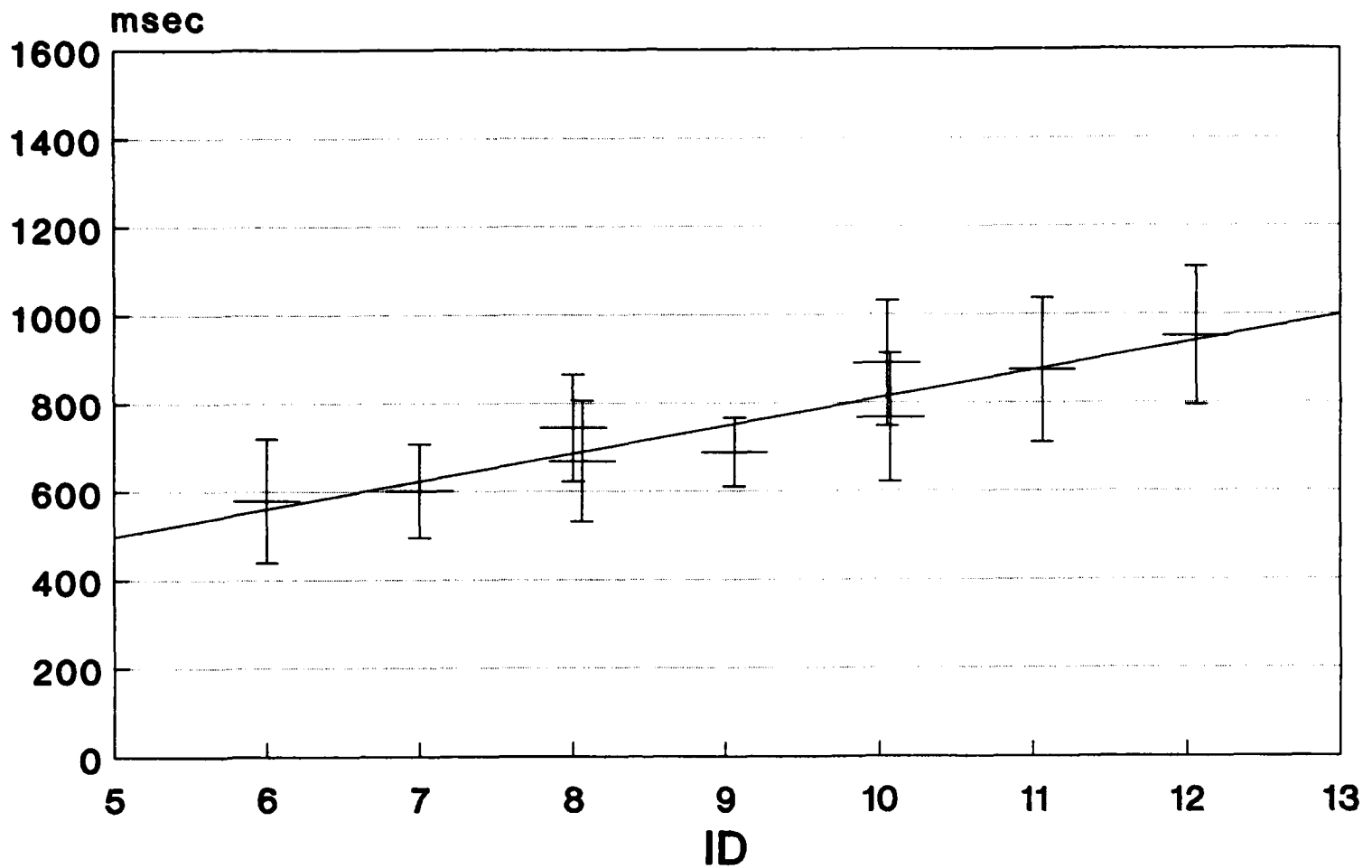

Subject 5 Unencumbered
All Data Points

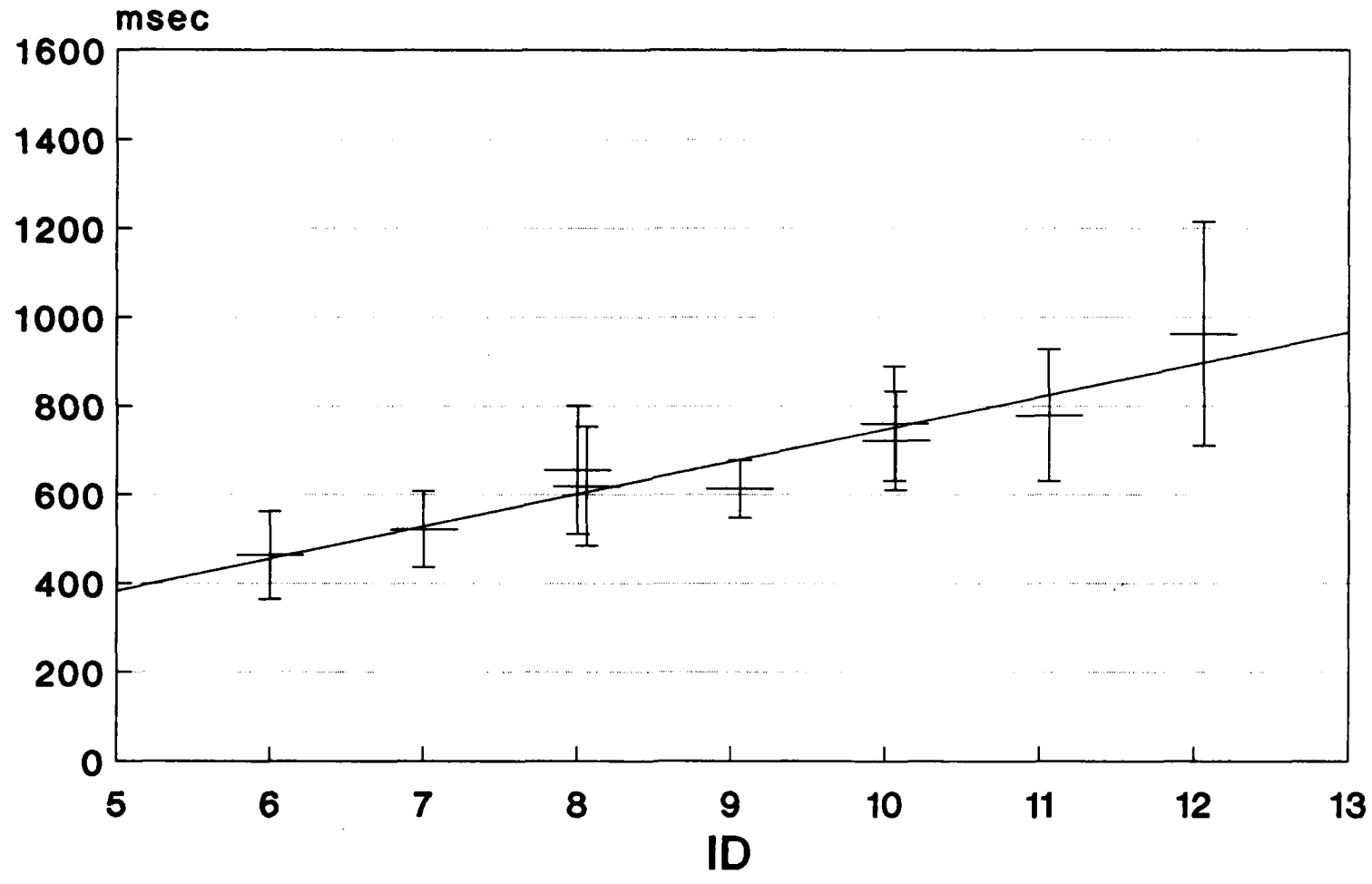

Subject 6 Unencumbered
All Data Points

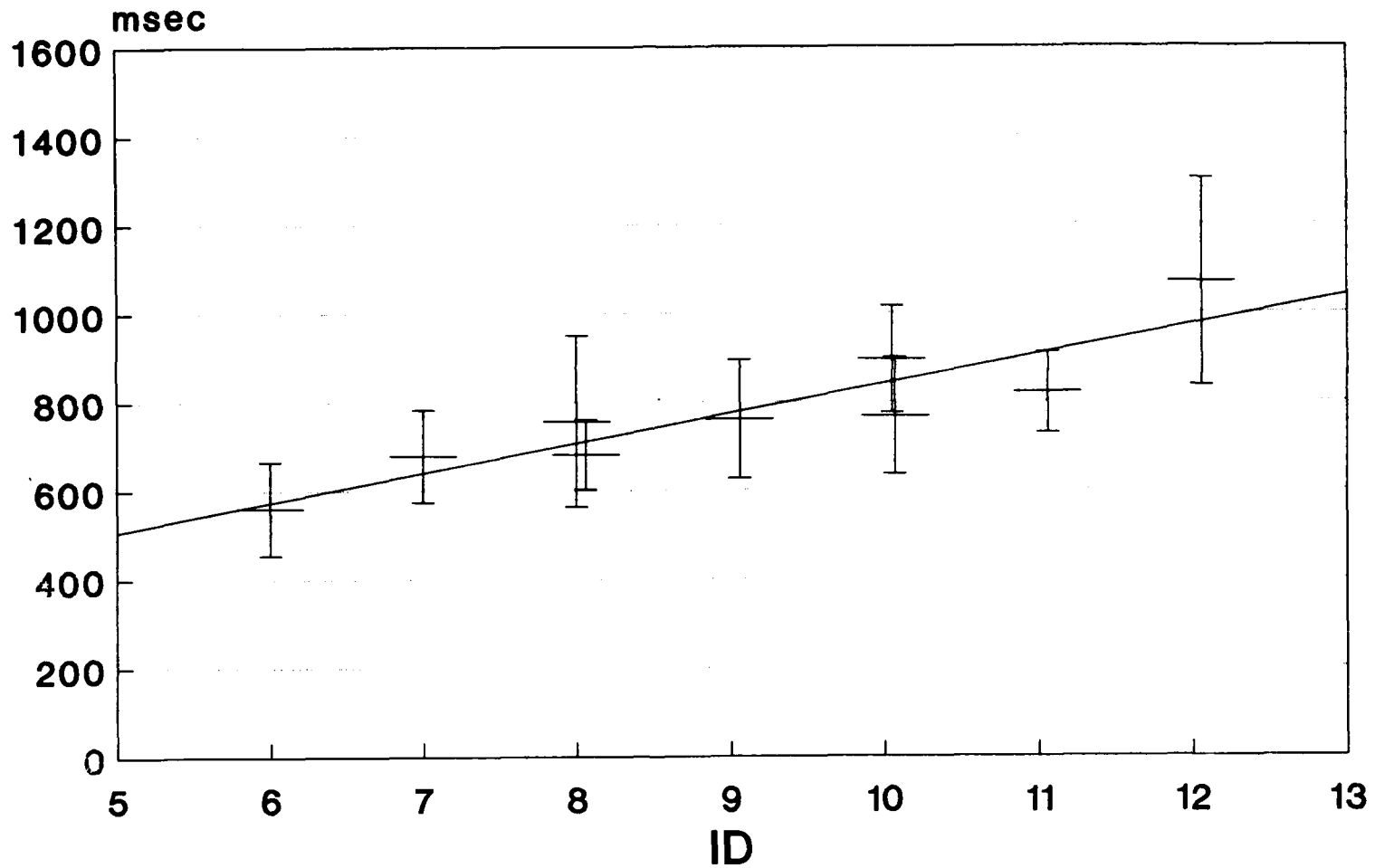

Subject 7 Unencumbered
All Data Points

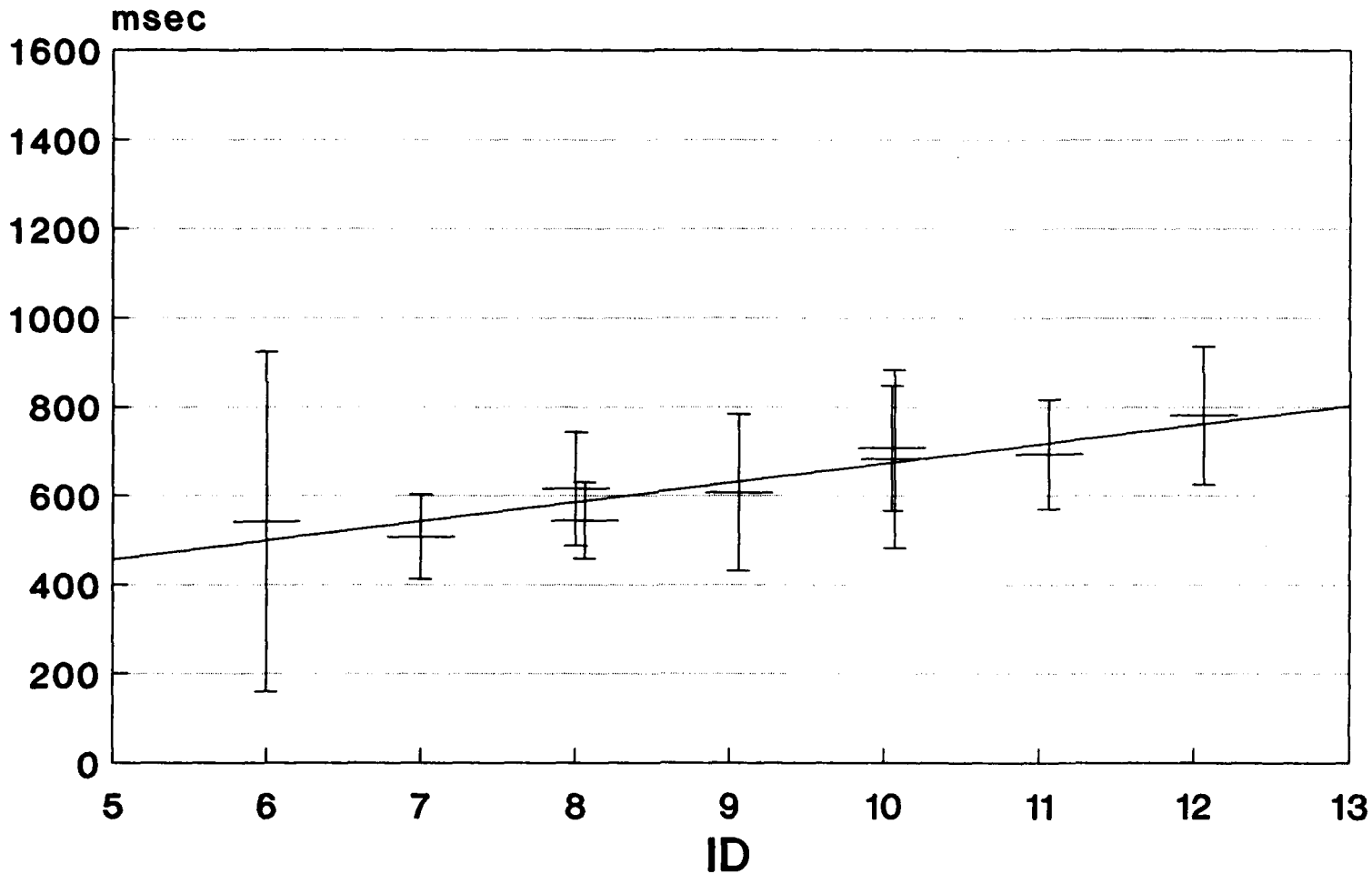

Appendix C

Unencumbered *mt vs. ID*, Excluding Nonlinear Data Points

Subject 1 Unencumbered

Linear Data Points

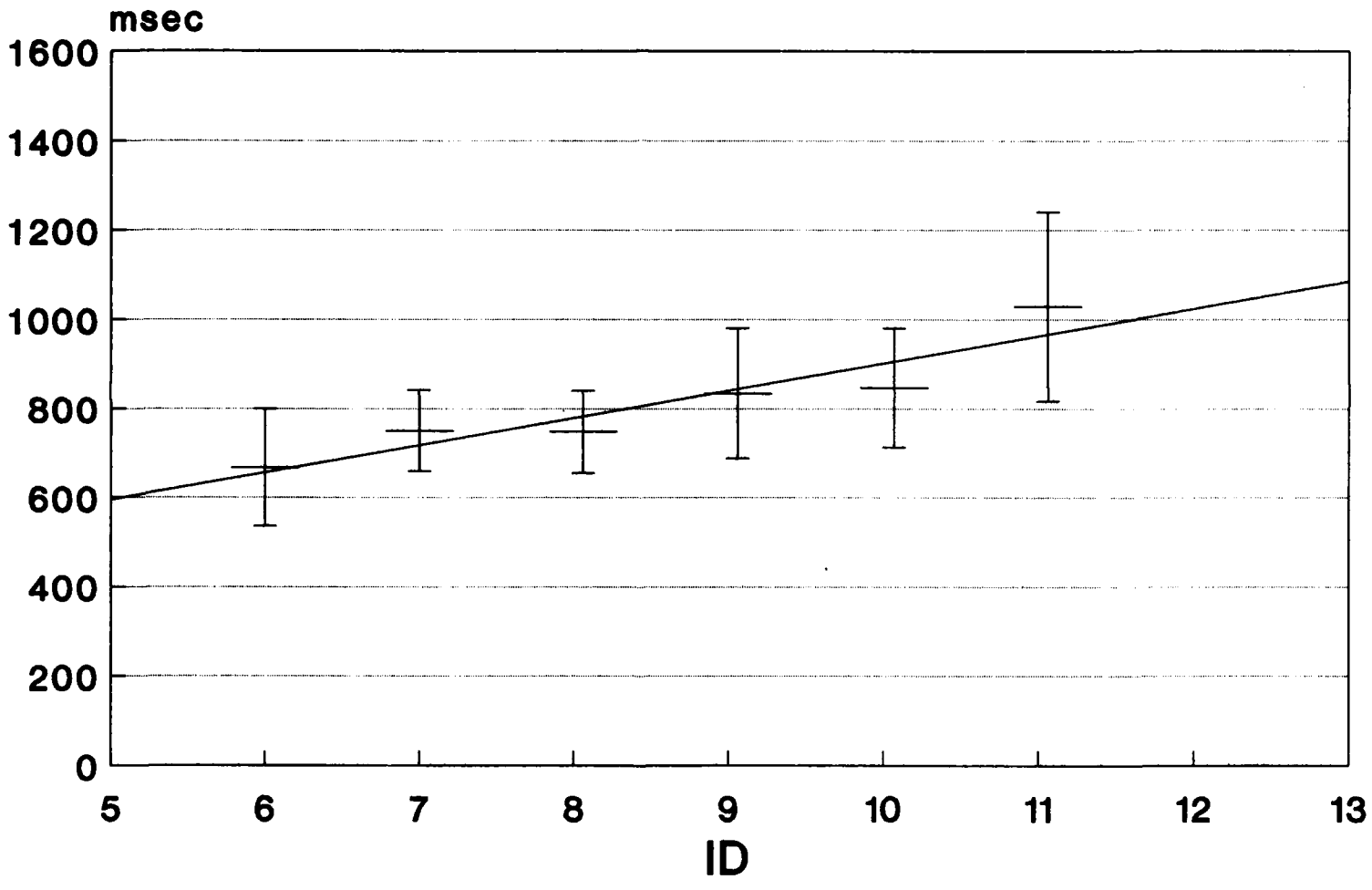

Subject 2 Unencumbered
Linear Data Points

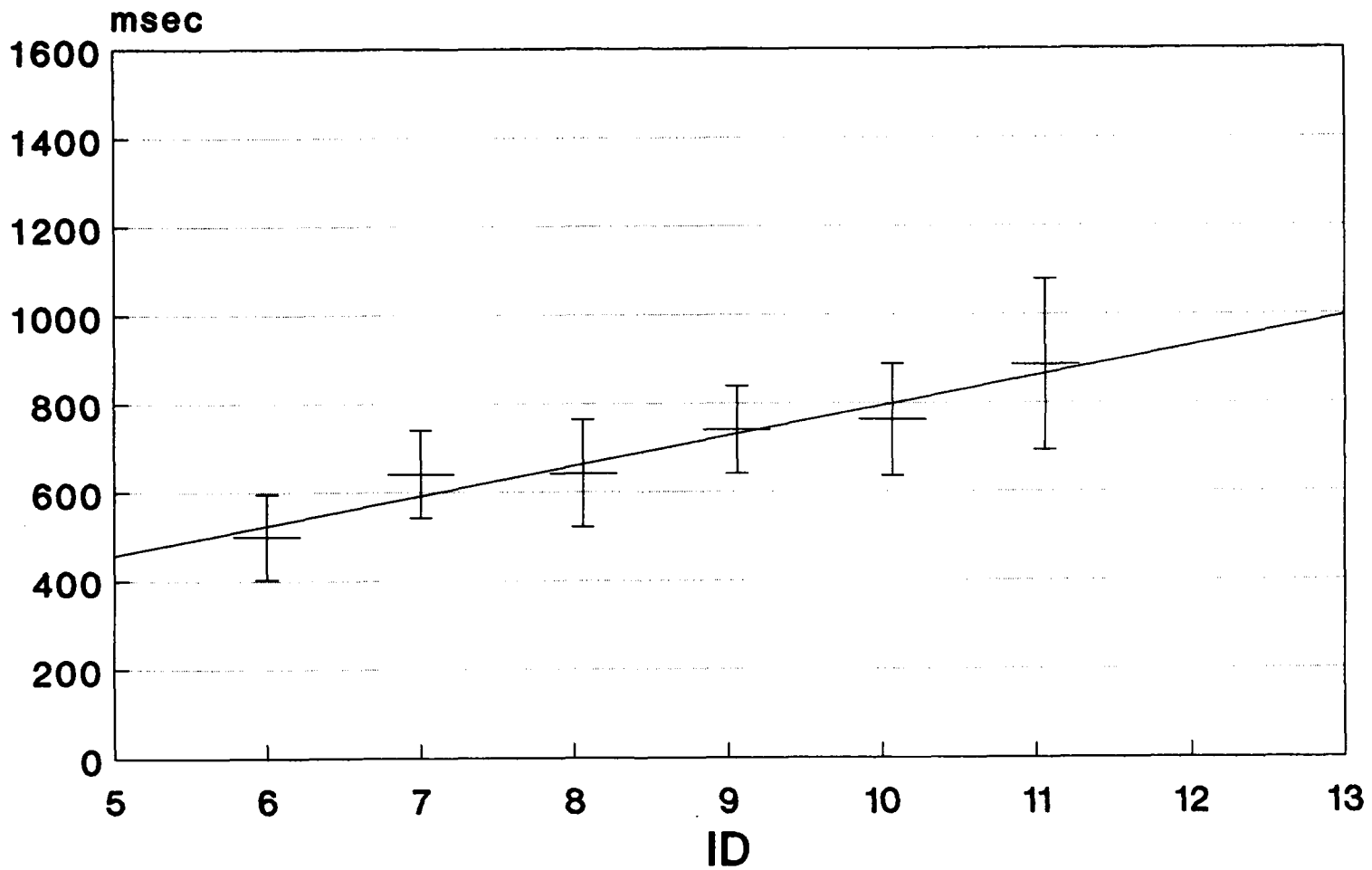

Subject 3 Unencumbered
Linear Data Points

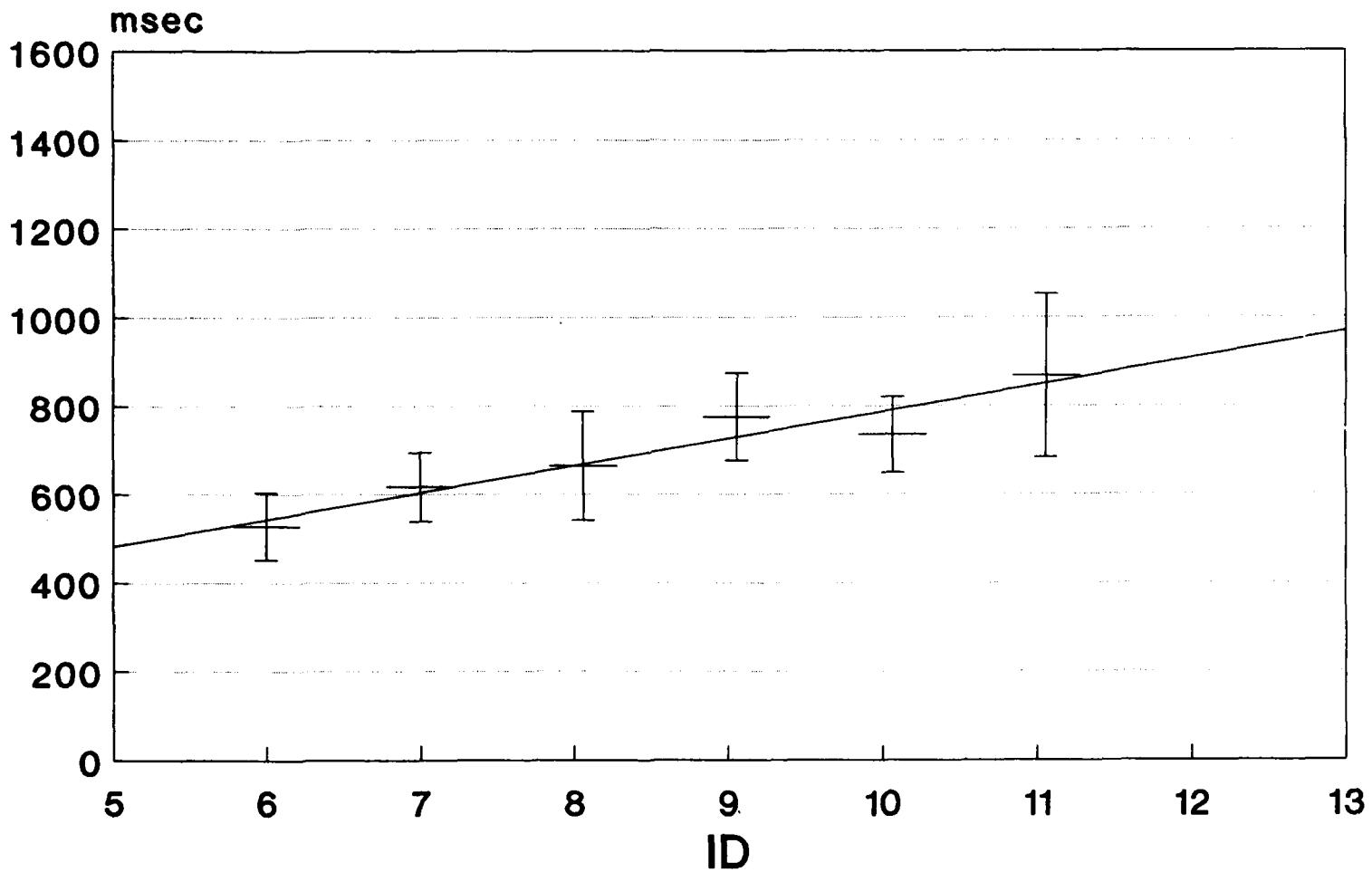

Subject 4 Unencumbered

Linear Data Points

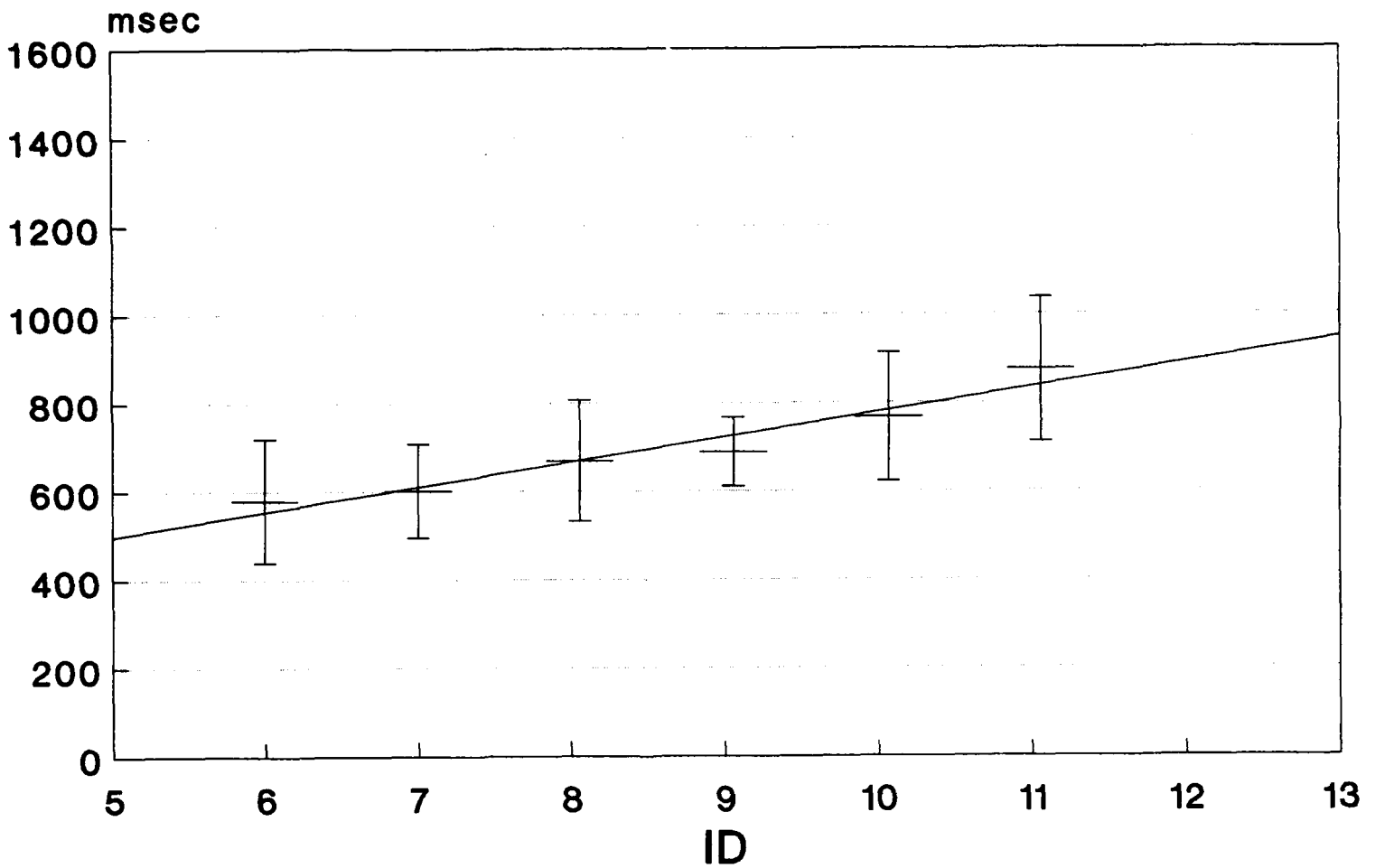

Subject 5 Unencumbered
Linear Data Points

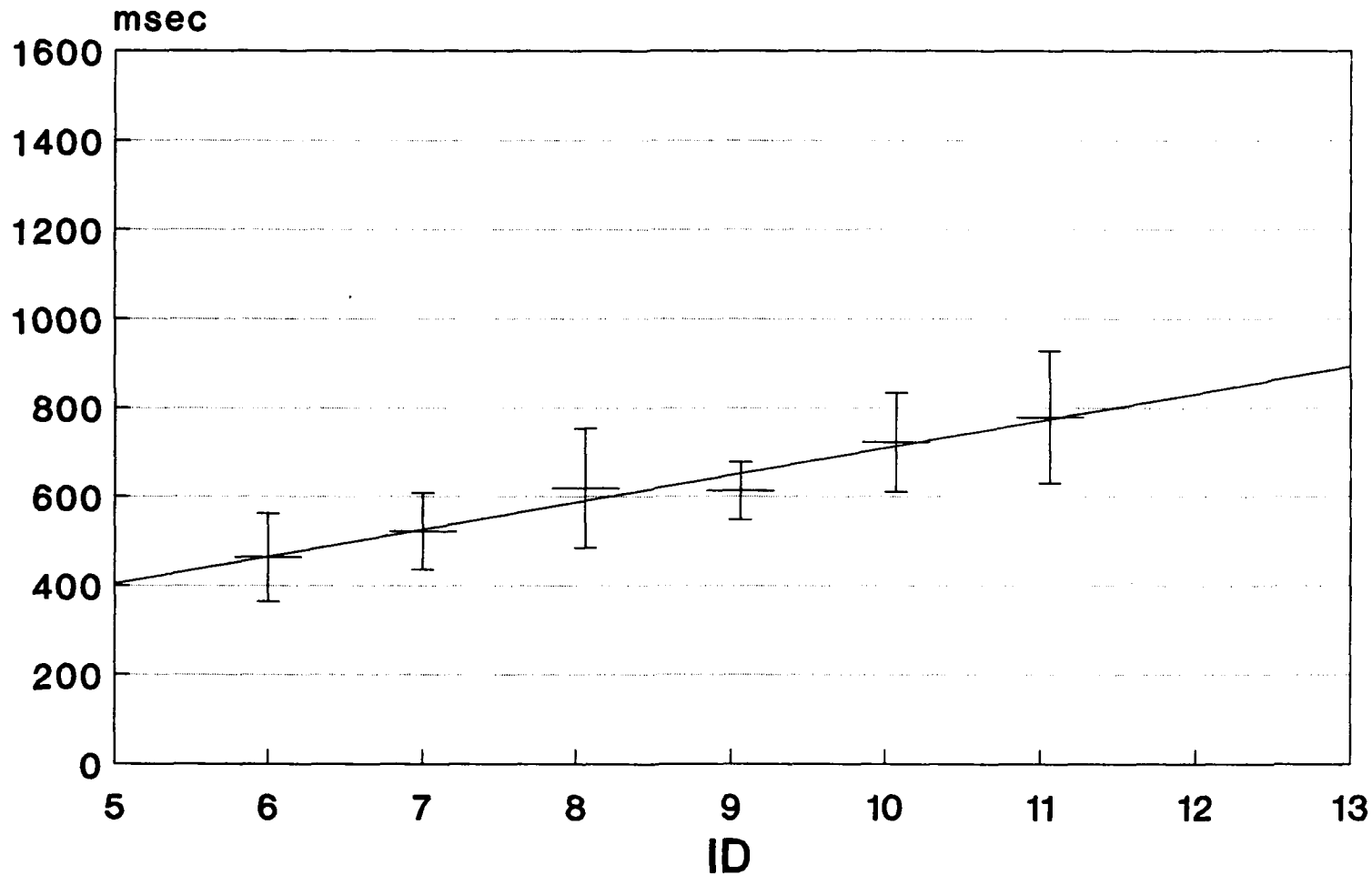

Subject 6 Unencumbered
Linear Data Points

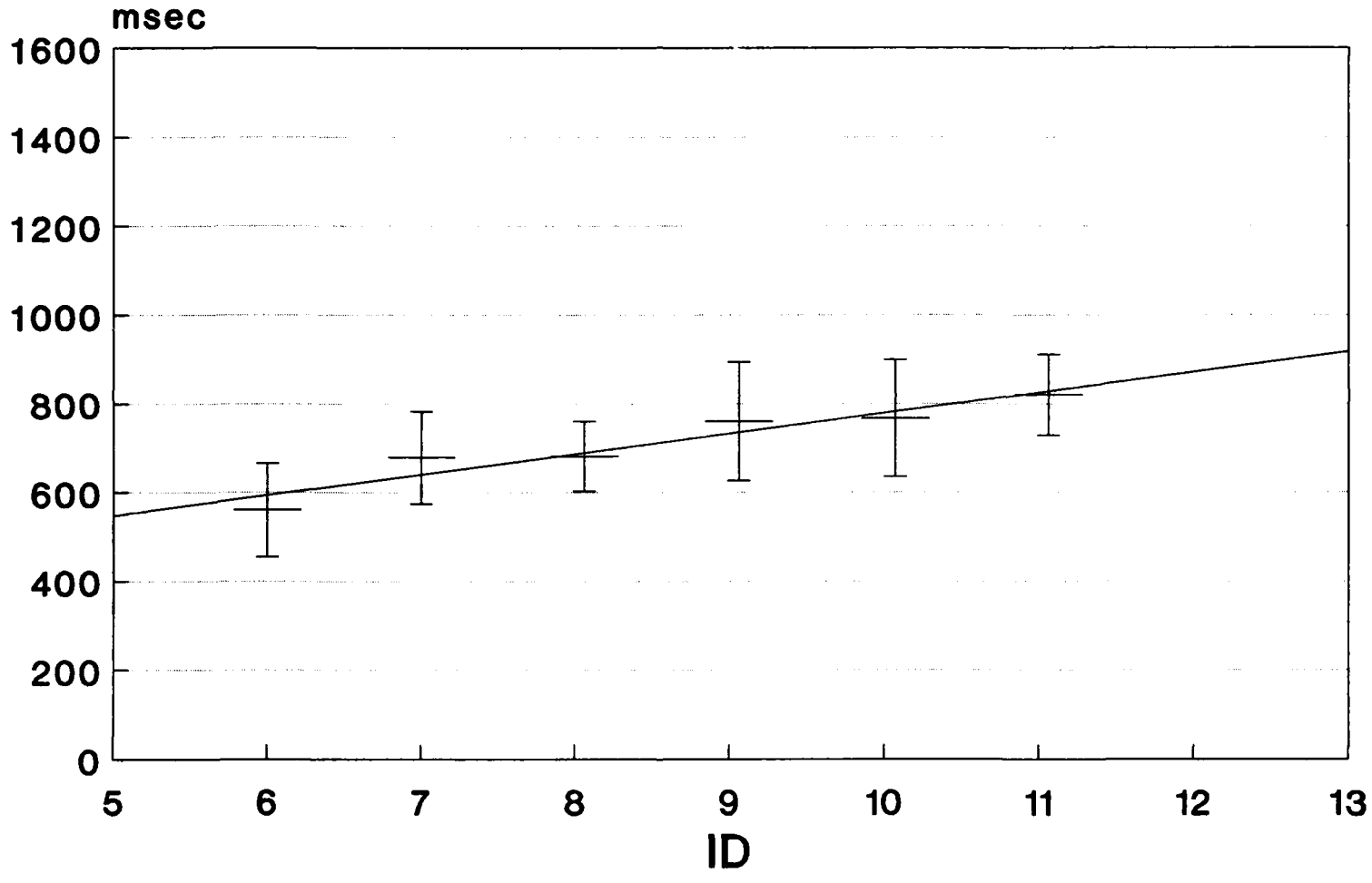

Subject 7 Unencumbered

Linear Data Points

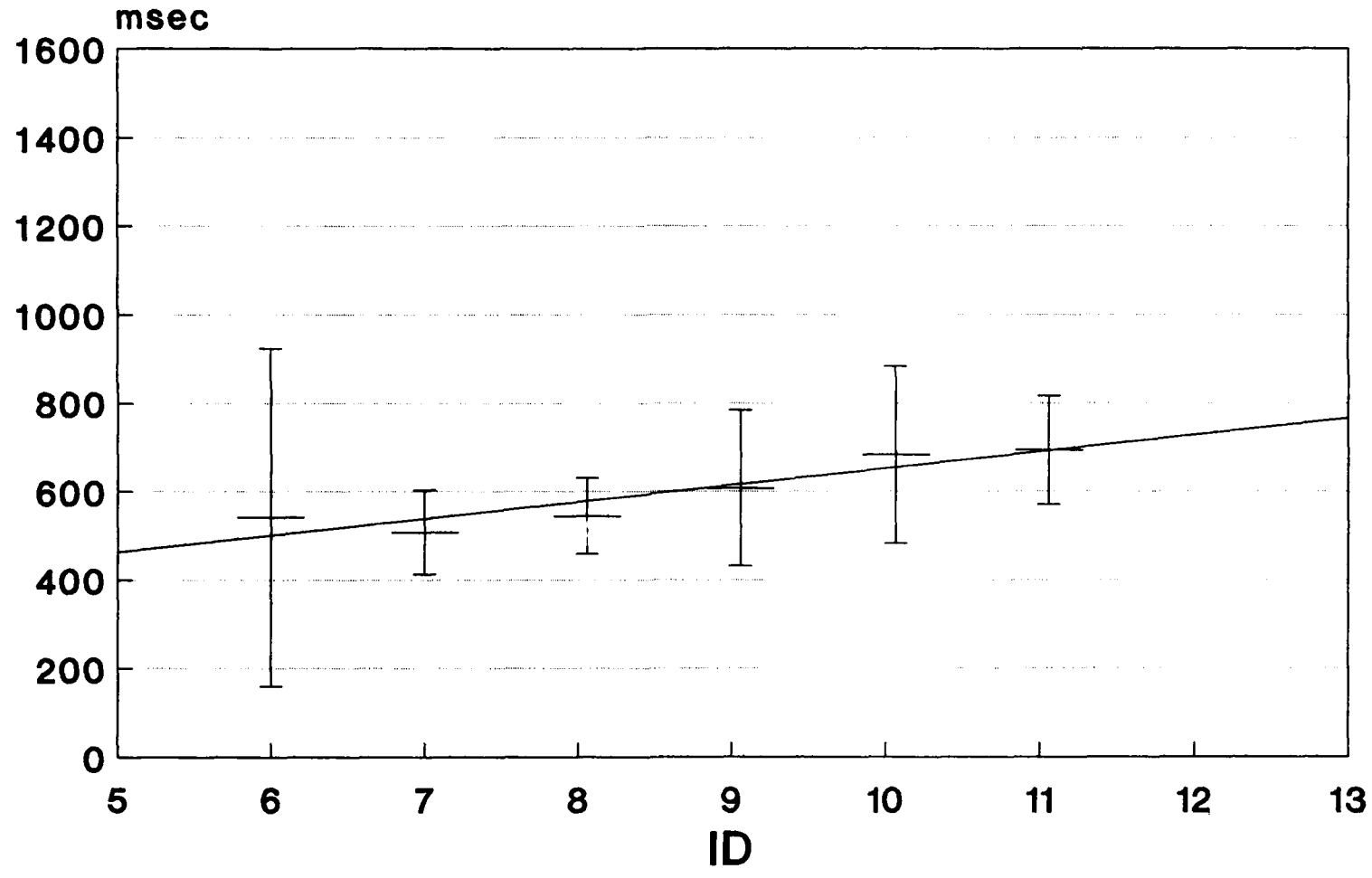

Appendix D

Unencumbered *mt vs.* ID Extrapolated to $ID = 0$

Subject 1 Unencumbered
Linear Data Points

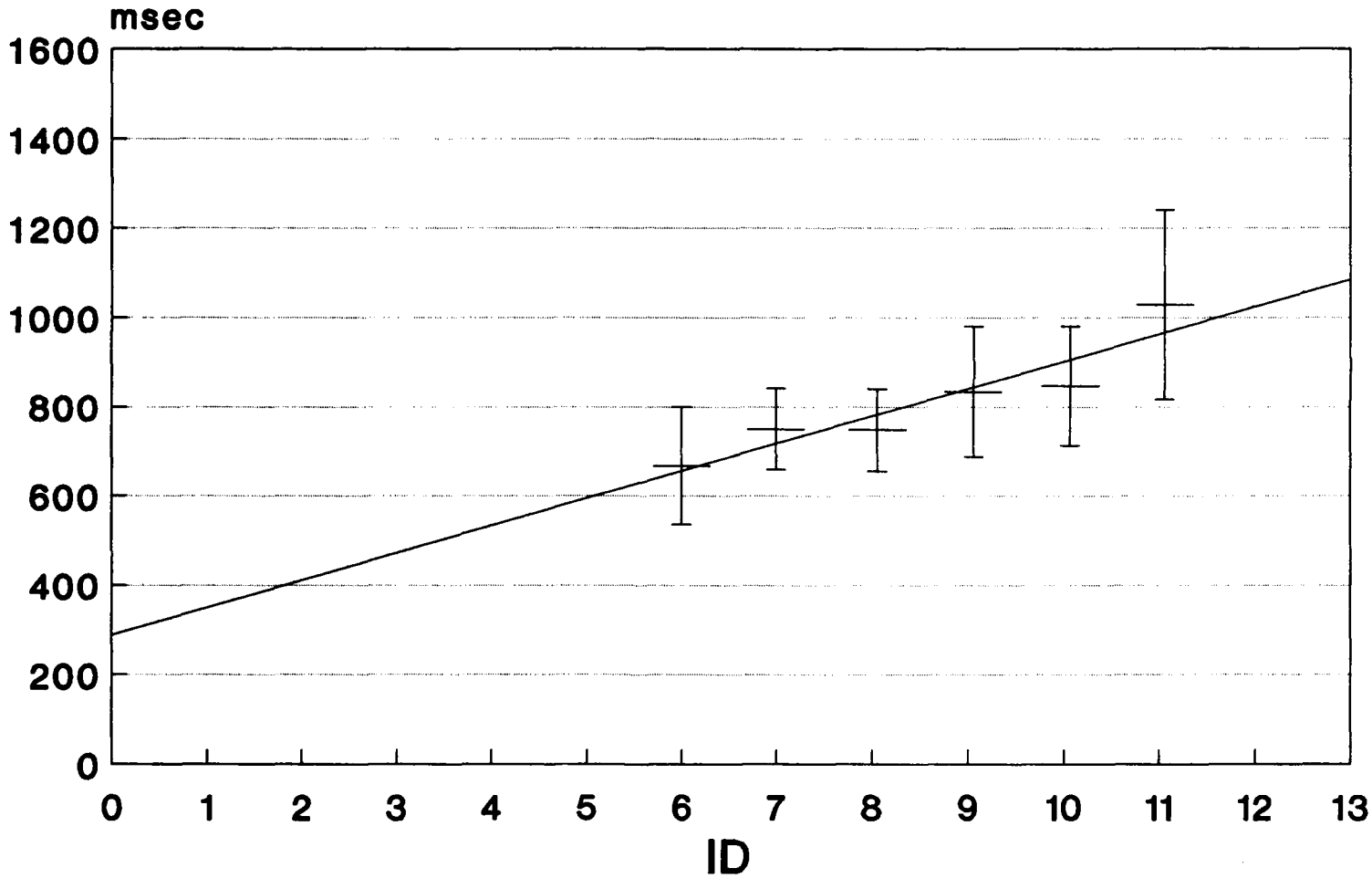

Subject 2 Unencumbered
Linear Data Points

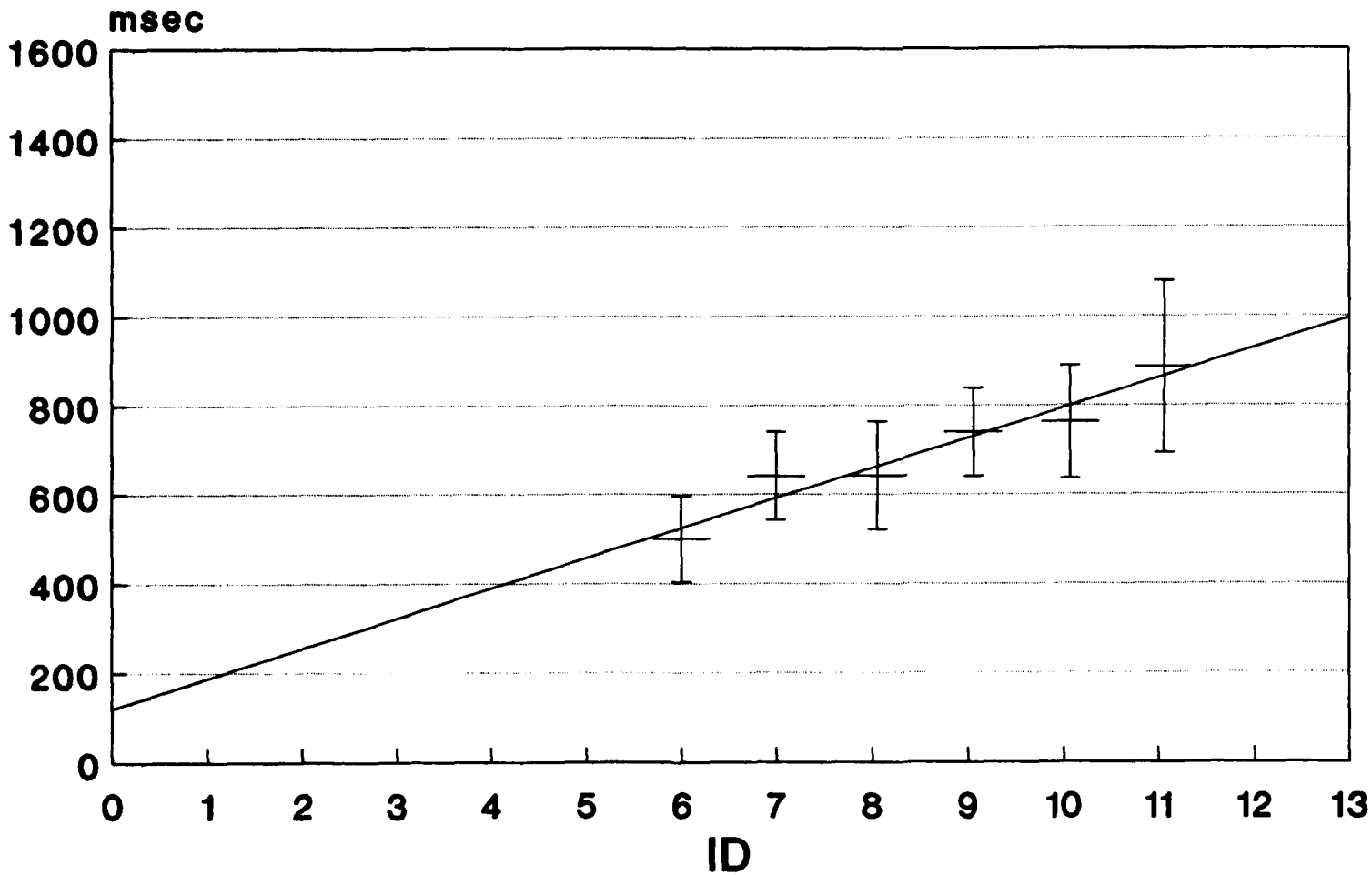

Subject 3 Unencumbered
Linear Data Points

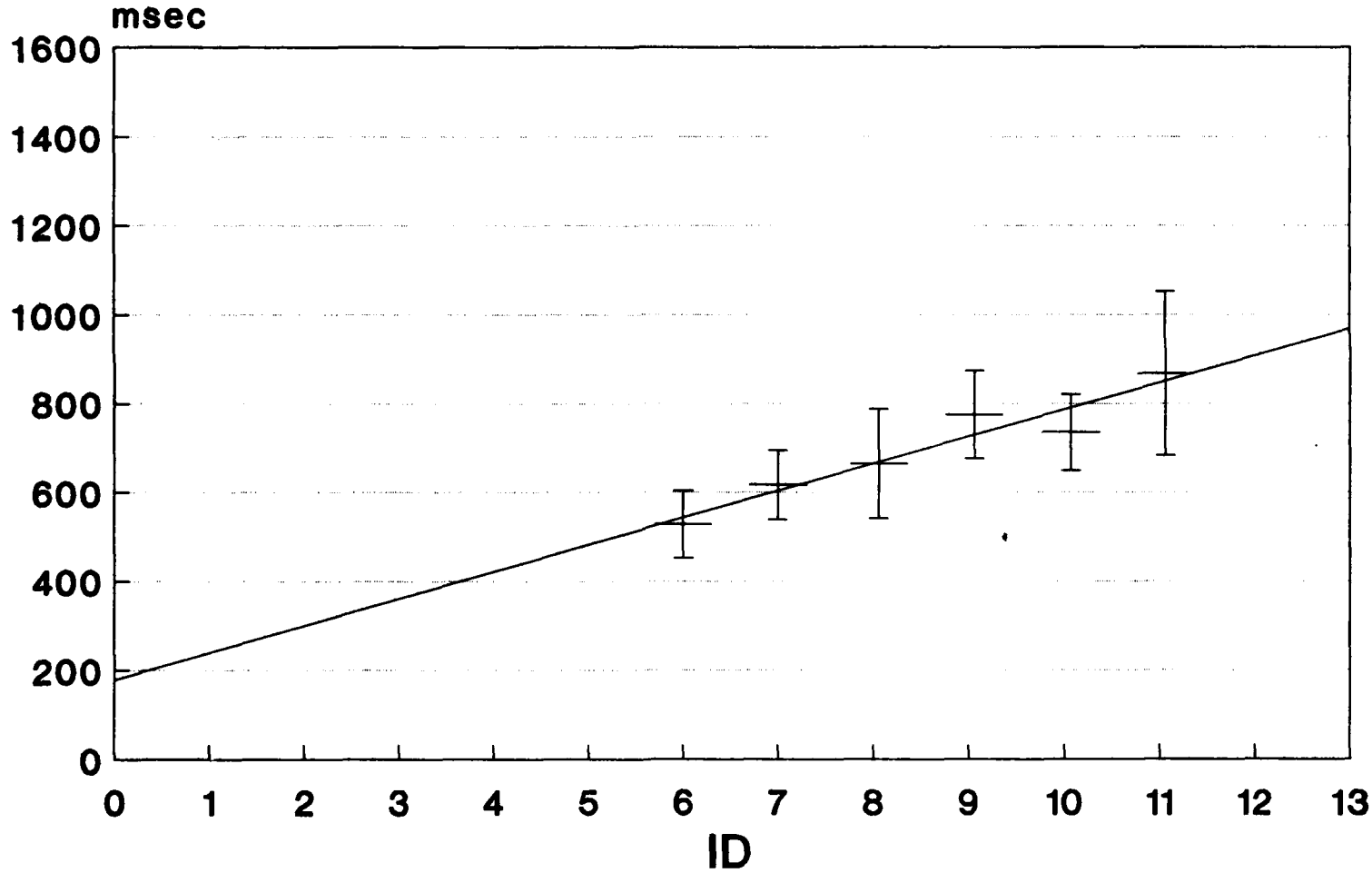

Subject 4 Unencumbered

Linear Data Points

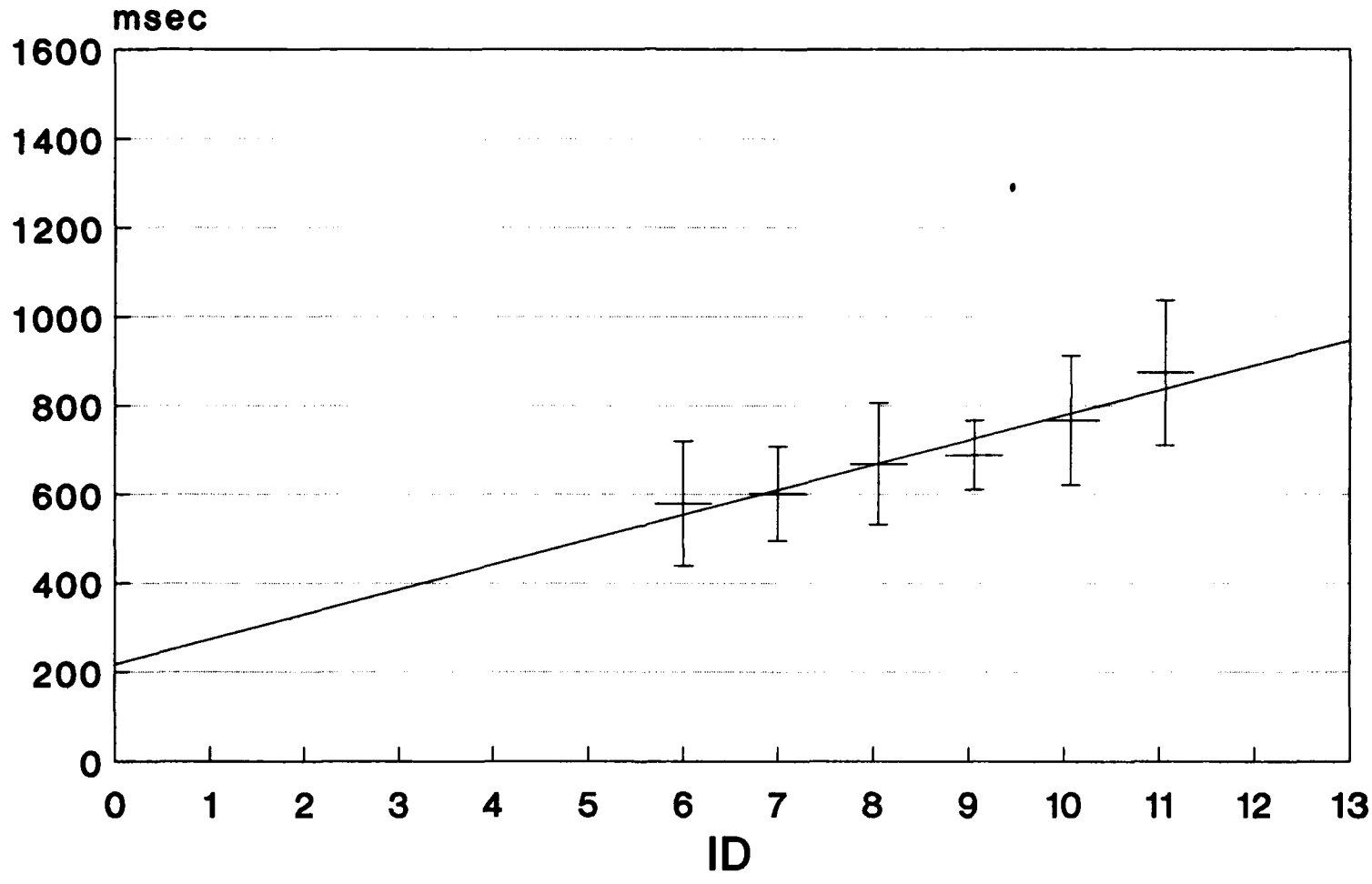

Subject 5 Unencumbered

Linear Data Points

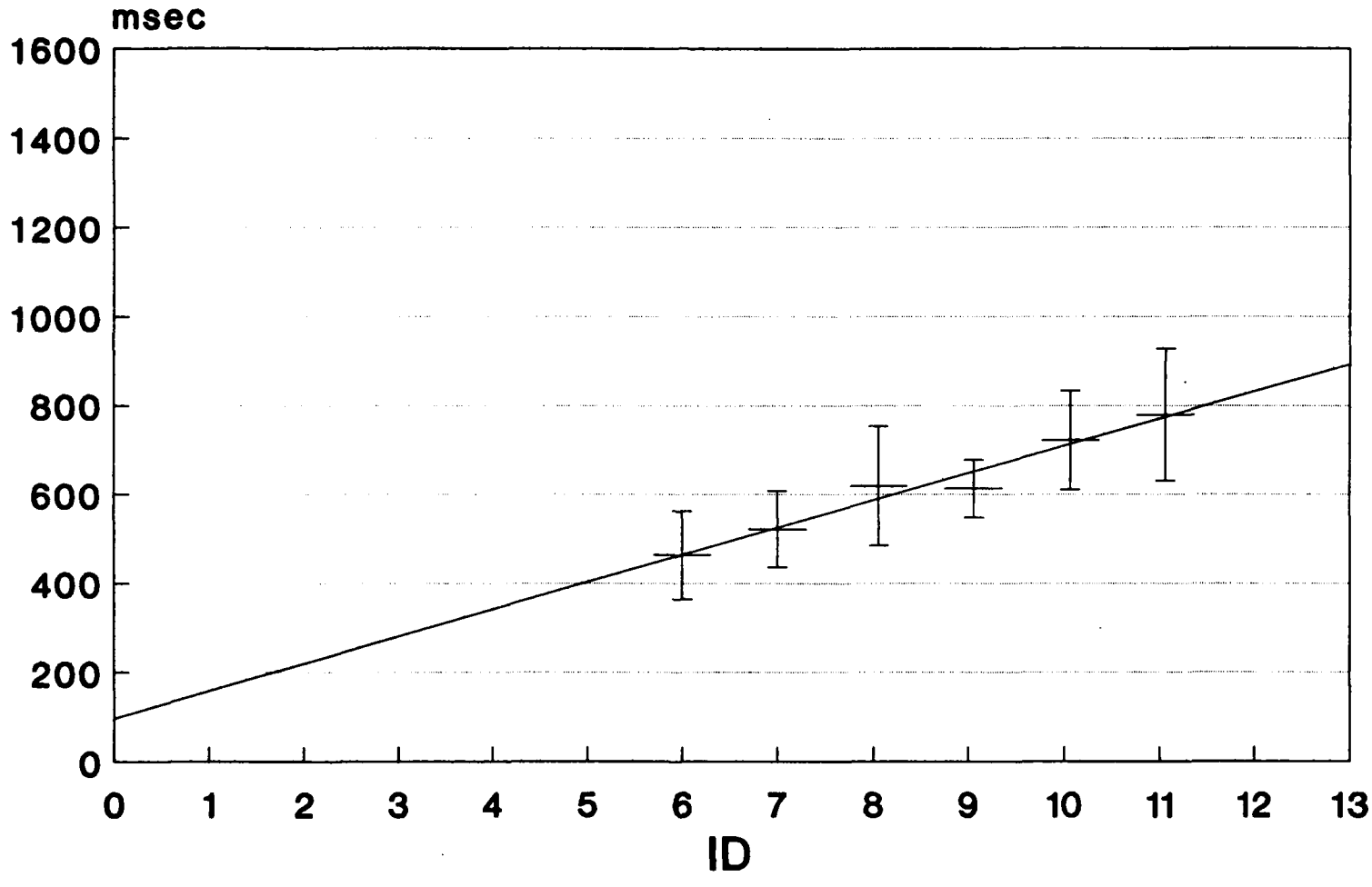

Subject 6 Unencumbered
Linear Data Points

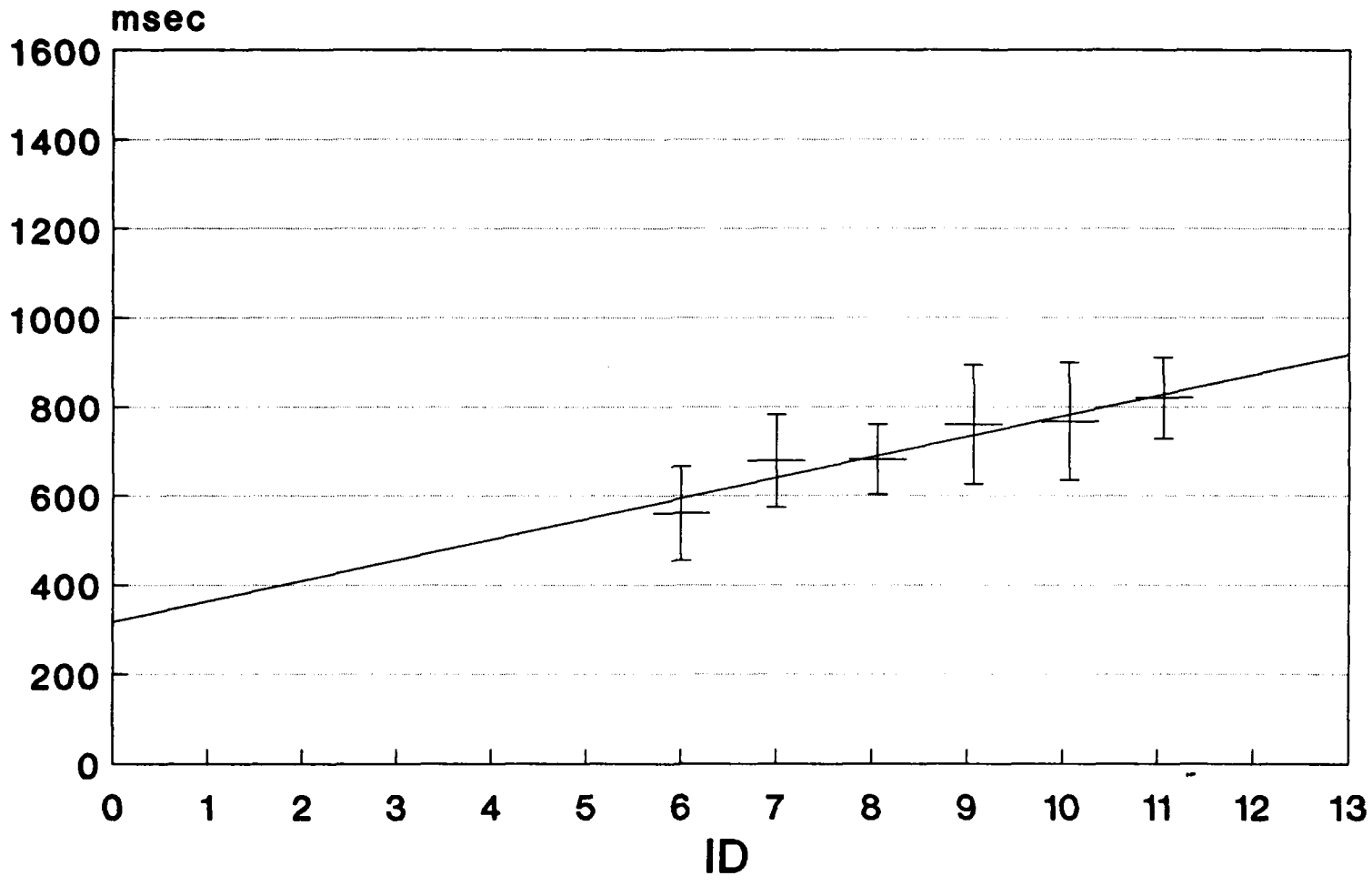

Subject 7 Unencumbered
Linear Data Points

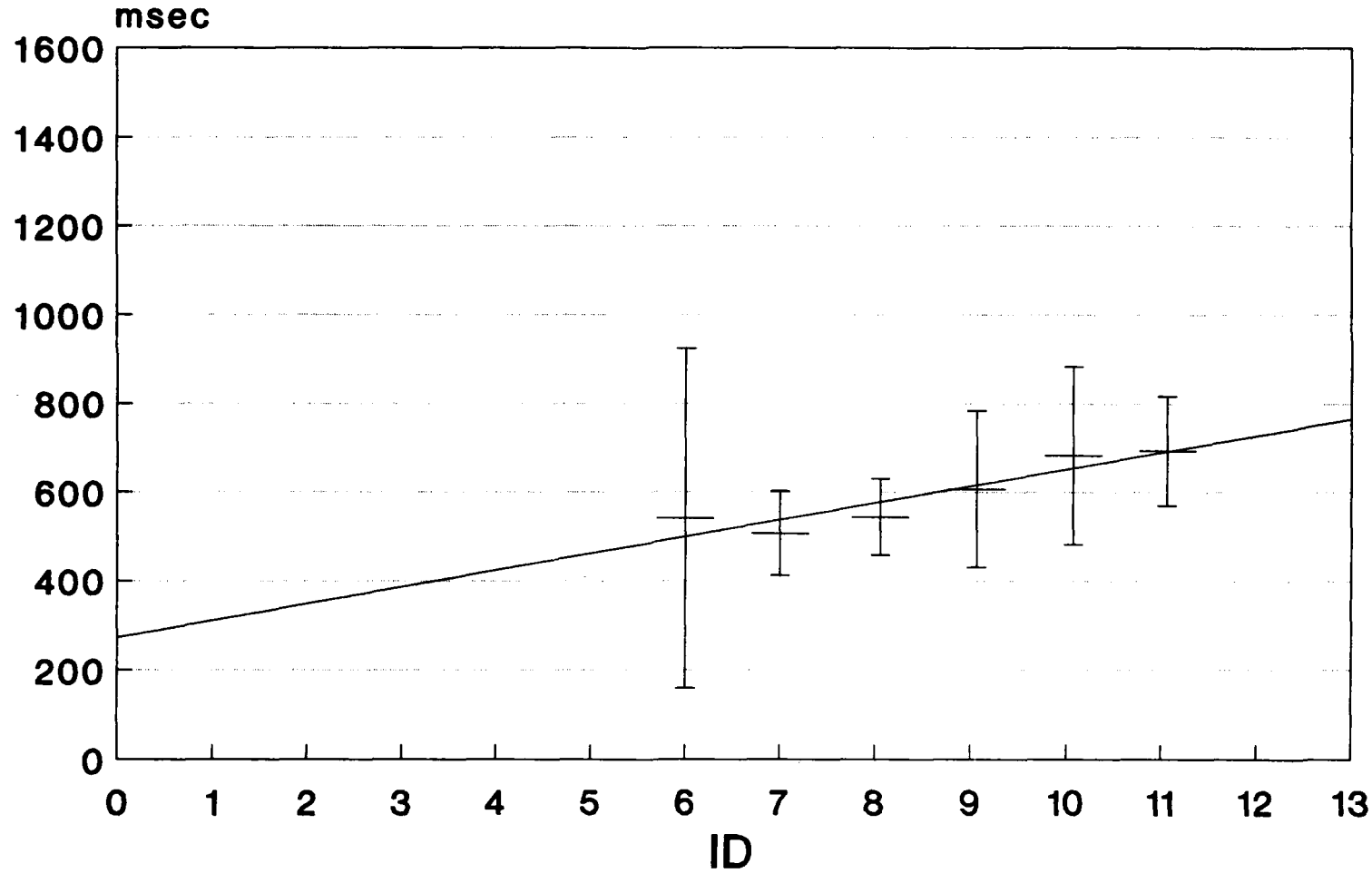

Appendix E

Raw Data Wearing MBA Exoskeleton Grouped by Task *ID*

Subject 1 - Wearing MBA Exoskeleton

Peg diameter (cm)	$\frac{W}{2}$ (cm)	A (cm)	ID $\frac{bits}{response}$	n	$\overline{mt}$ (msec)	σ (msec)
1.50	0.250	16	6.000	24	741.958	87.053
1.88	0.060	32	7.000	24	851.542	168.478
1.97	0.015	64	8.000	24	1129.833	321.515
1.50	0.250	16	8.006	24	924.250	175.081
1.88	0.060	32	9.006	24	999.833	156.009
1.97	0.015	64	10.006	24	1153.375	112.317
1.50	0.250	16	10.060	24	1009.125	125.178
1.88	0.060	32	11.060	24	1150.583	173.395
1.97	0.015	64	12.060	24	1438.750	266.706

Subject 2 - Wearing MBA Exoskeleton

Peg diameter (cm)	$\frac{W}{2}$ (cm)	A (cm)	ID $\frac{bits}{response}$	n	$\overline{mt}$ (msec)	σ (msec)
1.50	0.250	16	6.000	24	616.250	102.382
1.88	0.060	32	7.000	24	721.375	111.502
1.97	0.015	64	8.000	24	962.833	151.676
1.50	0.250	16	8.006	24	724.833	90.738
1.88	0.060	32	9.006	24	862.458	114.188
1.97	0.015	64	10.006	24	1067.583	164.955
1.50	0.250	16	10.060	24	897.333	147.651
1.88	0.060	32	11.060	24	1034.417	132.109
1.97	0.015	64	12.060	24	1259.750	235.352

Subject 3 - Wearing MBA Exoskeleton

Peg diameter (cm)	$\frac{W}{2}$ (cm)	A (cm)	ID $\frac{bits}{response}$	n	$\overline{mt}$ (msec)	σ (msec)
1.50	0.250	16	6.000	24	630.958	62.509
1.88	0.060	32	7.000	24	695.167	60.930
1.97	0.015	64	8.000	24	922.958	165.700
1.50	0.250	16	8.006	24	741.500	75.983
1.88	0.060	32	9.006	24	883.167	134.213
1.97	0.015	64	10.006	24	1050.208	127.230
1.50	0.250	16	10.060	24	928.708	154.933
1.88	0.060	32	11.060	24	978.917	125.329
1.97	0.015	64	12.060	24	1230.875	135.345

Subject 4 - Wearing MBA Exoskeleton

Peg diameter (cm)	$\frac{W}{2}$ (cm)	A (cm)	ID $\frac{bits}{response}$	n	$\overline{mt}$ (msec)	σ (msec)
1.50	0.250	16	6.000	24	773.875	177.820
1.88	0.060	32	7.000	24	769.875	122.446
1.97	0.015	64	8.000	24	870.125	96.008
1.50	0.250	16	8.006	24	847.792	147.792
1.88	0.060	32	9.006	24	955.500	220.640
1.97	0.015	64	10.006	24	1114.083	227.601
1.50	0.250	16	10.060	24	1042.042	247.264
1.88	0.060	32	11.060	24	1039.208	183.573
1.97	0.015	64	12.060	24	1199.250	184.737

Subject 5 - Wearing MBA Exoskeleton

Peg diameter (cm)	$\frac{W}{2}$ (cm)	A (cm)	ID $\frac{bits}{response}$	n	$\overline{mt}$ (msec)	σ (msec)
1.50	0.250	16	6.000	24	563.667	107.866
1.88	0.060	32	7.000	24	620.208	116.553
1.97	0.015	64	8.000	24	724.000	67.978
1.50	0.250	16	8.006	24	723.667	217.256
1.88	0.060	32	9.006	24	795.500	163.808
1.97	0.015	64	10.006	24	911.583	95.760
1.50	0.250	16	10.060	24	838.917	137.780
1.88	0.060	32	11.060	24	859.167	121.557
1.97	0.015	64	12.060	24	1101.375	182.706

Subject 6 - Wearing MBA Exoskeleton

Peg diameter (cm)	$\frac{W}{2}$ (cm)	A (cm)	ID $\frac{bits}{response}$	n	$\overline{mt}$ (msec)	σ (msec)
1.50	0.250	16	6.000	24	758.417	118.031
1.88	0.060	32	7.000	24	880.333	164.181
1.97	0.015	64	8.000	24	1090.333	233.457
1.50	0.250	16	8.006	24	890.958	233.213
1.88	0.060	32	9.006	24	1023.625	254.442
1.97	0.015	64	10.006	24	1195.958	231.045
1.50	0.250	16	10.060	24	1154.708	335.473
1.88	0.060	32	11.060	24	1269.333	565.412
1.97	0.015	64	12.060	24	1482.042	410.447

Subject 7 - Wearing MBA Exoskeleton

Peg diameter (cm)	$\frac{W}{2}$ (cm)	A (cm)	ID $\frac{bits}{response}$	n	$\overline{mt}$ (msec)	σ (msec)
1.50	0.250	16	6.000	24	498.833	120.133
1.88	0.060	32	7.000	24	592.083	100.542
1.97	0.015	64	8.000	24	808.958	167.076
1.50	0.250	16	8.006	24	675.042	191.861
1.88	0.060	32	9.006	24	827.875	172.390
1.97	0.015	64	10.006	24	951.875	153.700
1.50	0.250	16	10.060	24	821.542	155.990
1.88	0.060	32	11.060	24	970.333	144.413
1.97	0.015	64	12.060	24	1190.708	217.713

Appendix F

nst vs. ID Wearing MBA Exoskeleton for All Tasks

Subject 1 w/ Exoskeleton

All Data Points

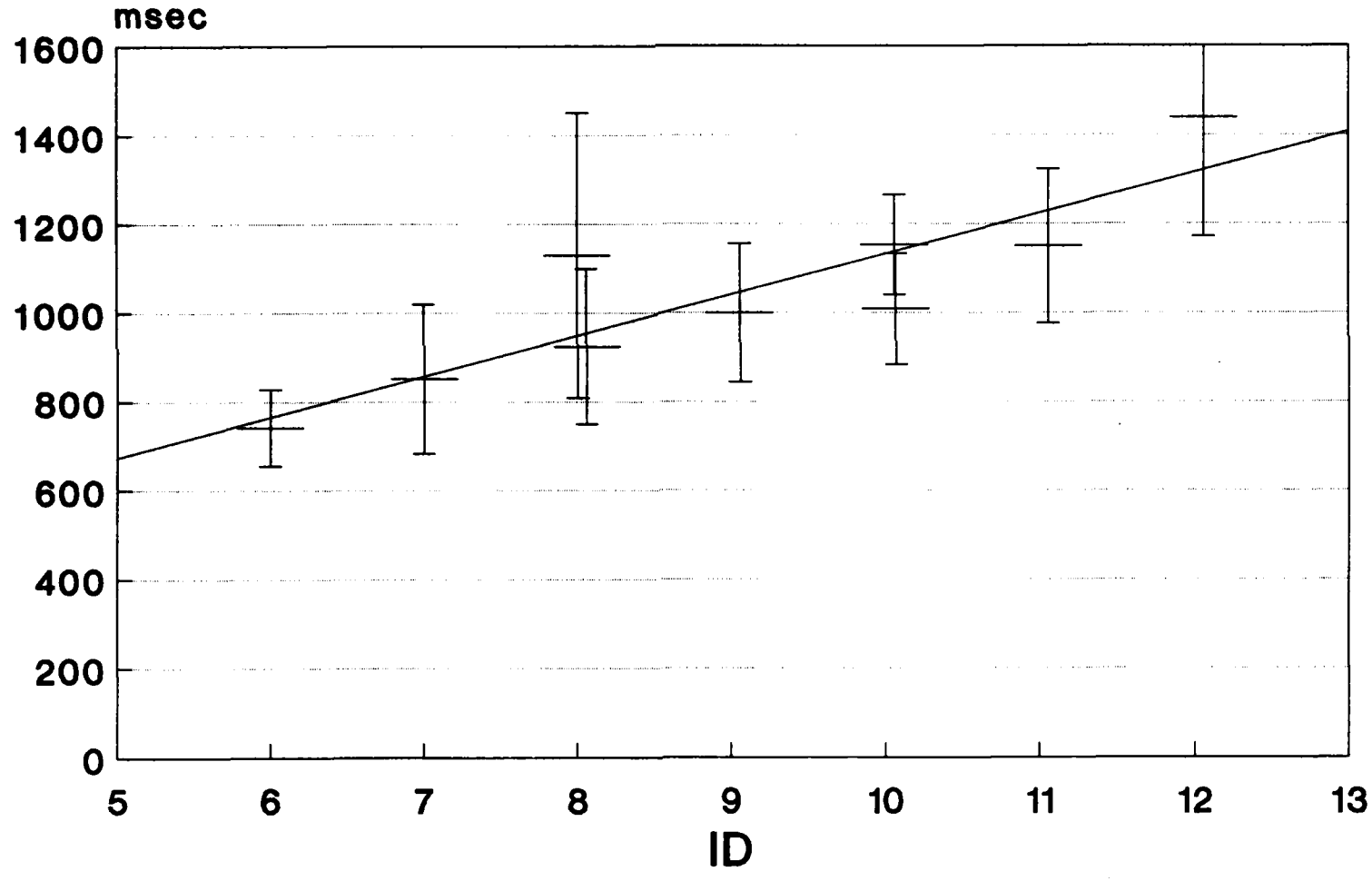

Subject 2 w/ Exoskeleton

All Data Points

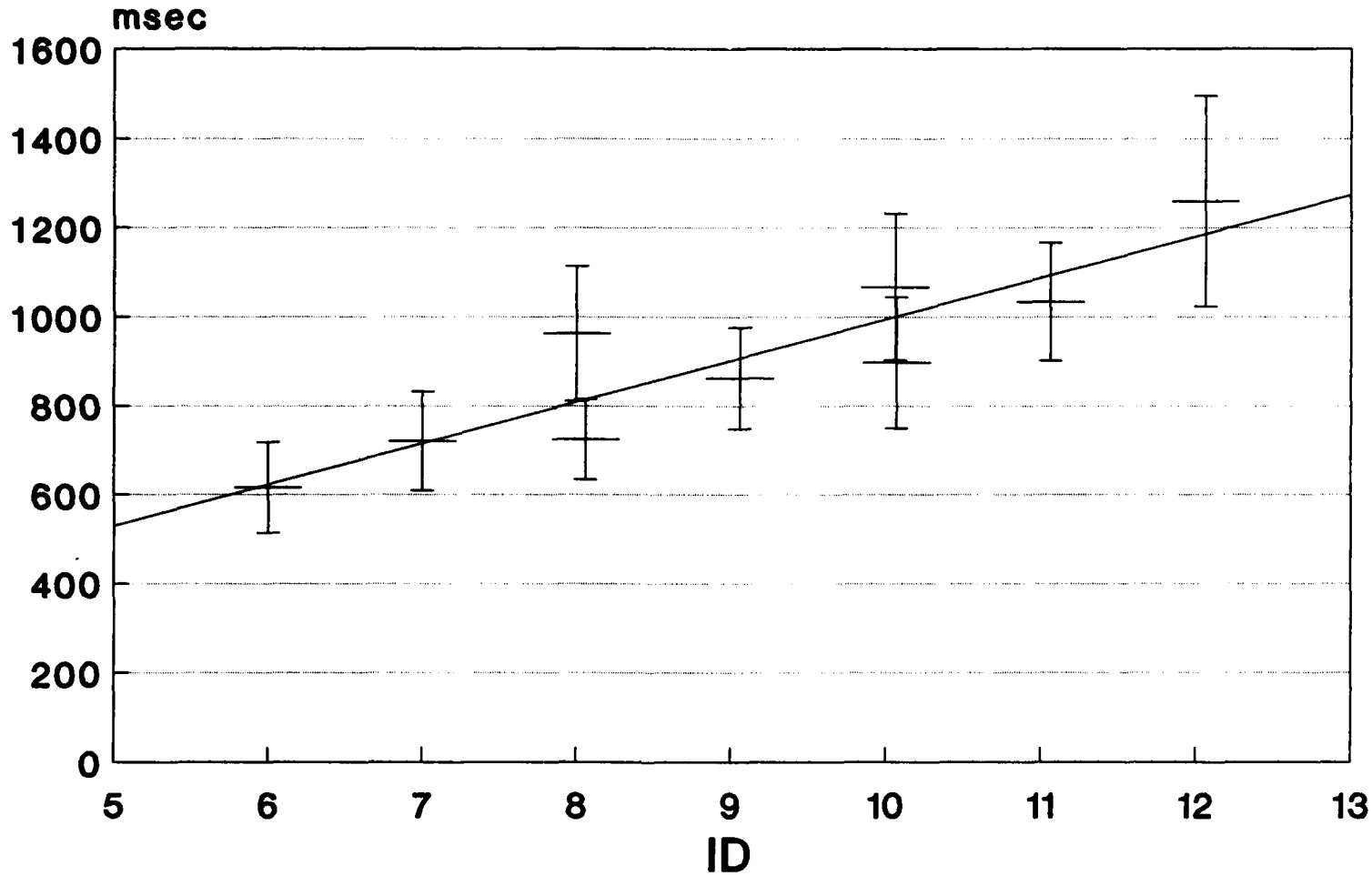

Subject 3 w/ Exoskeleton

All Data Points

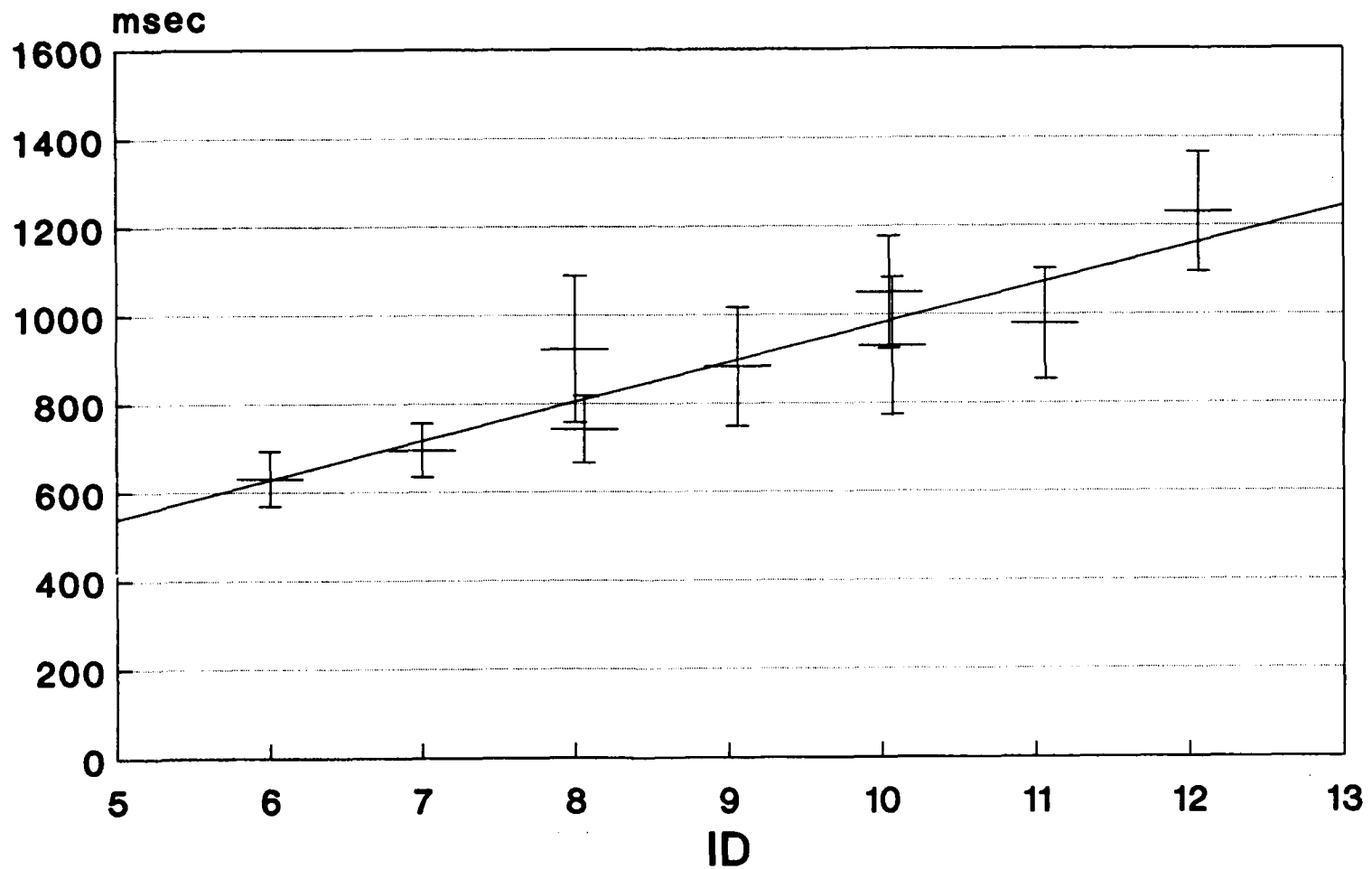

Subject 4 w/ Exoskeleton

All Data Points

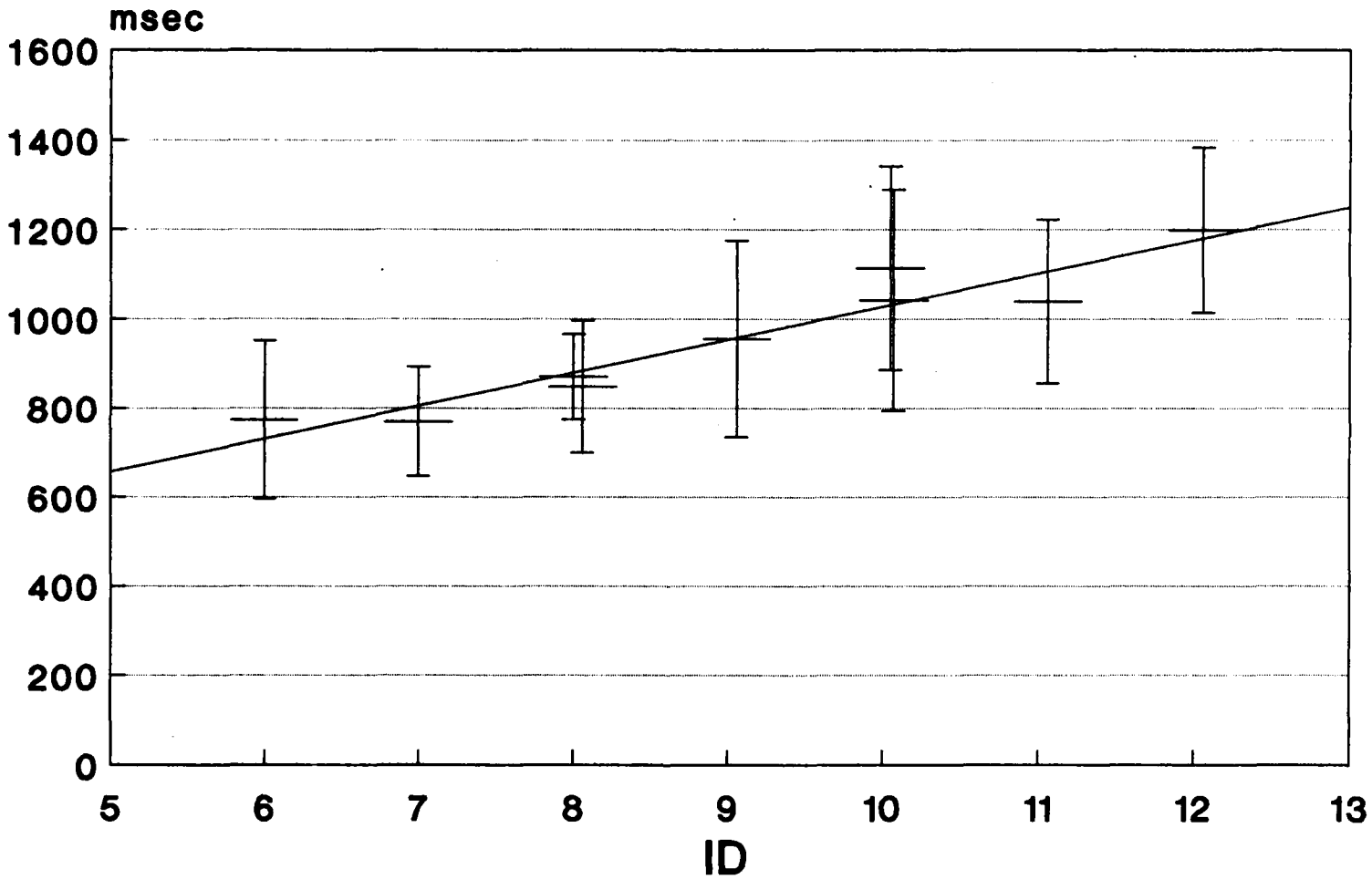

Subject 5 w/ Exoskeleton

All Data Points

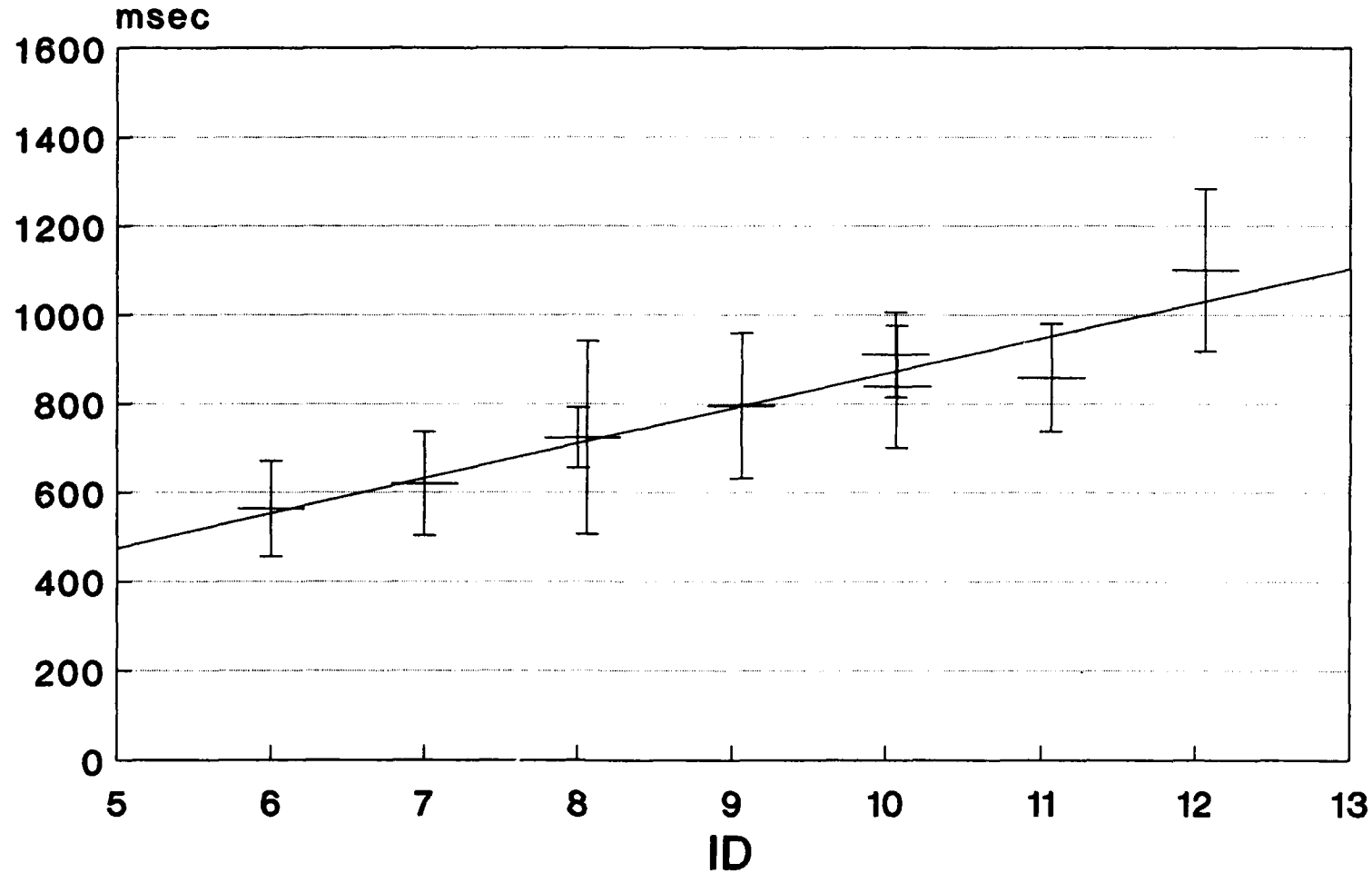

Subject 6 w/ Exoskeleton

All Data Points

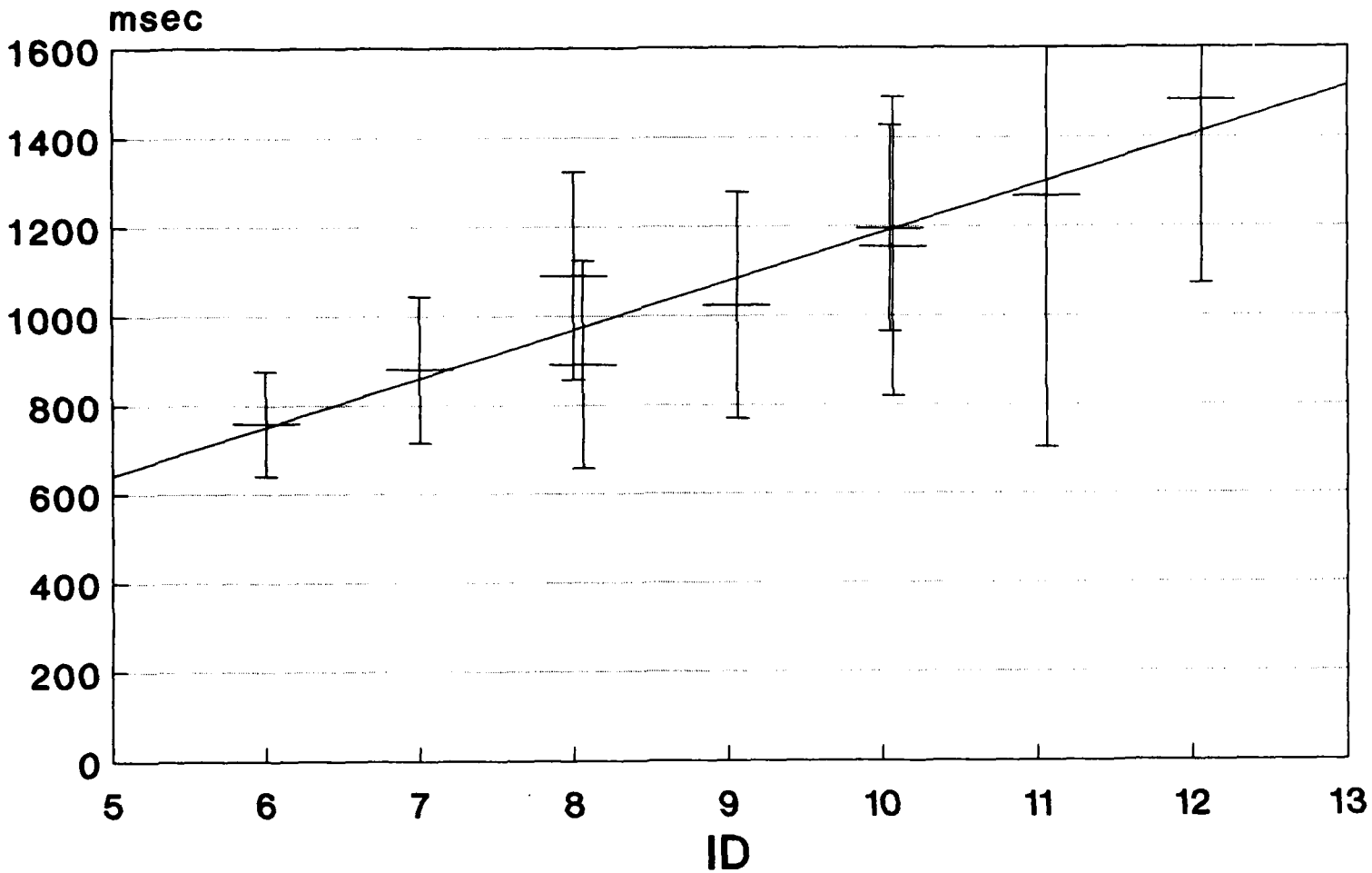

Subject 7 w/ Exoskeleton

All Data Points

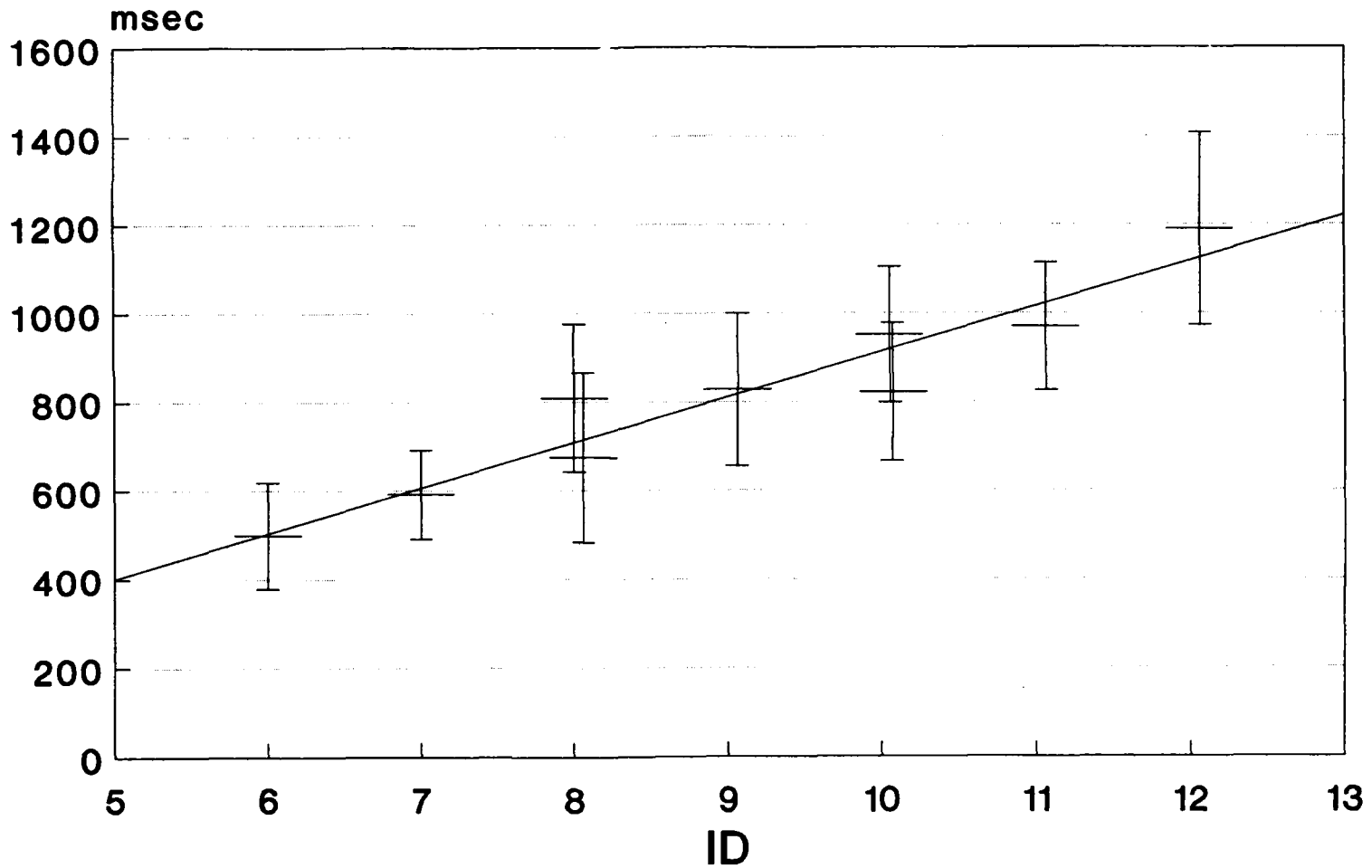

Appendix G

mt vs. ID Wearing MBA Exoskeleton, Excluding Nonlinear Data Points

Subject 1 w/ Exoskeleton

Linear Data Points

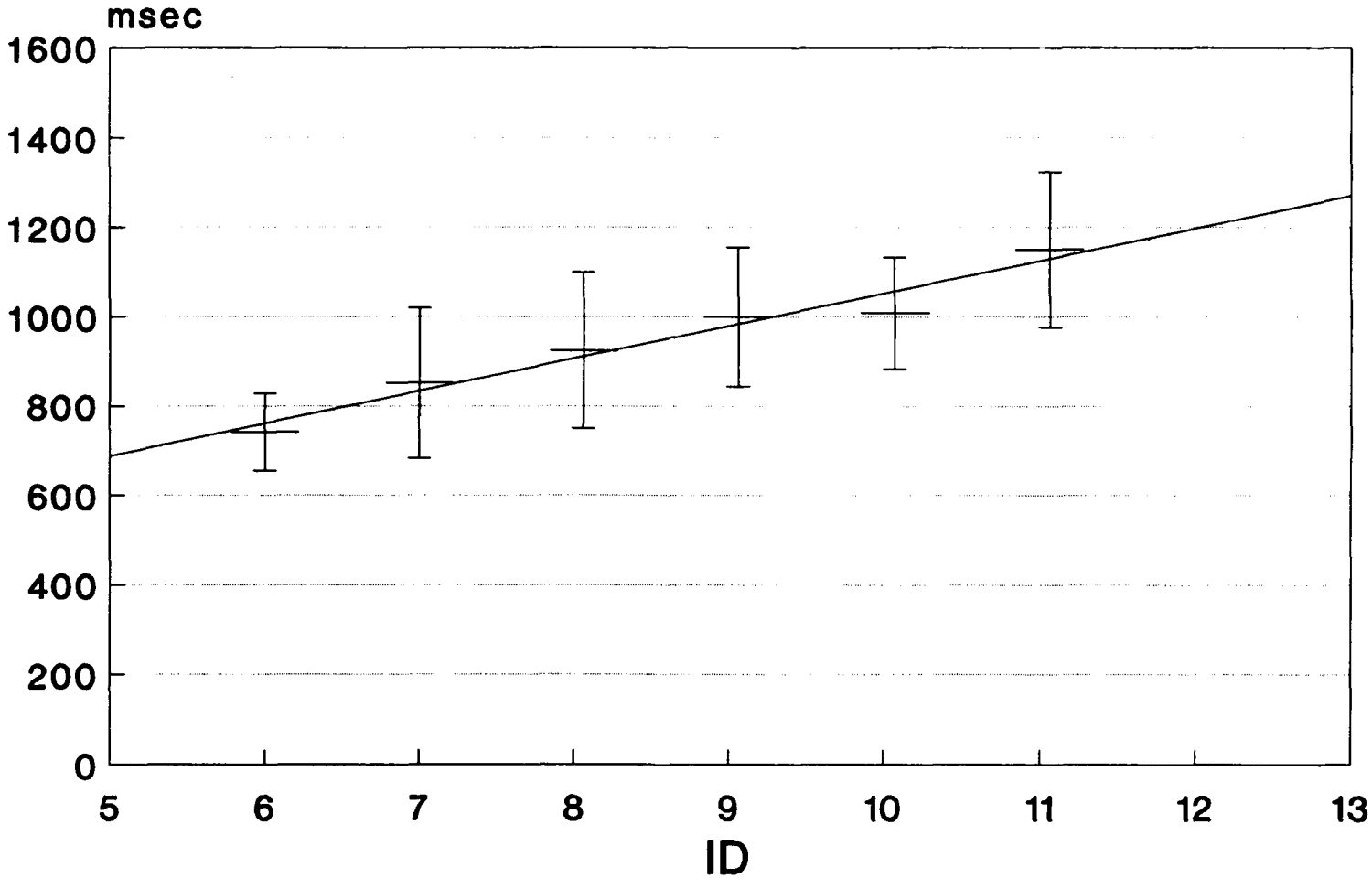

Subject 2 w/ Exoskeleton

Linear Data Points

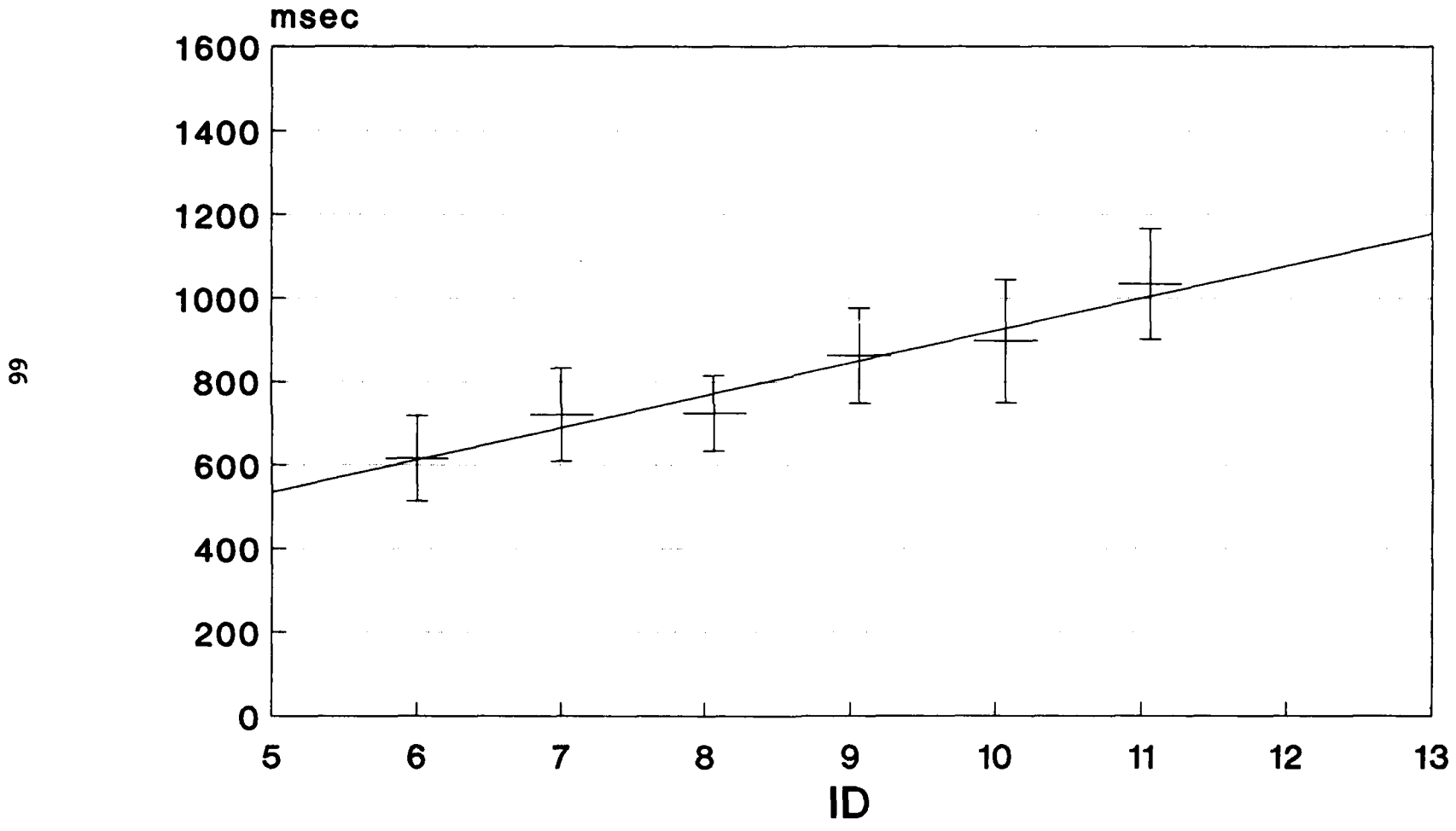

Subject 3 w/ Exoskeleton

Linear Data Points

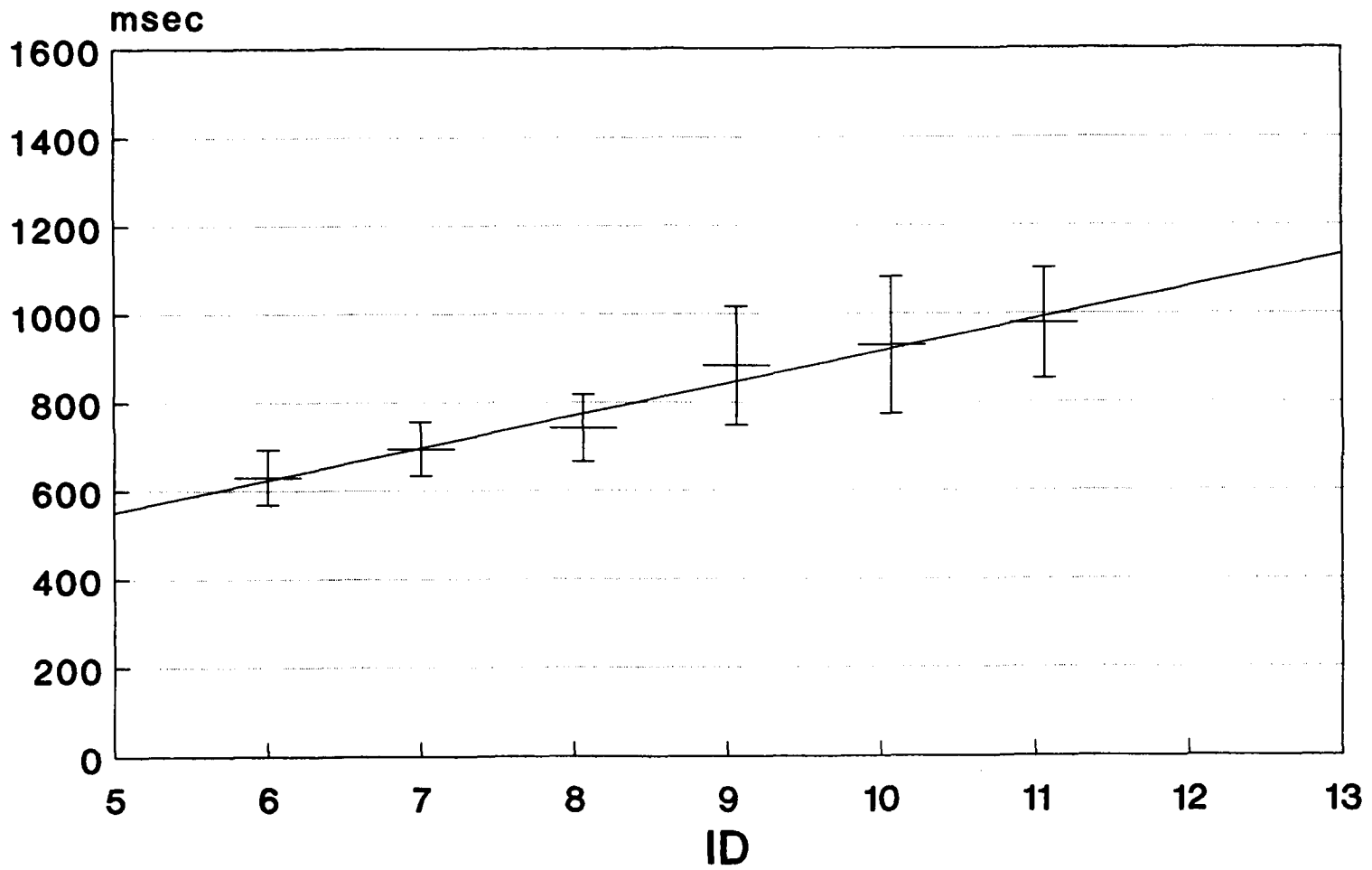

Subject 4 w/ Exoskeleton

Linear Data Points

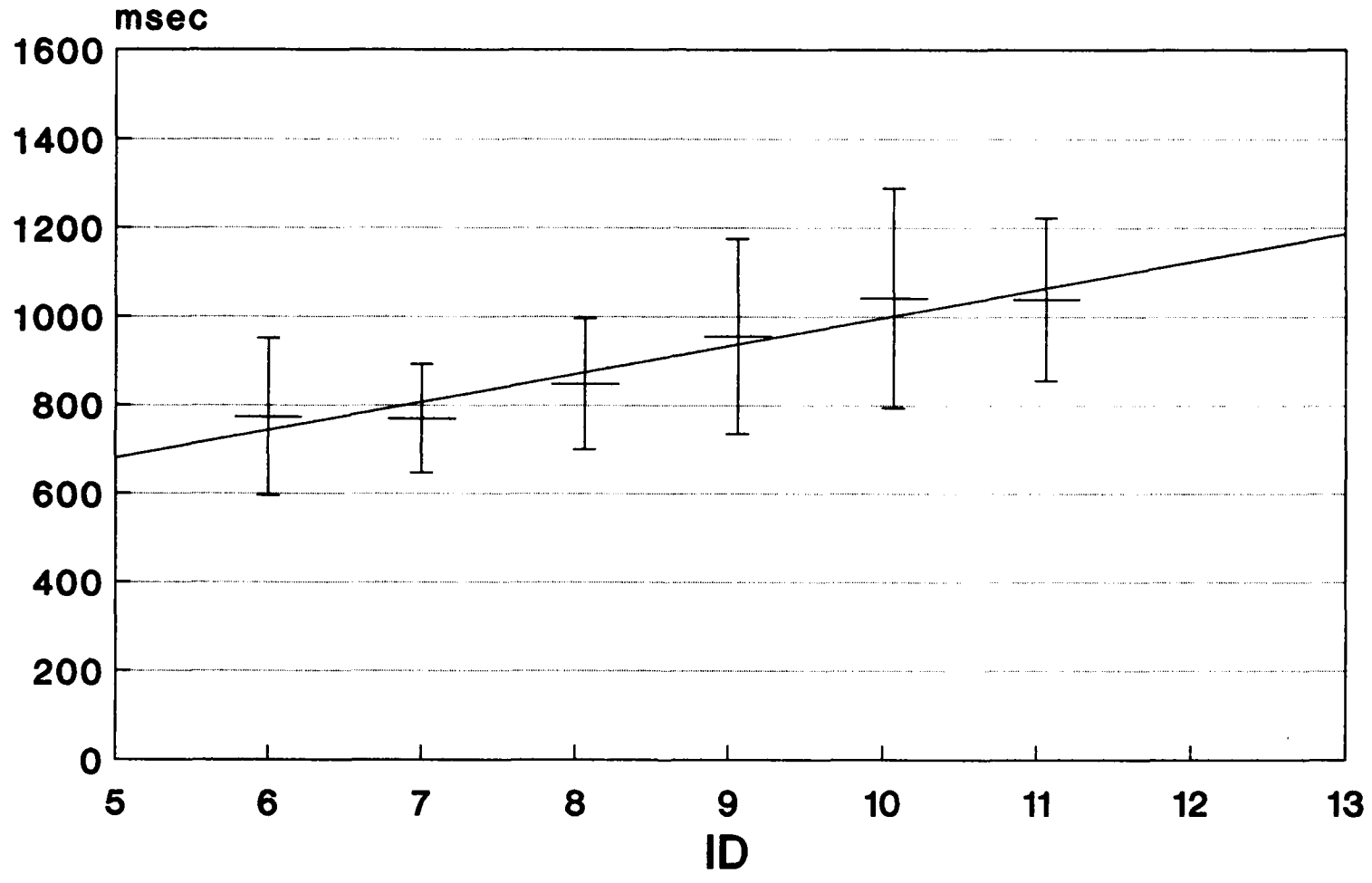

Subject 5 w/ Exoskeleton

Linear Data Points

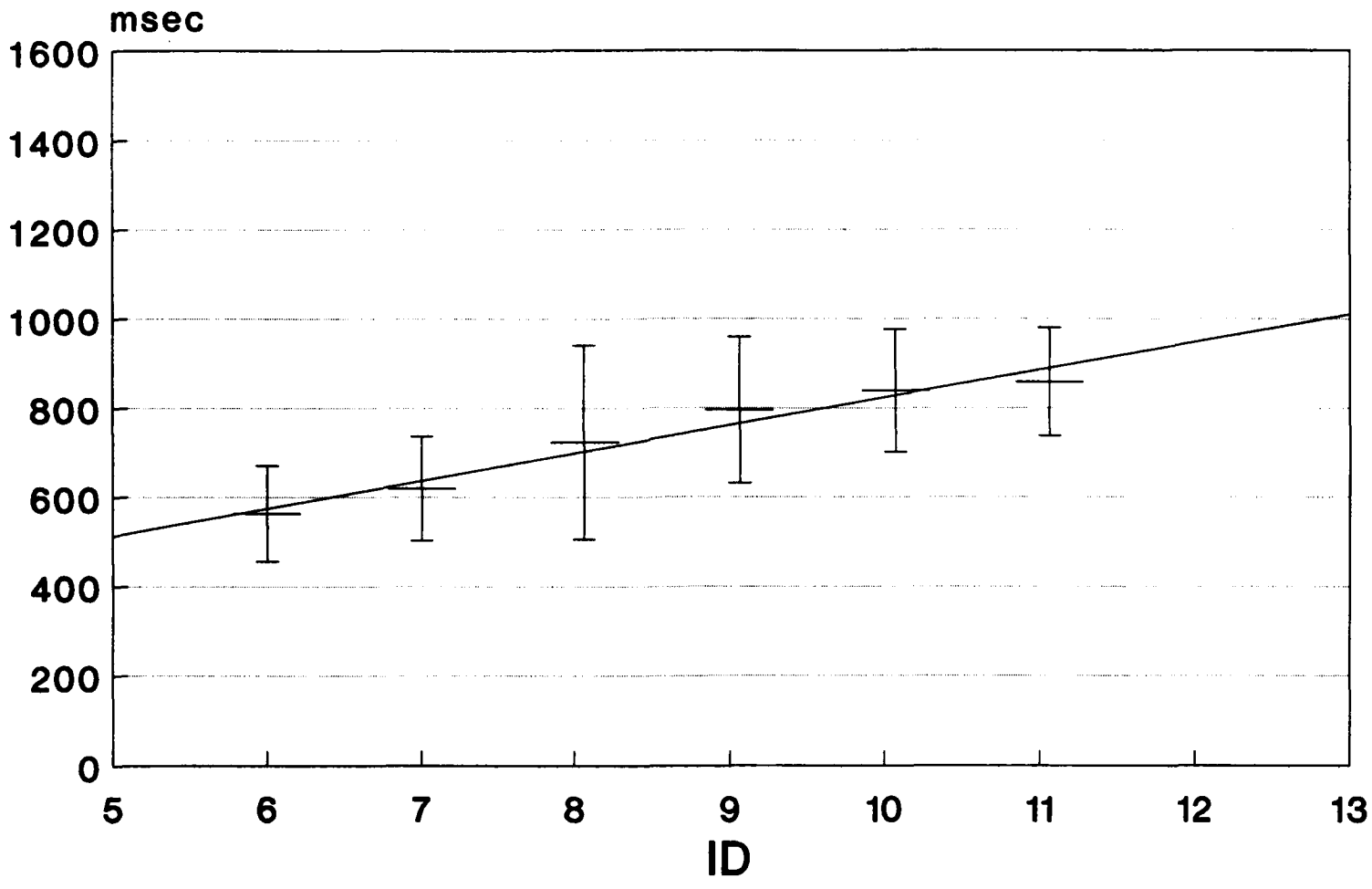

Subject 6 w/ Exoskeleton

Linear Data Points

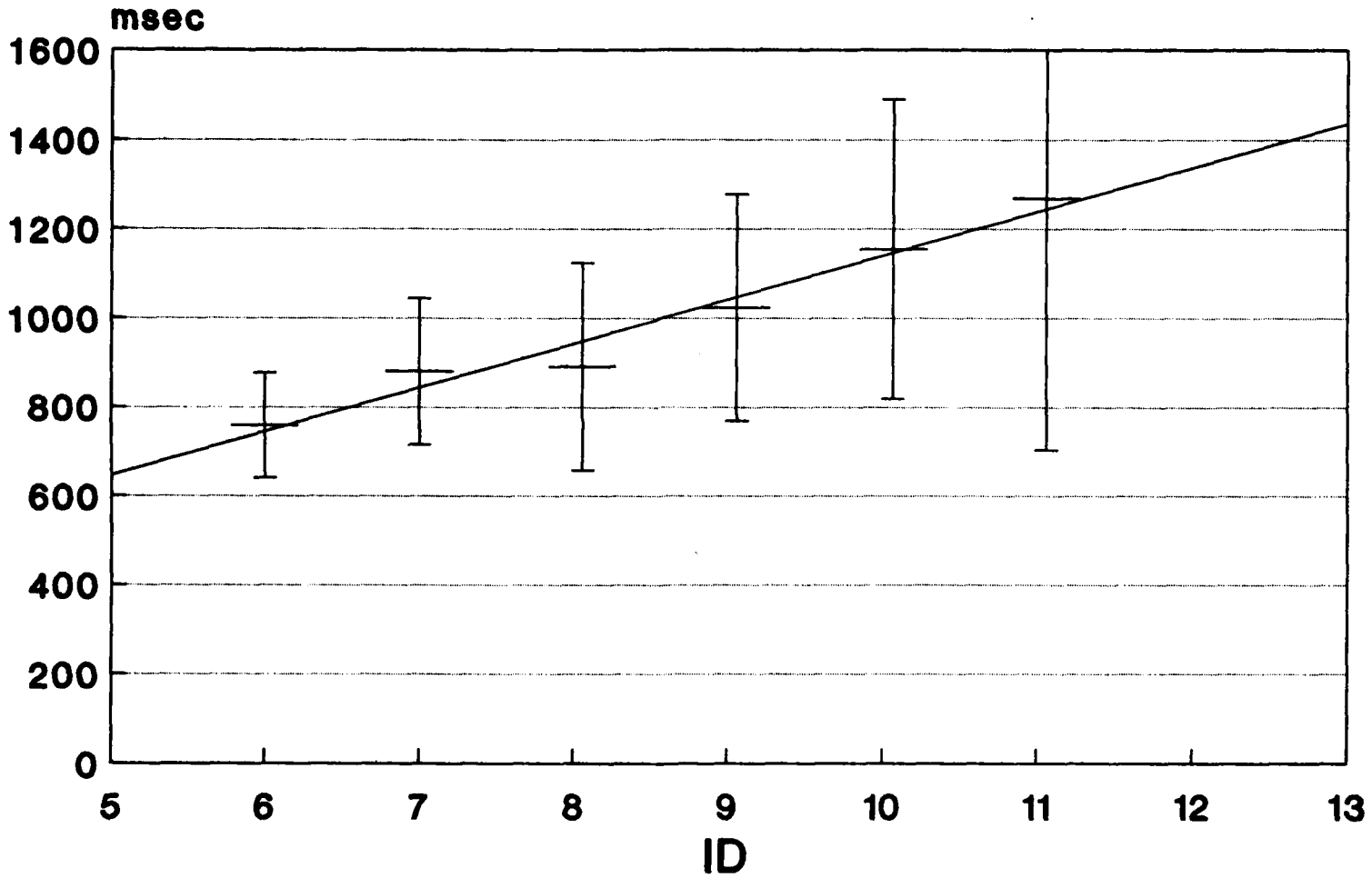

Subject 7 w/ Exoskeleton

Linear Data Points

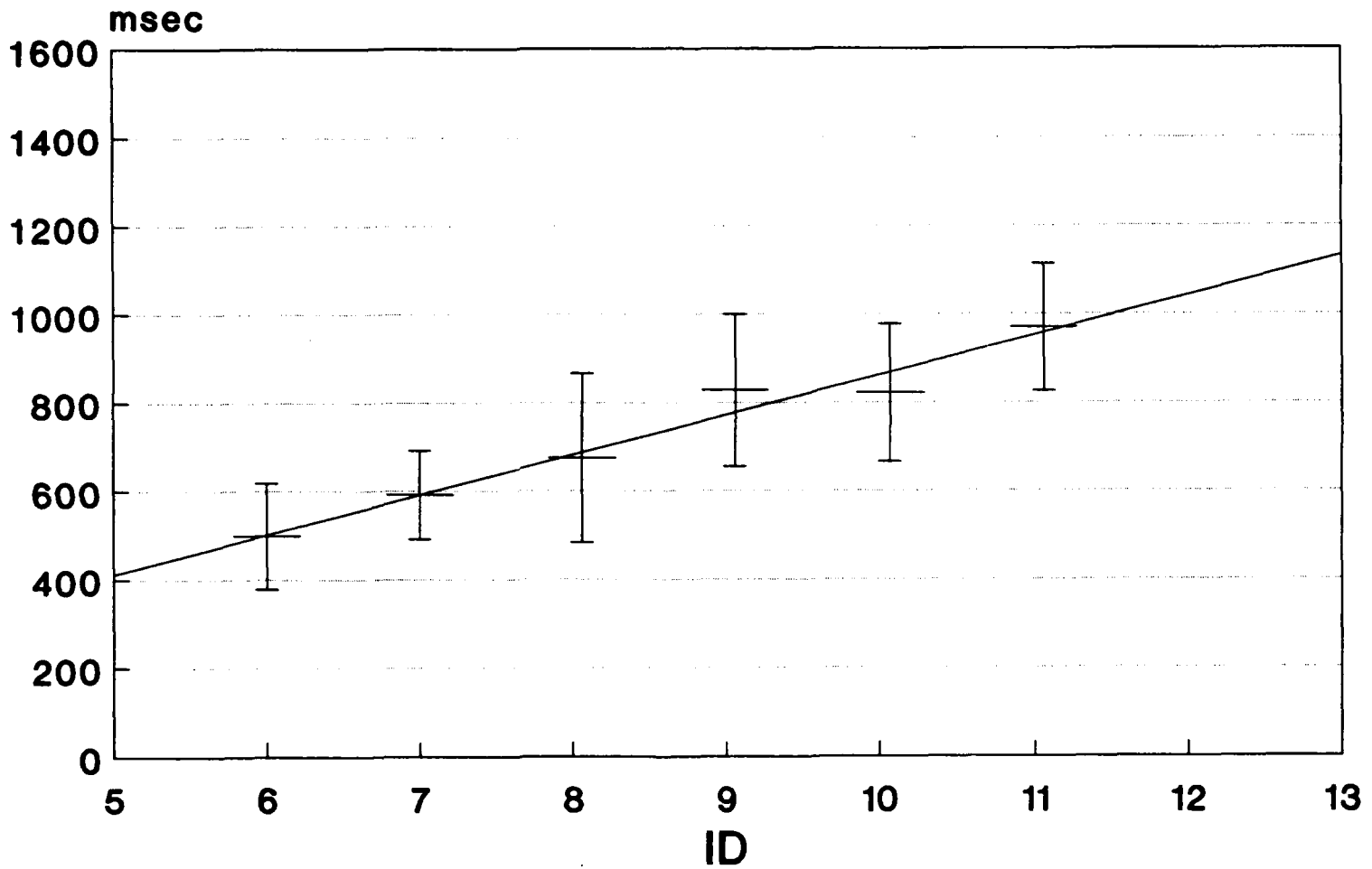

Appendix H

mt vs. ID **Wearing MBA Exoskeleton Extrapolated to** $ID = 0$

Subject 1 w/ Exoskeleton

Linear Data Points

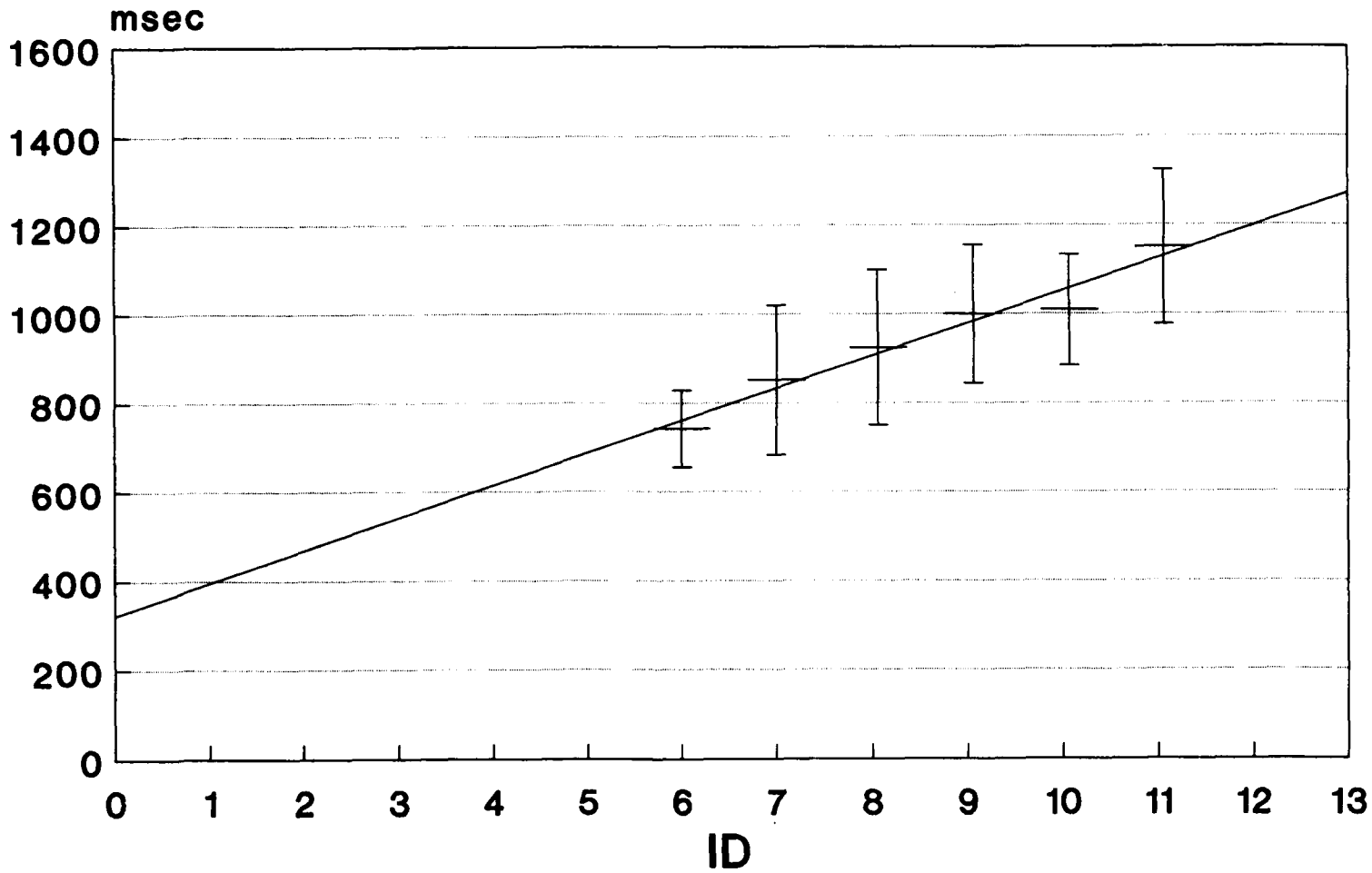

Subject 2 w/ Exoskeleton

Linear Data Points

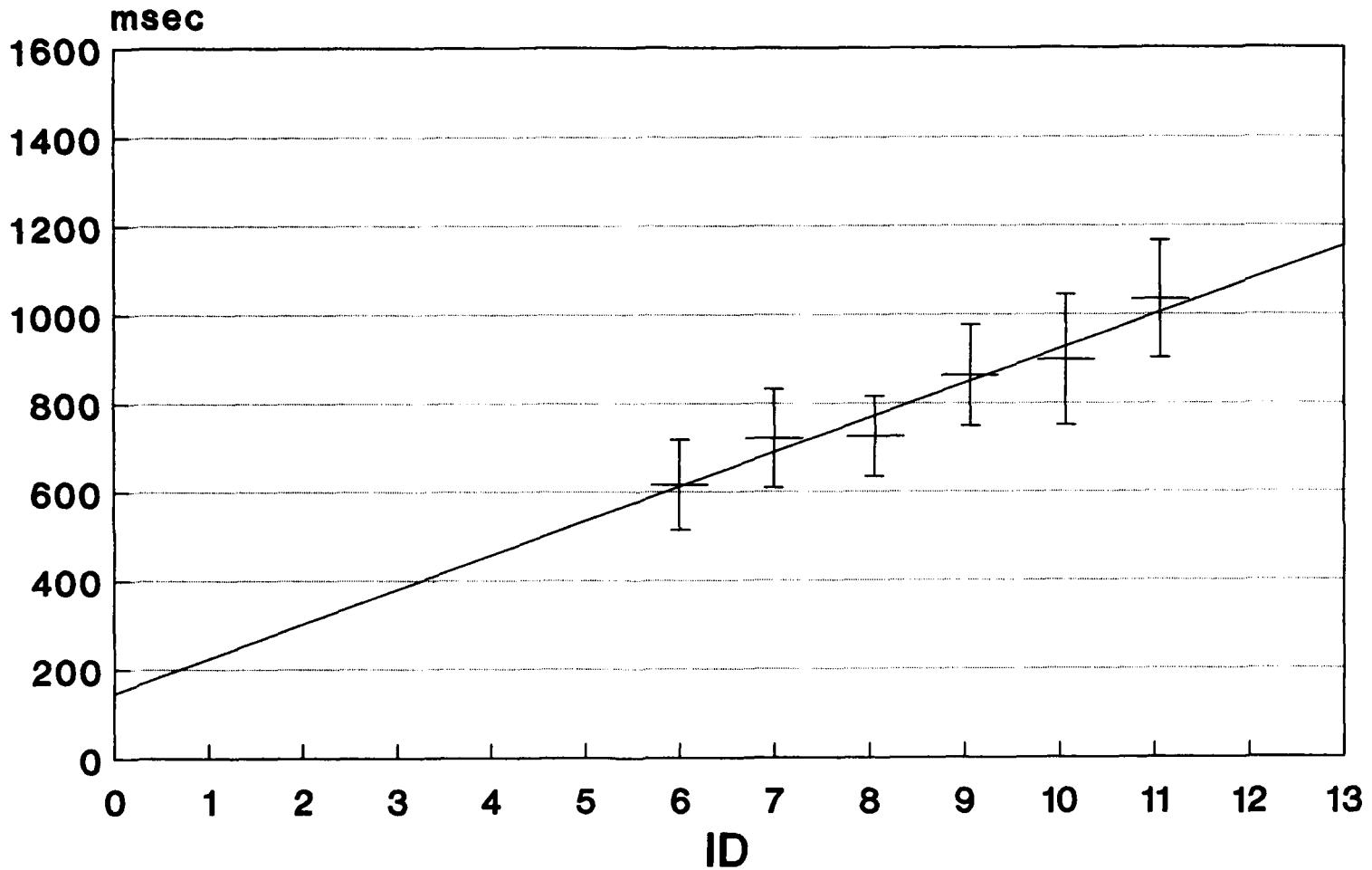

Subject 3 w/ Exoskeleton

Linear Data Points

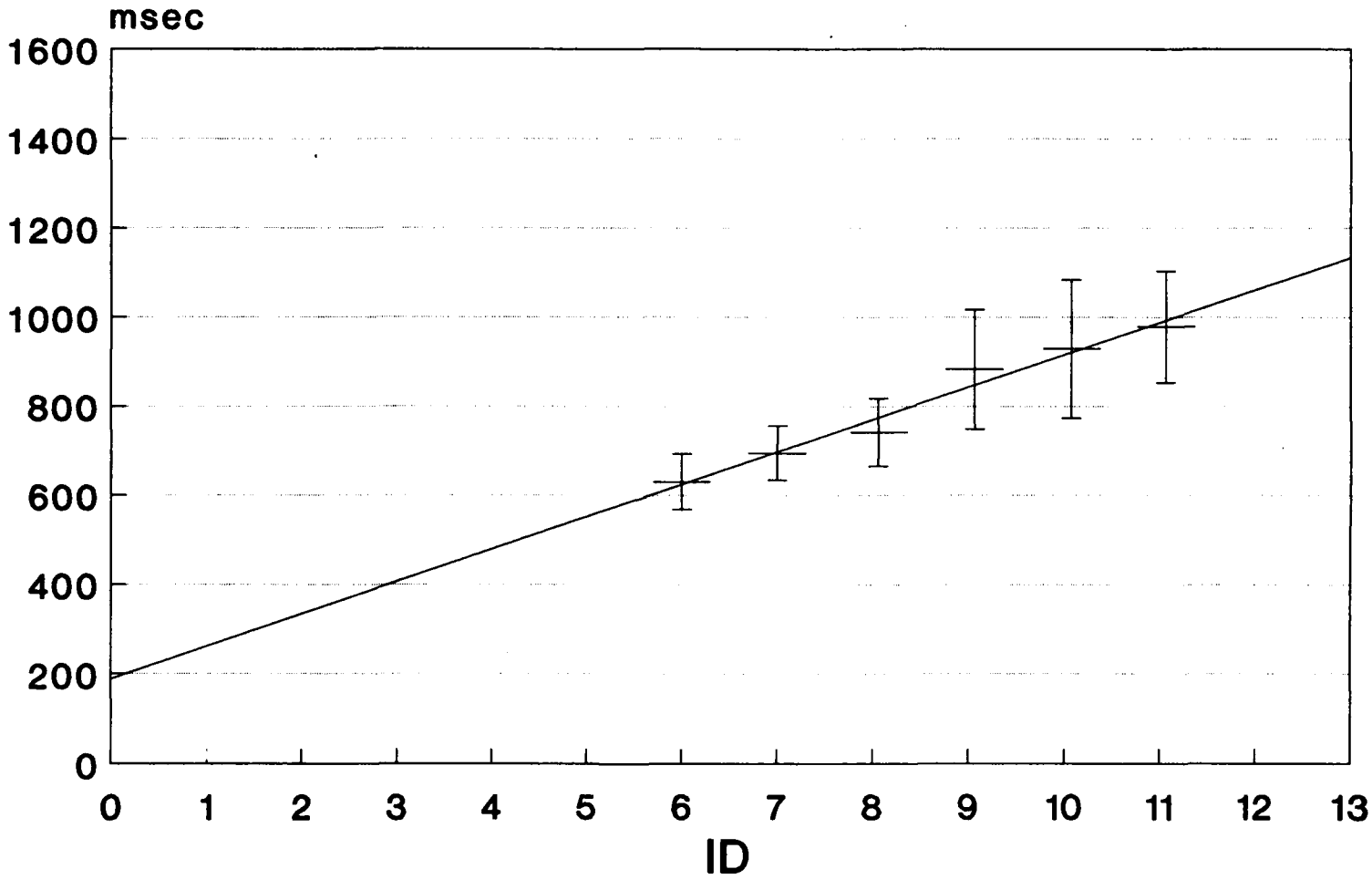

Subject 4 w/ Exoskeleton

Linear Data Points

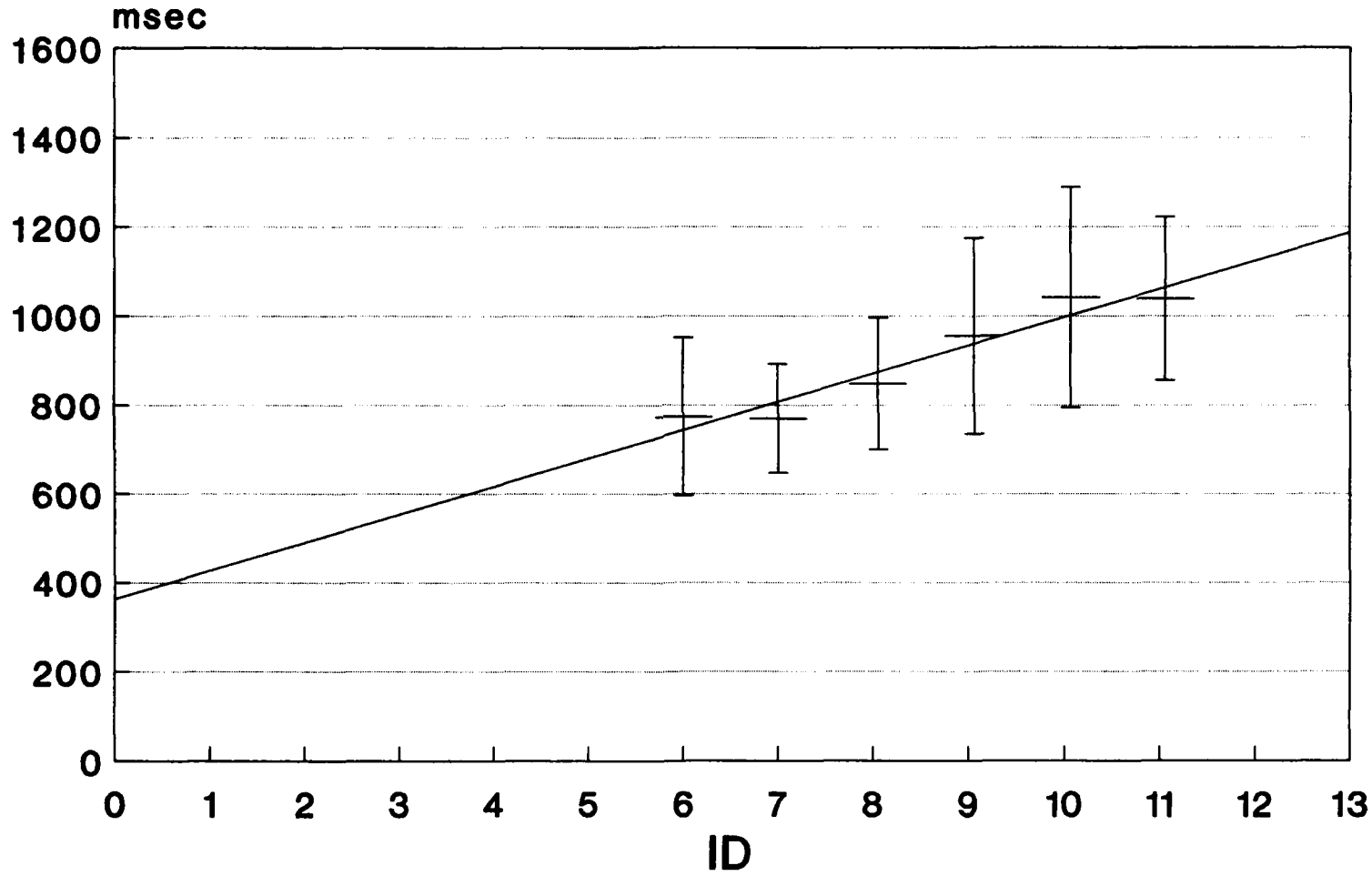

Subject 5 w/ Exoskeleton

Linear Data Points

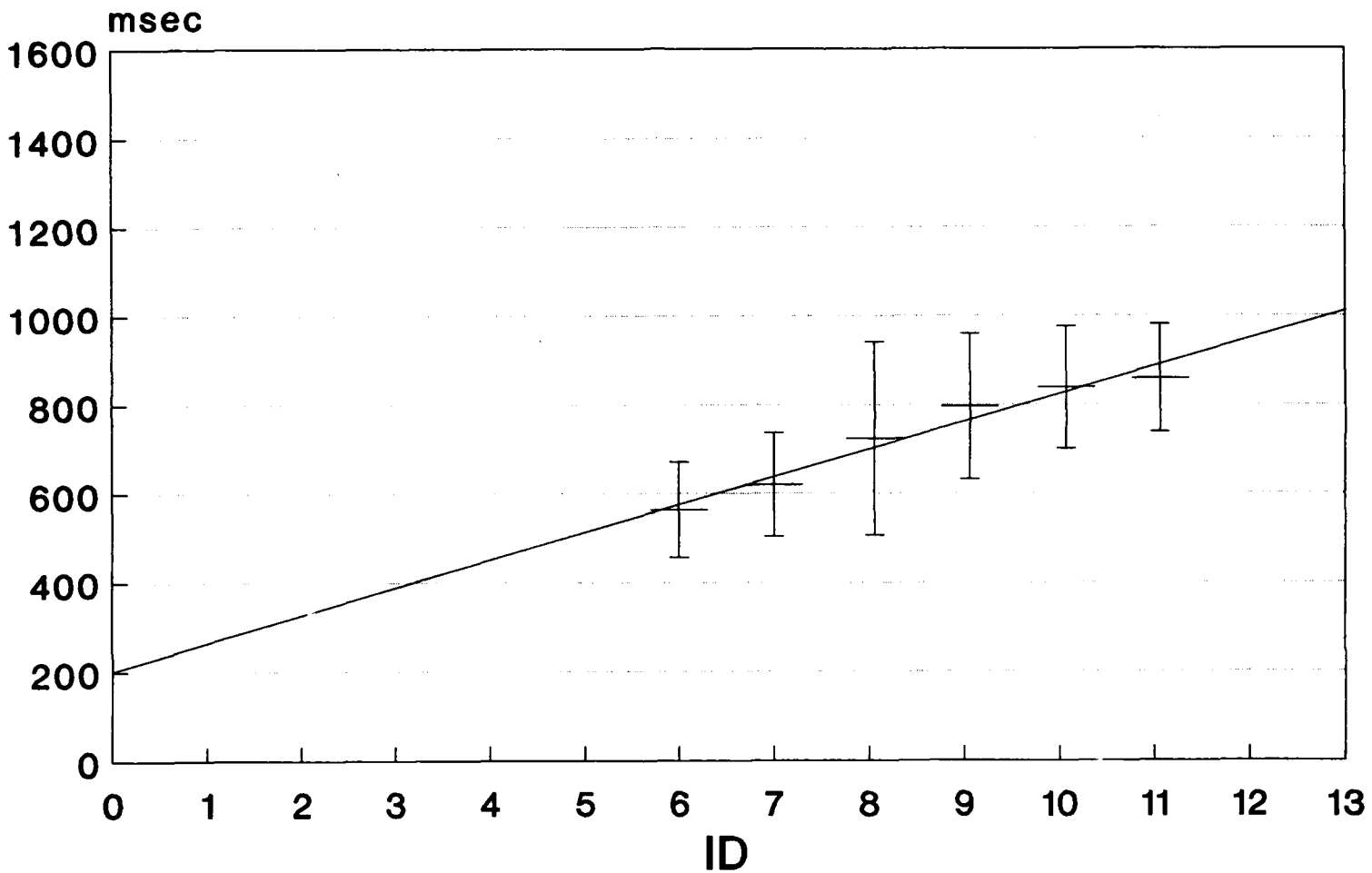

Subject 6 w/ Exoskeleton

Linear Data Points

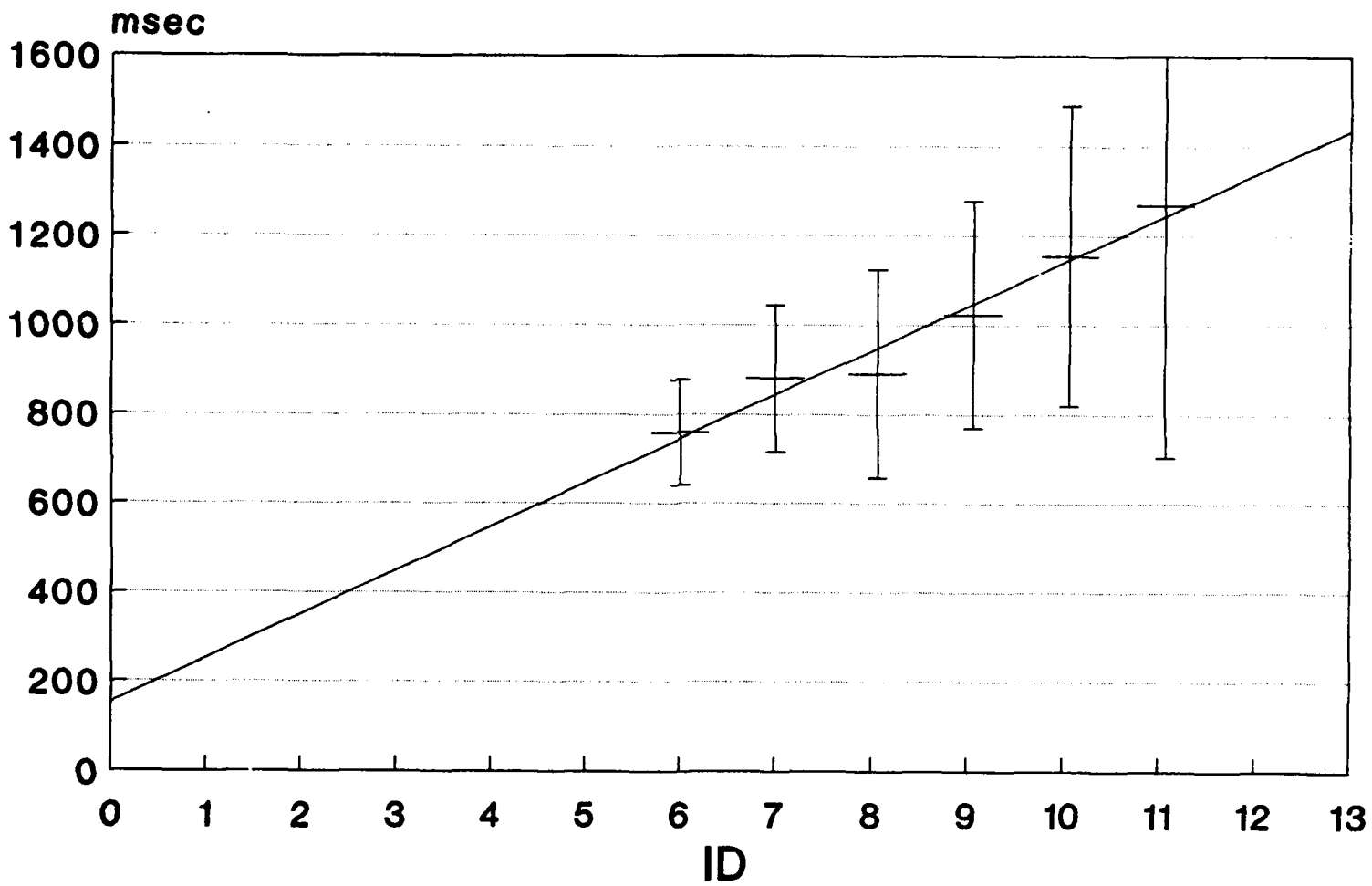

Subject 7 w/ Exoskeleton

Linear Data Points

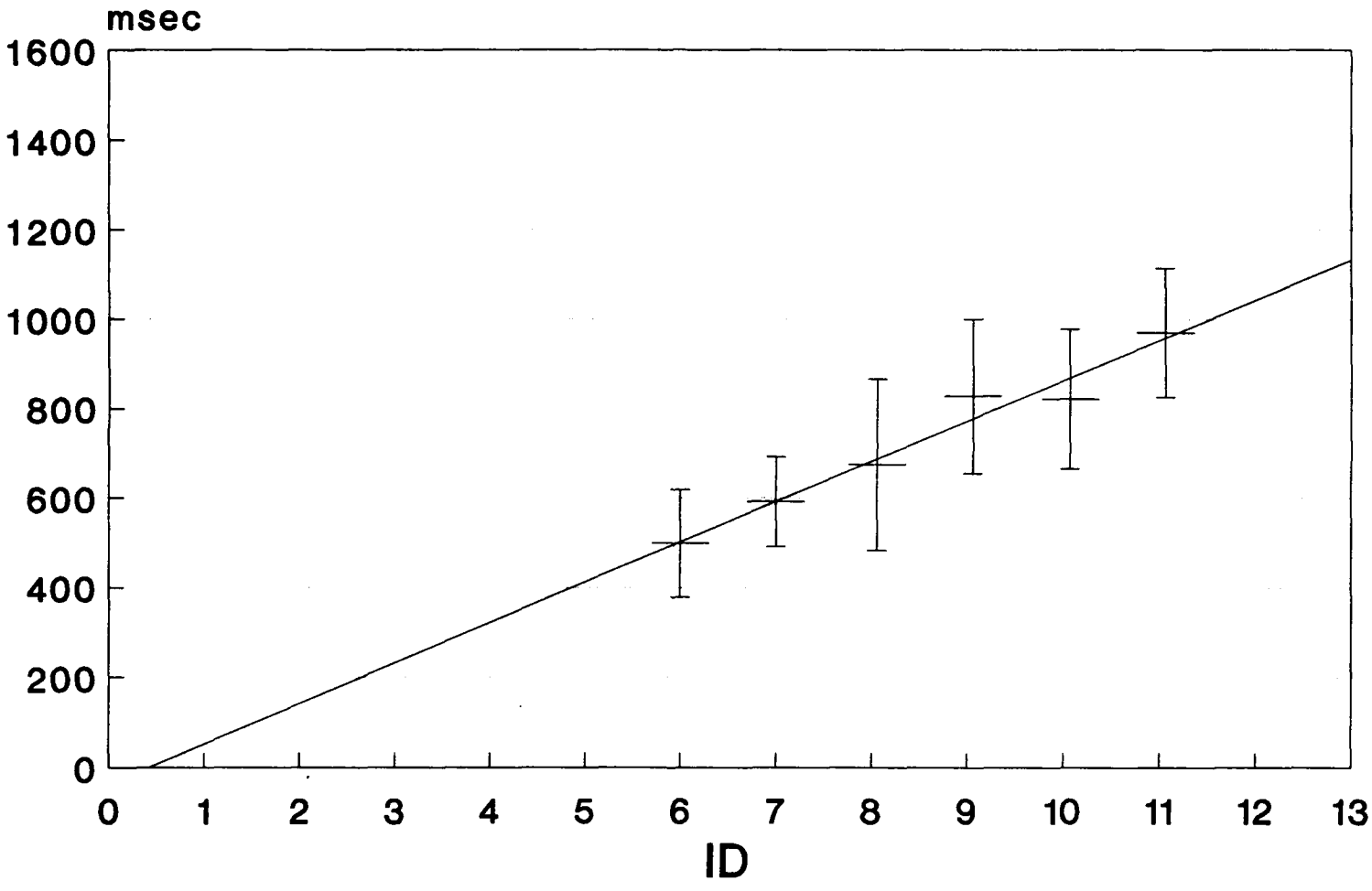

Appendix I

Coefficients of Variation

Coefficients of Variation
Average Across Seven Subjects

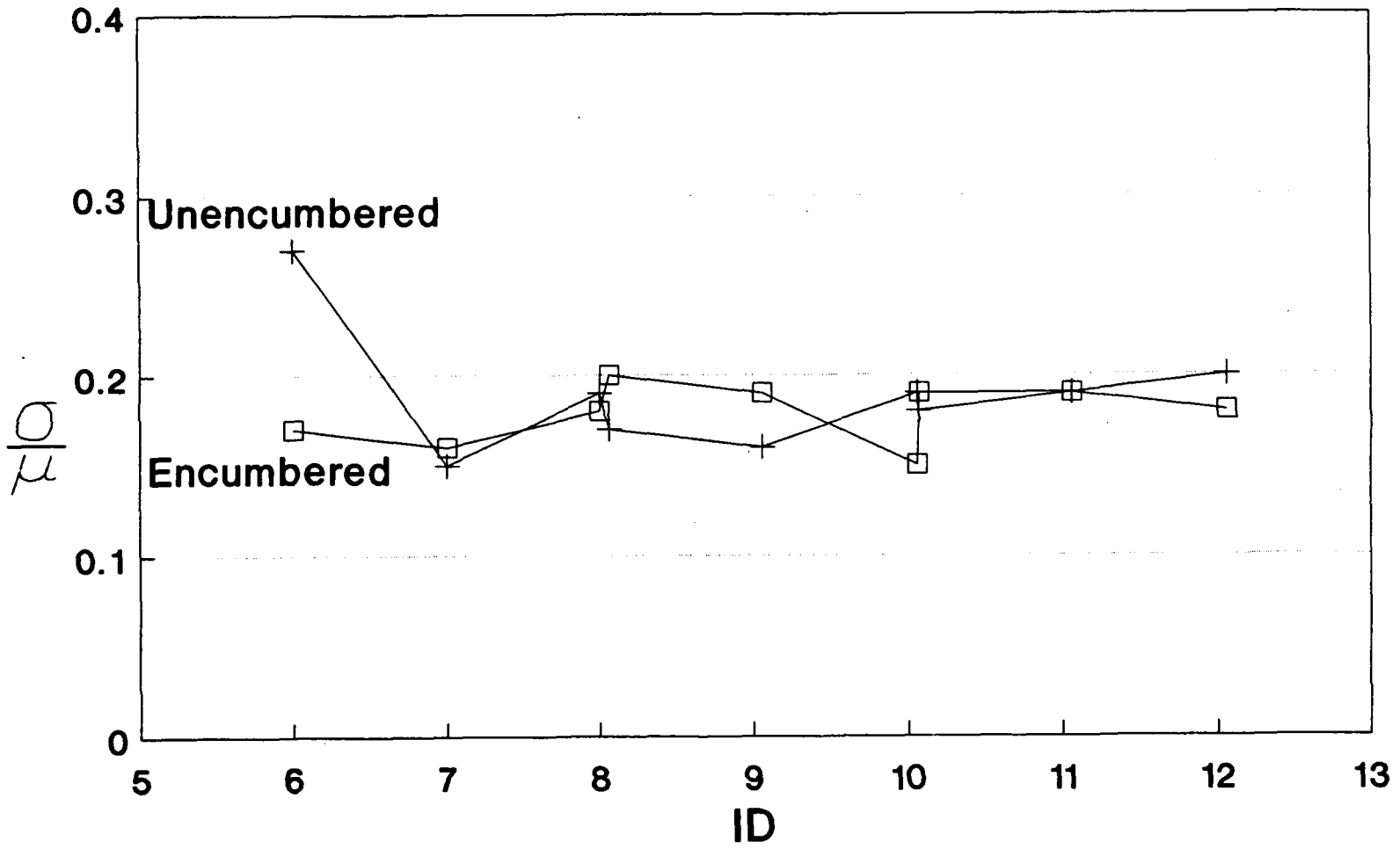

Subject 1
Coefficients of Variation

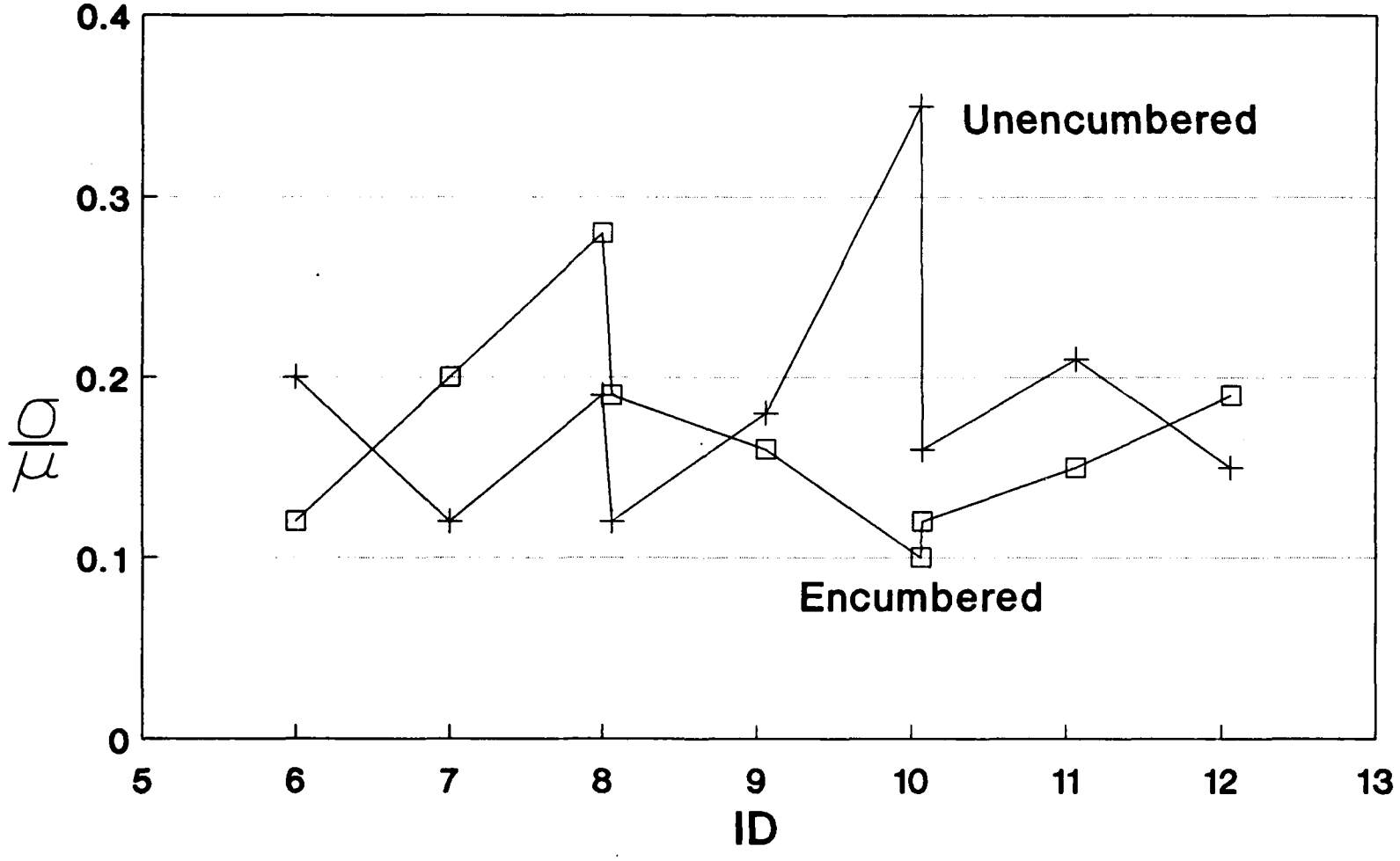

Subject 2
Coefficients of Variation

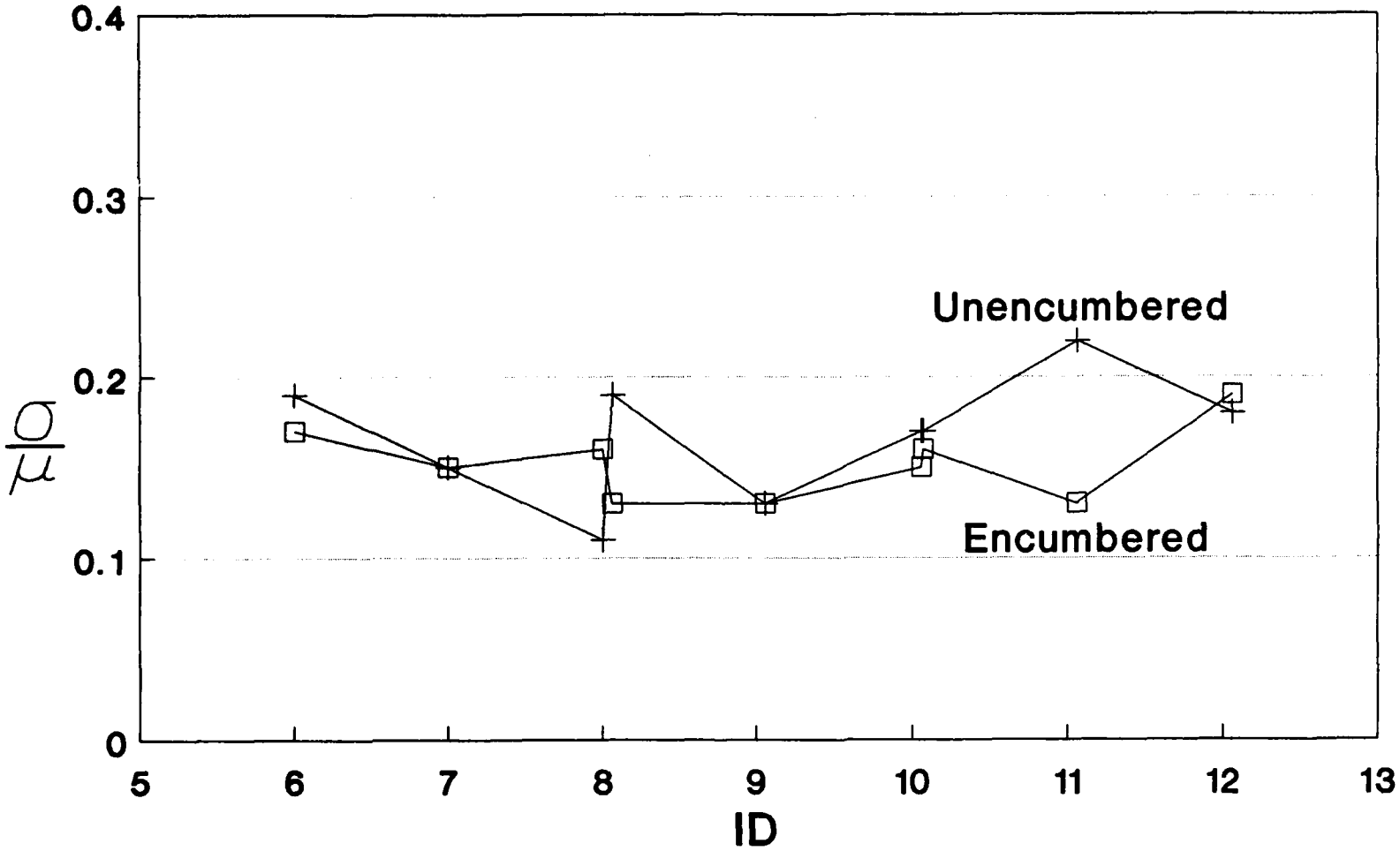

Subject 3
Coefficients of Variation

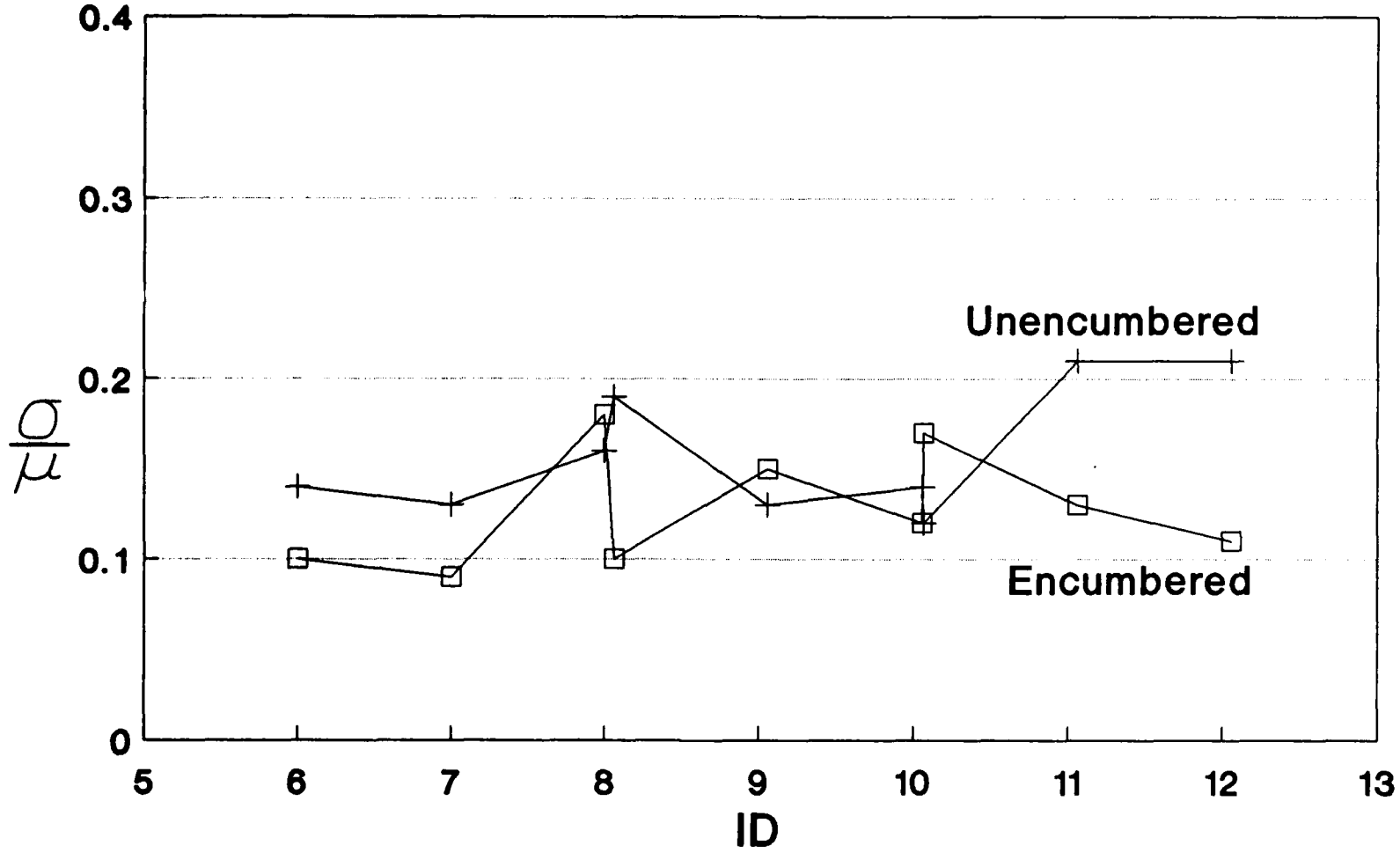

Subject 4
Coefficients of Variation

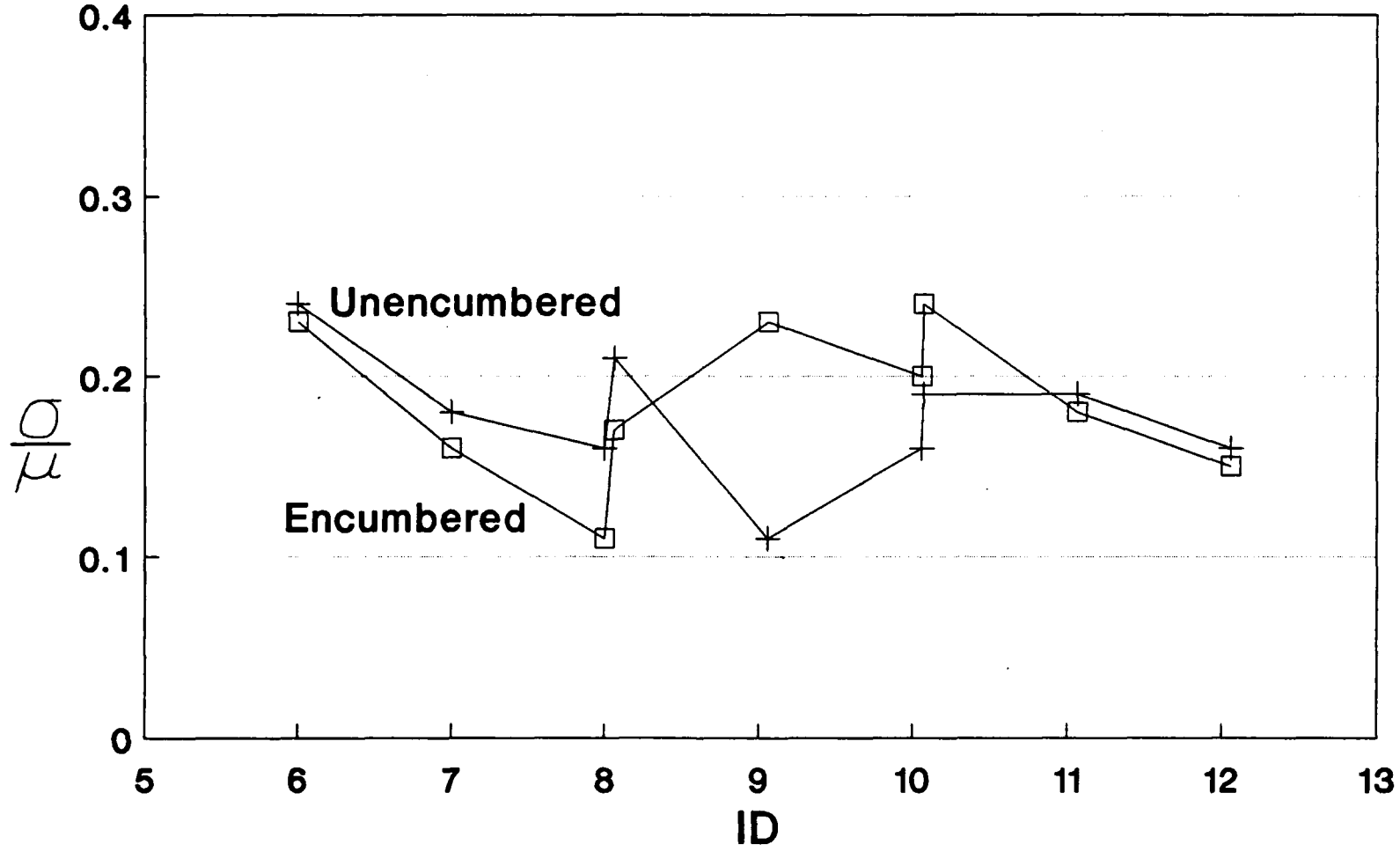

Subject 5
Coefficients of Variation

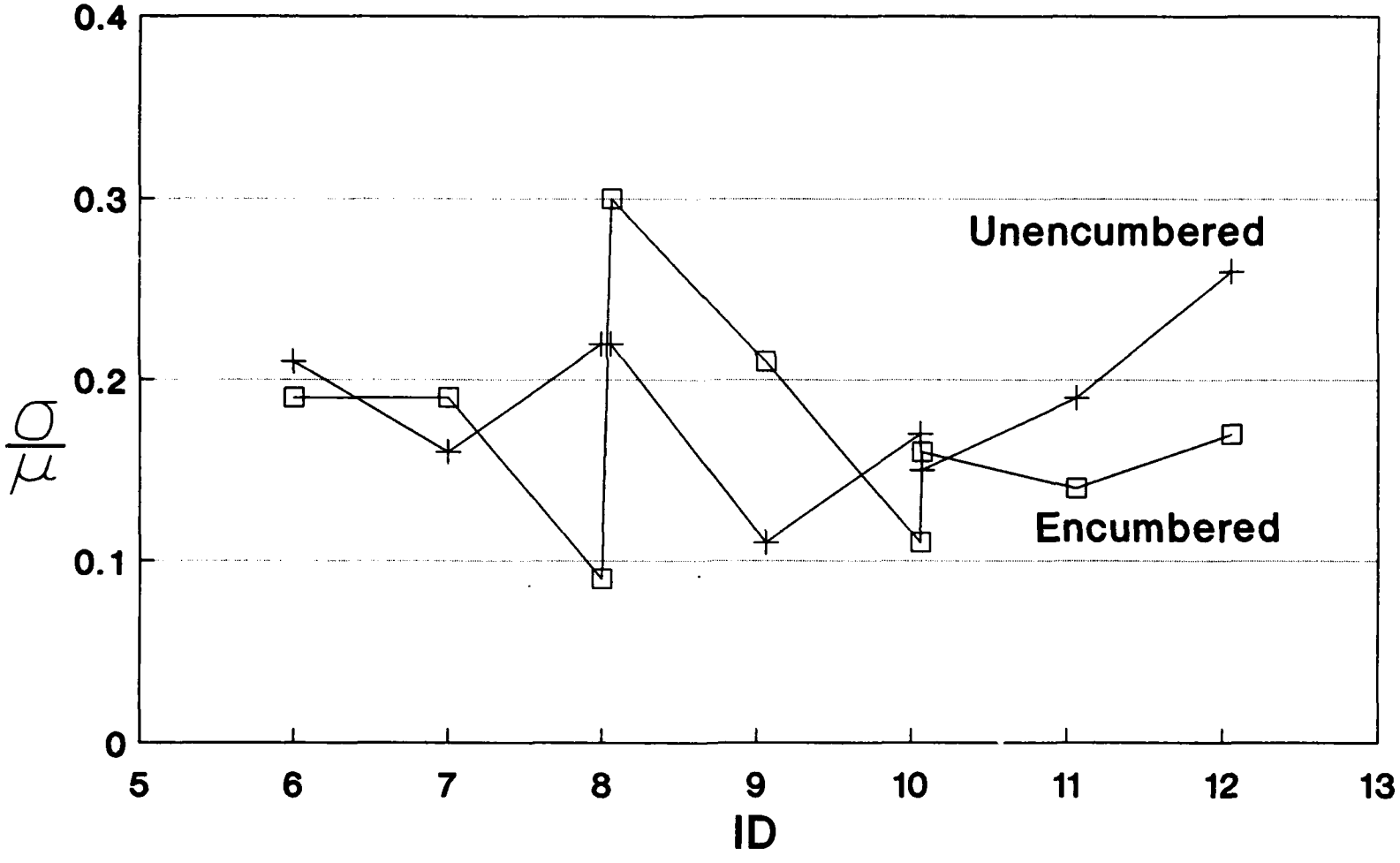

Subject 6
Coefficients of Variation

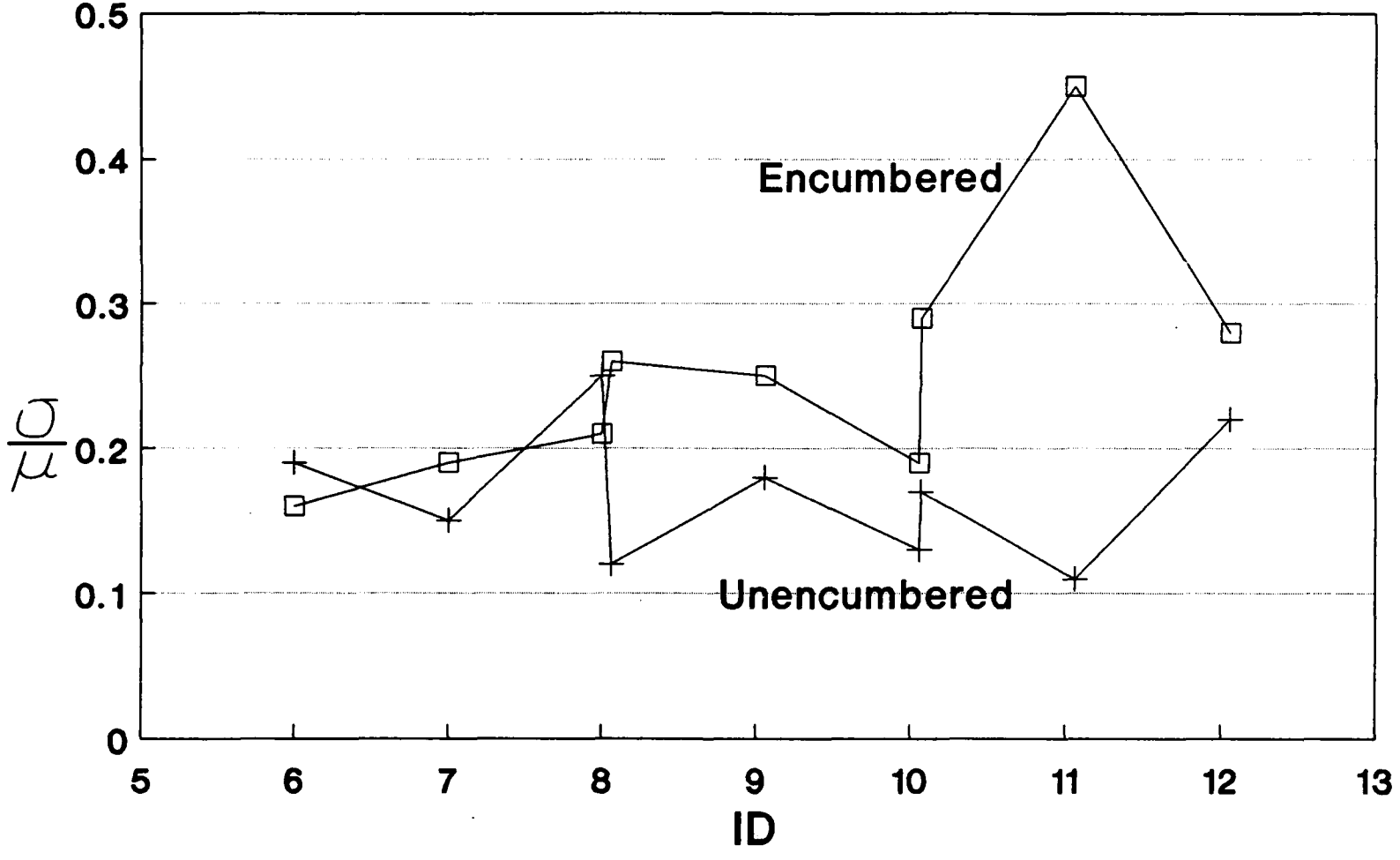

Subject 7
Coefficients of Variation

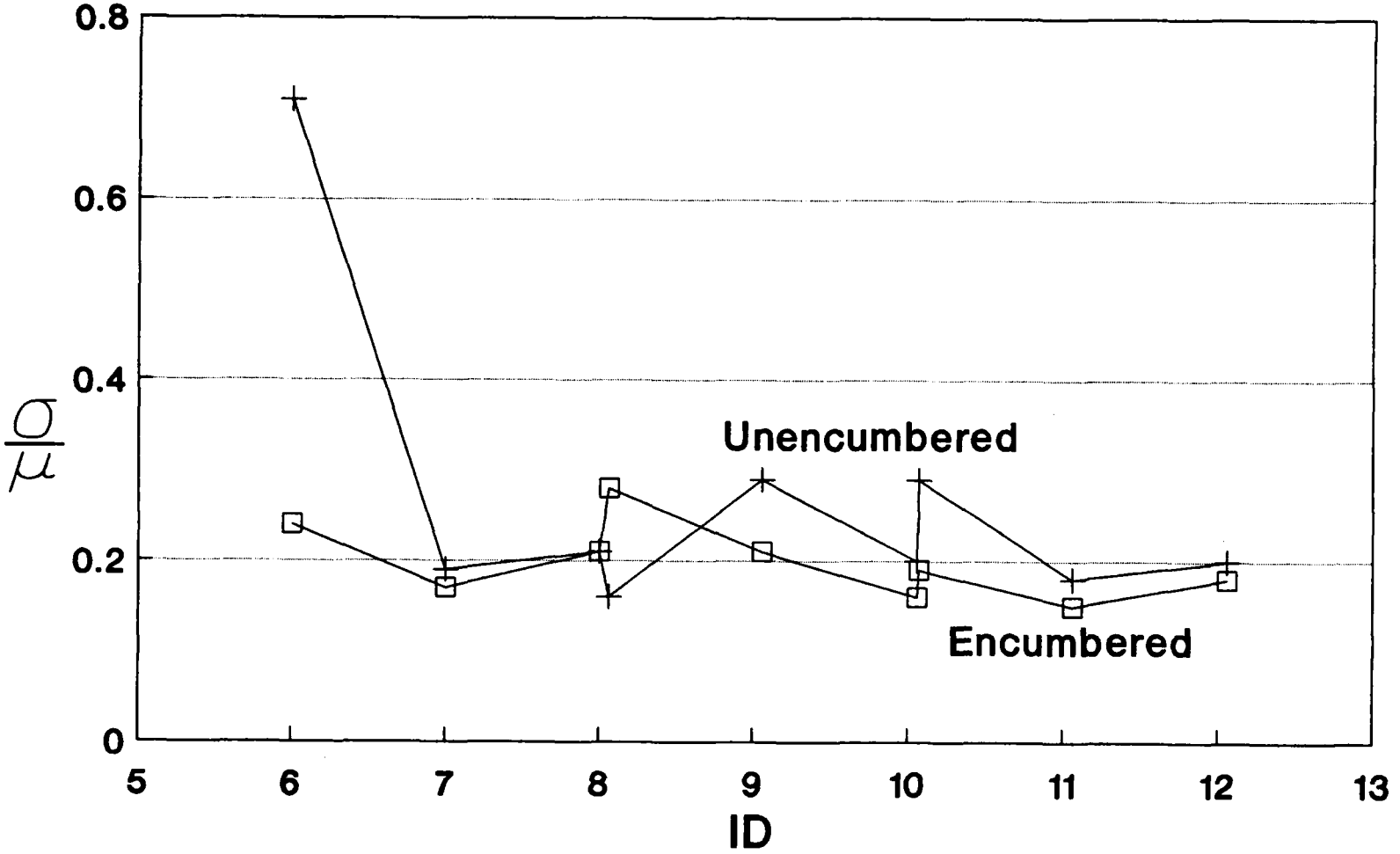

Appendix J

Two-dimensional Analysis of Data

Subject 1
Dual Task Paradigm

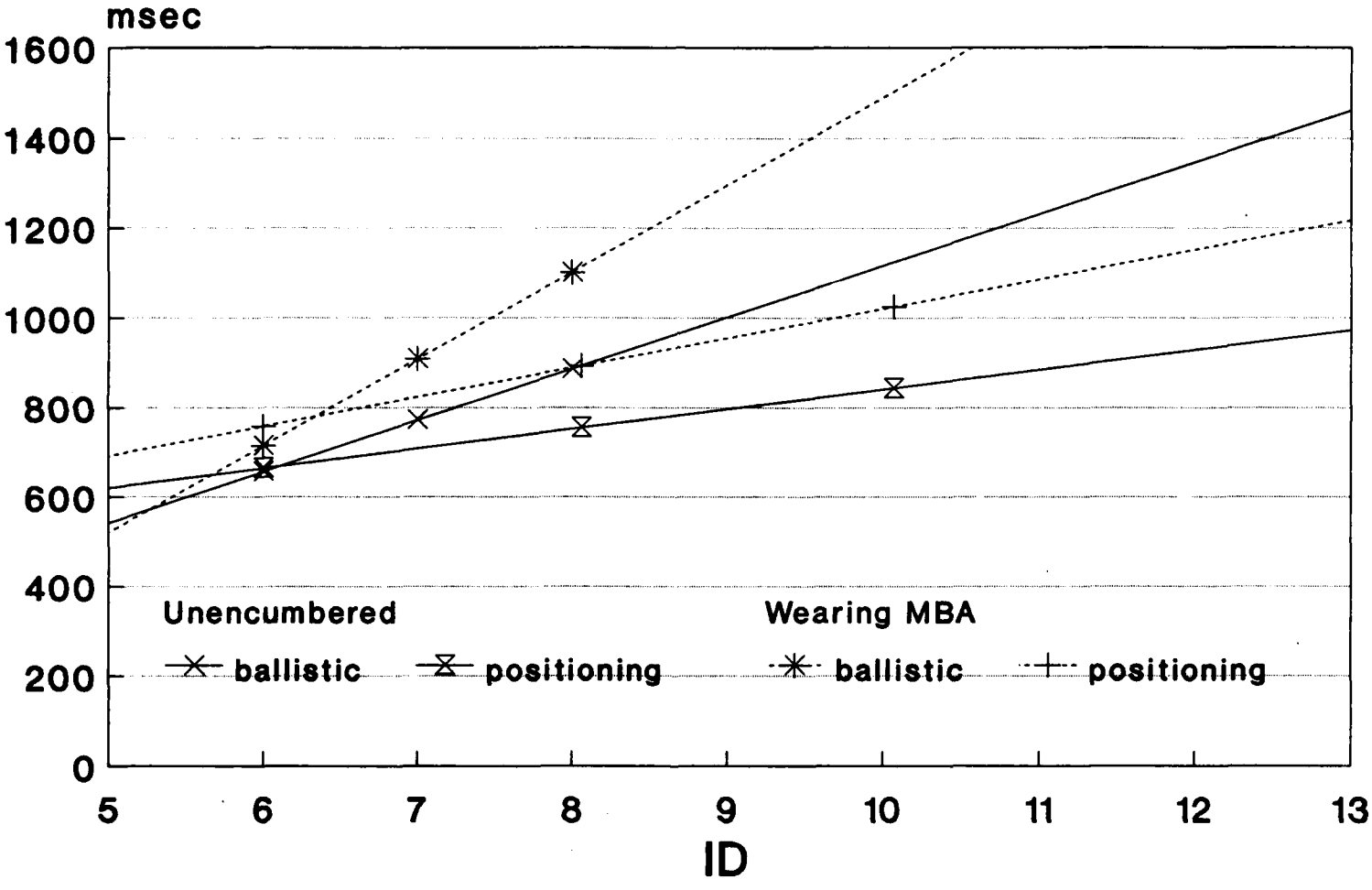

To differentiate between lines, the data points have been adjusted to fall on the best-fit lines. For actual values see Appendices B and F.

Subject 2
Dual Task Paradigm

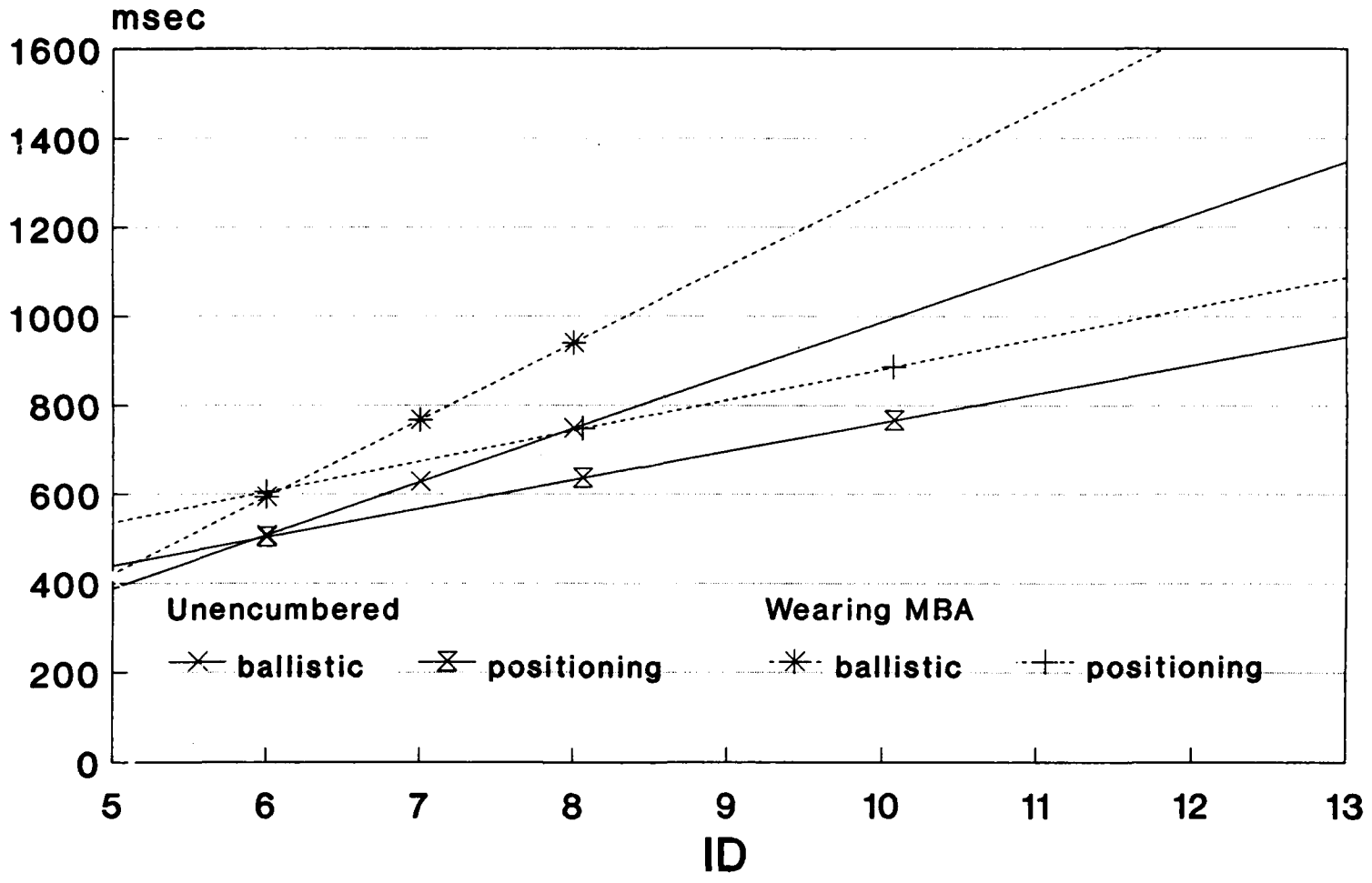

To differentiate between lines, the data points have been adjusted to fall on the best-fit lines. For actual values see Appendices B and F.

Subject 3
Dual Task Paradigm

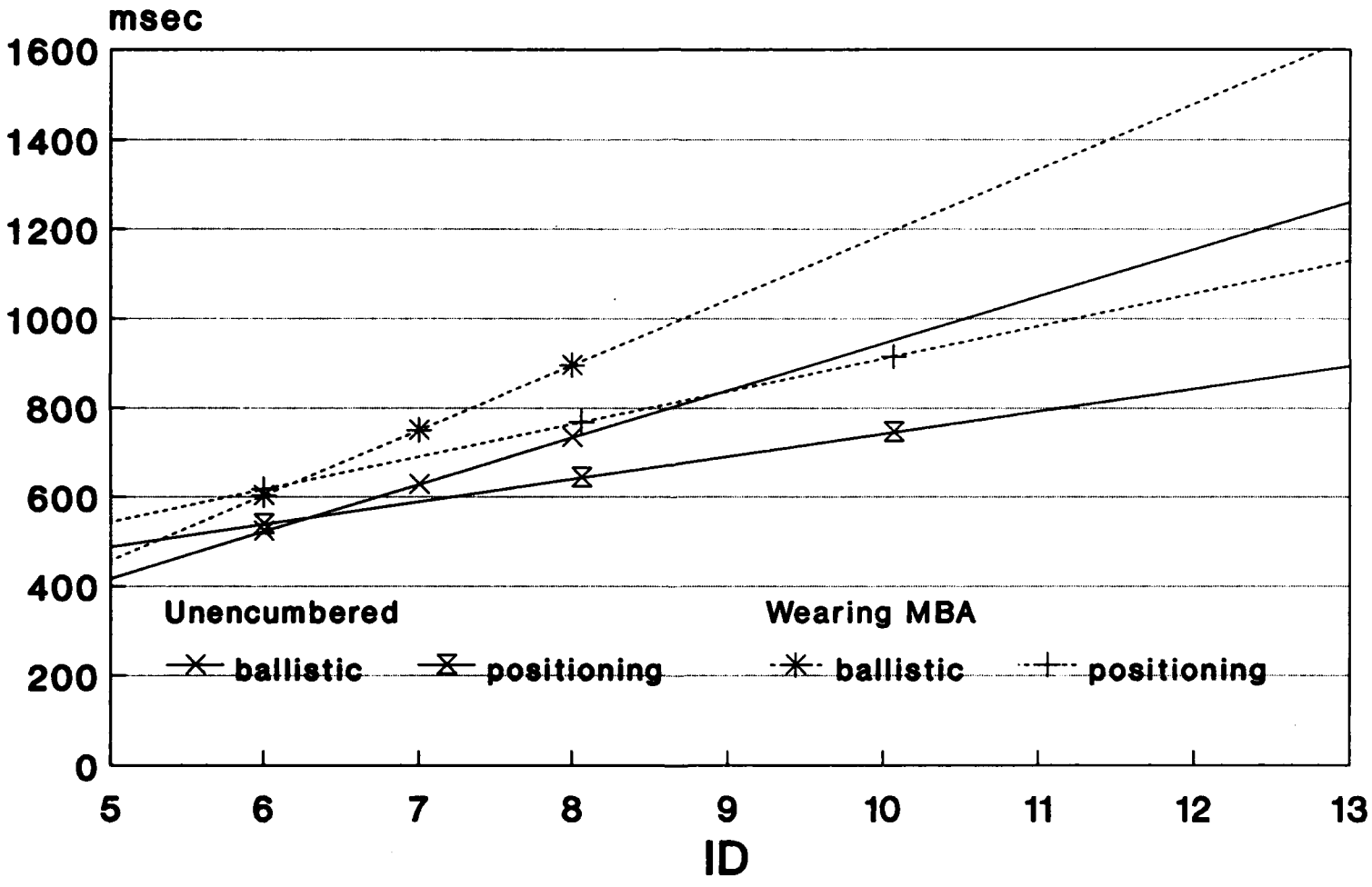

To differentiate between lines, the data points have been adjusted to fall on the best-fit lines. For actual values see Appendices B and F.

Subject 4
Dual Task Paradigm

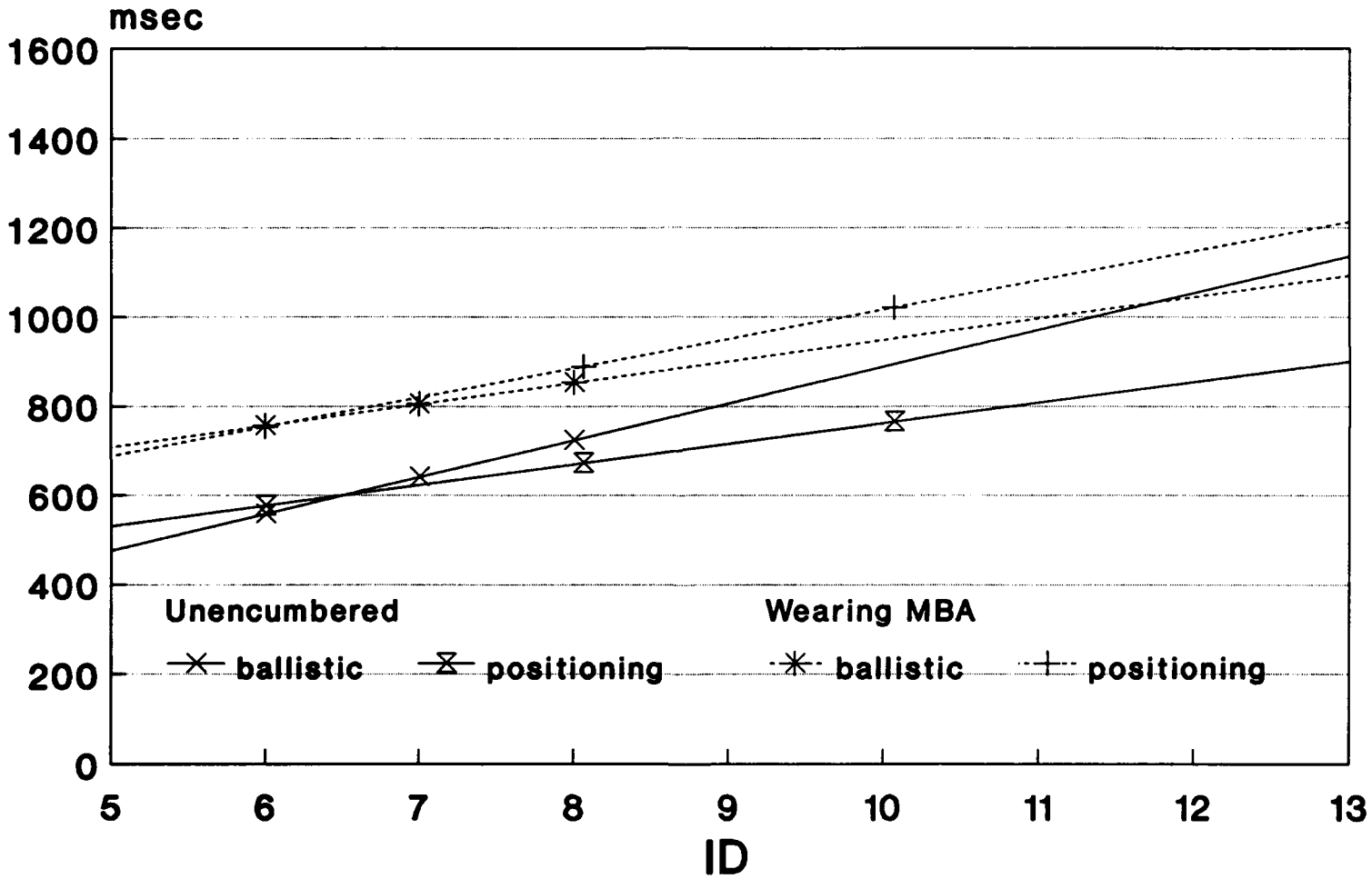

To differentiate between lines, the data points have been adjusted to fall on the best-fit lines. For actual values see Appendices B and F.

Subject 5
Dual Task Paradigm

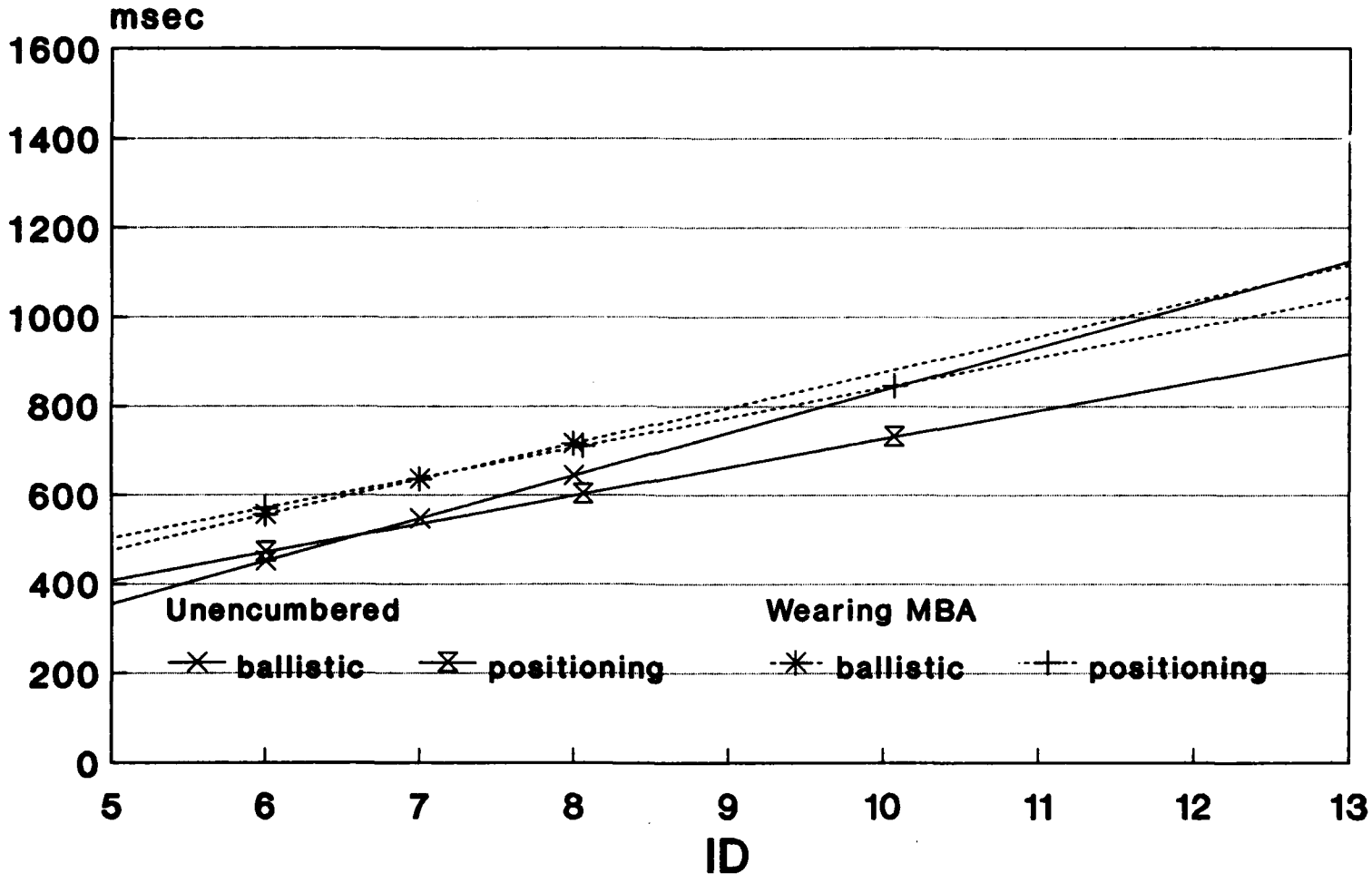

To differentiate between lines, the data points have been adjusted to fall on the best-fit lines. For actual values see Appendices B and F.

Subject 6
Dual Task Paradigm

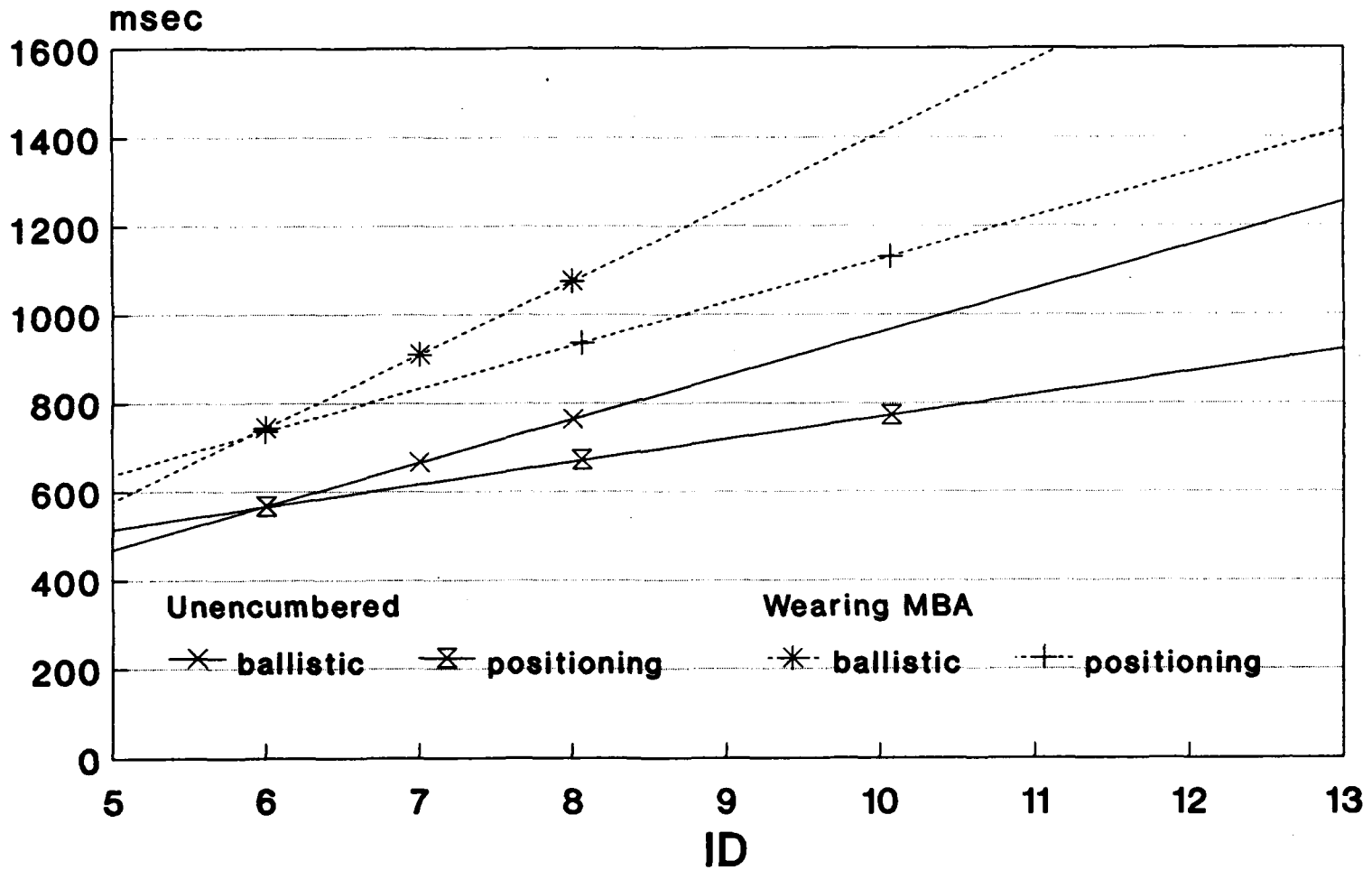

To differentiate between lines, the data points have been adjusted to fall on the best-fit lines. For actual values see Appendices B and F.

*U.S.Government Printing Office: 1991—548-017/20227

Subject 7
Dual Task Paradigm

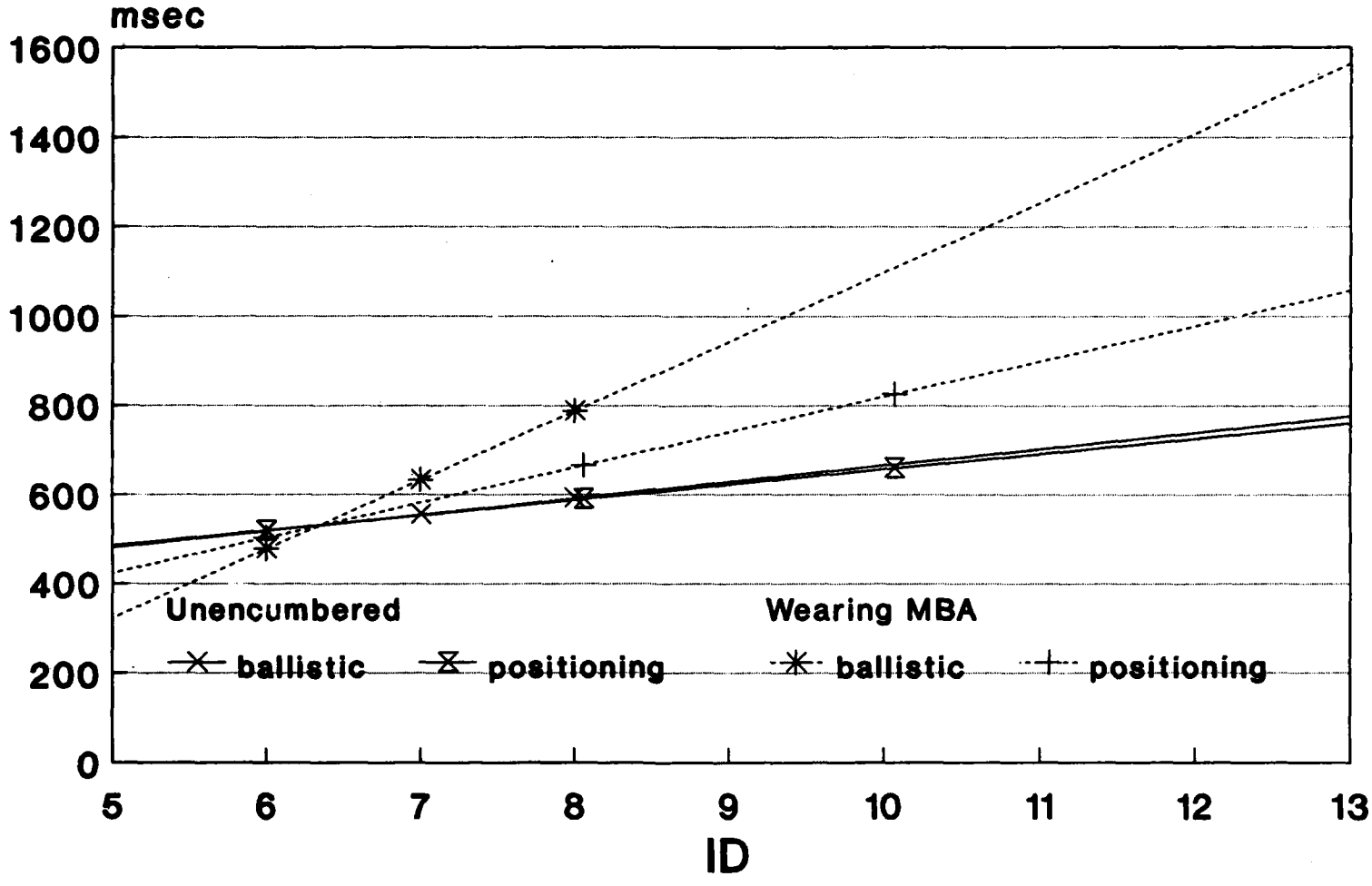

To differentiate between lines, the data points have been adjusted to fall on the best-fit lines. For actual values see Appendices B and F.